Universidade de Aveiro Departamento de Química
2009

Catarina Maia Seco Seiça Neves

Sistemas Aquosos Bifásicos com Líquidos Iónicos

Aqueous Biphasic Systems with Ionic Liquids

Universidade de Aveiro Departamento de Química
2009

Catarina Maia Seco Seiça Neves

Sistemas Aquosos Bifásicos com Líquidos Iónicos

Aqueous Biphasic Systems with Ionic Liquids

Dissertação apresentada à Universidade de Aveiro para cumprimento dos requisitos necessários à obtenção do grau de Mestre em Química Analítica e Controlo de Qualidade, realizada sob a orientação científica do Prof. Dr. João António Baptista Pereira de Oliveira, Professor Associado do Departamento de Química da Universidade de Aveiro, e co-orientação do Prof. Dr. João Manuel da Costa e Araújo Pereira Coutinho, Professor Associado com Agregação do Departamento de Química da Universidade de Aveiro.

Ao meu Pai e ao meu Avô…

o júri

presidente

Prof. Dr. Valdemar Inocêncio Esteves
Professor Auxiliar do Departamento de Química da Universidade de Aveiro

Prof. Dr. João Manuel da Costa e Araújo Pereira Coutinho
Professor Associado com Agregação do Departamento de Química da Universidade de Aveiro

Prof. Dr. João António Baptista Pereira de Oliveira
Professor Associado do Departamento de Química da Universidade de Aveiro

Prof. Dr. Luís Manuel das Neves Belchior Faia dos Santos
Professor Associado da Faculdade de Ciências da Universidade do Porto

agradecimentos

Gostaria de começar por agradecer aos meus orientadores Prof. Dr. João Coutinho e Prof. Dr. João Oliveira pela oportunidade dada e pela confiança depositada em mim. Obrigada por despertarem em mim o bichinho da investigação, já que este era um mundo no qual nunca julguei me vir a apaixonar.

Agradeço também à Profª. Drª. Isabel Marrucho, à Profª. Drª. Ana Fernandes e ao Prof. Dr. Artur Silva pelas sugestões e disponibilidade que sempre demonstraram para a discussão e esclarecimento de dúvidas, não só sobre este trabalho, mas ao longo do meu ainda pequeno percurso na investigação.

À Mara, por tudo o que fez por mim neste percurso: pelo incentivo, pelo apoio, pela dedicação, pela paciência… enfim, por acreditar nas minhas capacidades e não me deixar desistir nem baixar os braços, mesmo quando tudo parecia correr mal.

A todos os membros do grupo Path (indissociável dos minis) que me proporcionaram momentos divertidos enquanto se trabalhava. Deste grupo saliento algumas pessoas: o Pedro, imbatível nas partidas e nas bocas divertidas; à Jorge pela paciência e ajuda ao longo deste trabalho; à Sónia pela herança que me deixou; à Vera pelas horas tardias no laboratório sempre que precisei e acima de tudo pelo companheirismo; à Ana Caço pela boa disposição (mesmo quando parecia menos disposta) sempre mantida no laboratório, e claro, pelo material emprestado.

Aos jantares da comunidade, clube privado e clube ultra mega privado sempre divertidos, sempre cheios de assuntos para debater. Às powerpuff girls pelas parolices, palermices, parvoíces e gulodices partilhadas, por me ouvirem e por nunca deixarem que as minhas inseguranças e incertezas me deixassem andar para trás.

Aos meus amigos de sempre agradeço os convívios, as brincadeiras, os desabafos, as noitadas, por serem meus amigos e por estarem sempre disponíveis para mim, de uma ou outra forma.

À minha mãe que me permitiu chegar até aqui, aturou muitas vezes o meu mau feitio e nunca me deixou desistir. À minha família que me acompanhou e sempre torceu por mim o meu muito obrigada. Sem a força de todos não teria chegado aqui.

Para o Sérgio não encontro palavras para agradecer… és o melhor de mim!

palavras-chave líquidos iónicos, água, solubilidade, QSPR, sistemas aquosos bifásicos.

resumo

O objectivo principal deste trabalho é estudar o equilíbrio de fases de líquidos iónicos em sistemas aquosos bifásicos. Para isso foram estudadas as solubilidades mútuas entre água e líquidos iónicos hidrofóbicos, e foi criado um modelo que descreve esta propriedade. Além disso, foram realizados e estudados sistemas aquosos bifásicos com líquidos iónicos hidrofílicos e o sal inorgânico K_3PO_4.

Os líquidos iónicos são sais compostos por iões grandes que não formam uma rede cristalina bem definida, e assim permanecem líquidos à temperatura ambiente ou perto desta. Estes compostos são solventes interessantes, em reacções orgânicas convencionais do tipo liquido-liquido e em processos de separação, devido às suas propriedades termofísicas, à sua grande capacidade de solvatação e à sua pressão de vapor desprezável. Em particular, o conhecimento de solubilidades mútuas com água é muito importante para a extracção de compostos orgânicos em meios aquosos, uma vez que são necessários líquidos iónicos com baixa solubilidade na água, e para tal o conhecimento das solubilidades mútuas é de elevada importância. Com este propósito, as solubilidades mútuas entre a água e os líquidos iónicos foram determinadas no intervalo de temperatura entre 288,15 K até 318,15 K e à pressão atmosférica. Os líquidos iónicos seleccionados permitiram o estudo da influência da estrutura do catião e do anião. De forma a complementar este estudo foi criado um modelo QSPR de forma a prever as solubilidades mútuas entre a água e os líquidos iónicos a 303,15 K.

Os sistemas aquosos bifásicos com líquidos iónicos podem ser de especial interesse em aplicações de biotecnologia na separação e purificação de biomoléculas vitais. Assim, foi realizado um estudo sistemático envolvendo um grande número de líquidos iónicos baseados no catião imidazólio afim de se obter nova informação acerca da capacidade dos líquidos iónicos promoverem a formação de sistemas aquosos bifásicos e extraírem biomoléculas. Com este propósito, foi avaliada a influência da natureza do anião, bem como a estrutura do catião. Foram determinados diagramas de fase com líquidos iónicos, água e K_3PO_4, assim como as respectivas linhas de equilíbrio. Como complemento, os sistemas aqui estudados foram também caracterizados pelo seu potencial em extrair aminoácidos, para o qual o L-triptofano foi seleccionado como uma biomolécula modelo.

keywords Ionic liquids, water, solubility, QSPR, aqueous biphasic systems.

abstract

The main goal of this work is to study the behavior of ionic liquids in aqueous biphasic systems. For that purpose it was studied the mutual solubilities of water and hydrophobic ionic liquids and created a model to describe that property. In addition, aqueous biphasic systems employing hydrophilic ionic liquids and an inorganic salt, K_3PO_4, were carried and analyzed.

Ionic liquids are salts composed of large ions that cannot easily form an ordered crystal and thus remain liquid at or near room temperature. Their intrinsic thermophysical properties, their high solvating ability and their negligible vapour pressures make them interesting solvents in conventional organic liquid-phase reactions and in separation processes. In particular, the knowledge of their mutual solubilities with water is very important for the extraction of organic products from chemical reactions that proceed in aqueous media and in liquid-liquid extractions from aqueous phases since ionic liquids with low solubility in water are required, and therefore the knowledge of their mutual solubilities with water is highly important. With that aim, the mutual solubilities between water and hydrophobic ionic liquids were determined from temperatures ranging from 288.15 K to 318.15 K and at atmospheric pressure.The selected ILs allowed the study of the cation and anion structure influence. In order to complement this experimental approach, a QSPR model was built to predict mutual solubilities between water and ionic liquids at 303.15 K.

Aqueous biphasic systems containing ionic liquids could be especially interesting in biotechnological applications for the separation and purification of vital biomolecules. Therefore, a systematic study involving a large number of imidazolium-based ILs was conducted to provide new information related to the ionic liquids ABS promoting capability and extraction ability. For that purpose, the influence of the anion nature as well as the cation structure composing the ionic liquids were evaluated. Phase diagrams of the aqueous biphasic systems formed by ionic liquids and K_3PO_4, and the respective tie-lines, were measured. In addition, the aqueous biphasic systems here investigated were also characterized according to their extractive potential of aminoacids, where L-tryptophan was selected as a model biomolecule.

Contents

List of Symbols

x_{IL}	mole fraction solubility of the IL in water
x_{w}	mole fraction solubility of the water in IL
T	temperature
δ	relative deviation
X_{T}	molar fraction of K_3PO_4 on top phase
X_{B}	molar fraction of K_3PO_4 on bottom phase
Y_{T}	molar fraction of IL on top phase
Y_{B}	molar fraction of IL on bottom phase
α'	ratio between the top mass and the total mass
K_{Trp}	partition coefficient of L-tryptophan
α	hydrogen bond acidity
β	hydrogen bond basicity

List of Abbreviations

ABS	Aqueous Biphasic Systems
KF	Karl Fischer
ILs	Ionic Liquids
LFER	Liner Free Energy Relationship
LSER	Linear Solvation Energy Relationship
PEG	Polyethylene glycol
QSAR	Quantitative Structure Activity Relationships
QSPR	Quantitative Structure Properties Relationships
TLs	Tie Lines
TLL	Tie Line Length
VOCs	Volatile Organic Compounds
$[C_3mim][PF_6]$	1-methyl-3-propylimidazolium hexafluorophosphate
$[C_4mim][PF_6]$	1-butyl-3-methylimidazolium hexafluorophosphate
$[C_6mim][PF_6]$	1-hexyl-3-methylimidazolium hexafluorophosphate
$[C_8mim][PF_6]$	1-methyl-3-octylimidazolium hexafluorophosphate
$[C_4C_1mim][PF_6]$	1-butyl-2,3-dimethylimidazolium hexafluorophosphate
$[C_3mpy][PF_6]$	1-methyl-3-propylpyridinium hexafluorophosphate
$[C_1mim][Tf_2N]$	1,3-dimethylimidazolium bis(trifluoromethylsulfonyl)imide
$[C_2mim][Tf_2N]$	1-ethyl-3-methylimidazolium bis(trifluoromethylsulfonyl)imide
$[C_3mim][Tf_2N]$	1-methyl-3-propylimidazolium bis(trifluoromethylsulfonyl)imide
$[C_4mim][Tf_2N]$	1-butyl-3-methylimidazolium bis(trifluoromethylsulfonyl)imide
$[C_5mim][Tf_2N]$	1-methyl-3-pentylimidazolium bis(trifluoromethylsulfonyl)imide
$[C_6mim][Tf_2N]$	1-hexyl-3-methylimidazolium bis(trifluoromethylsulfonyl)imide
$[C_7mim][Tf_2N]$	1-heptyl-3-methylimidazolium bis(trifluoromethylsulfonyl)imide
$[C_8mim][Tf_2N]$	1-methyl-3-octylimidazolium bis(trifluoromethylsulfonyl)imide
$[C_{10}mim][Tf_2N]$	1-decyl-3-methylimidazolium bis(trifluoromethylsulfonyl)imide
$[C_2C_2im][Tf_2N]$	1,3-diethylimidazolium bis(trifluoromethylsulfonyl)imide
$[C_4C_1mim][Tf_2N]$	1-butyl-2,3-dimethylimidazolium bis(trifluoromethylsulfonyl)imide
$[C_4py][Tf_2N]$	butylpyridinium bis(trifluoromethylsulfonyl)imide

$[C_6py][Tf_2N]$	hexylpyridinium bis(trifluoromethylsulfonyl)imide
$[C_8py][Tf_2N]$	octylpyridinium bis(trifluoromethylsulfonyl)imide
$[C_3mpy][Tf_2N]$	1-methyl-3-propylpyridinium bis(trifluoromethylsulfonyl)imide
$[C_4mpy][Tf_2N]$	1-butyl-3-methylpyridinium bis(trifluoromethylsulfonyl)imide
$[4\text{-}C_4mpy][Tf_2N]$	1-butyl-4-methylpyridinium bis(trifluoromethylsulfonyl)imide
$[C_3mpyr][Tf_2N]$	1-methyl-1-propylpyrrolidinium bis(trifluoromethylsulfonyl)imide
$[C_4mpyr][Tf_2N]$	1-butyl-1-methylpyrrolidinium bis(trifluoromethylsulfonyl)imide
$[C_3mpip][Tf_2N]$	1-methyl-1-propylpiperidinium bis(trifluoromethylsulfonyl)imide
[im][Cl]	imidazolium chloride
$[C_1im][Cl]$	methylimidazolium chloride
$[C_2im][Cl]$	ethylimidazolium chloride
$[C_1mim][Cl]$	1,3-dimethylimidazolium chloride
$[C_2mim][Cl]$	1-ethyl-3-methylimidazolium chloride
$[C_4mim][Cl]$	1-butyl-3-methylimidazolium chloride
$[C_6mim][Cl]$	1-hexyl-3-methylimidazolium chloride
[amim][Cl]	1-allyl-3-methylimidazolium chloride
$[OHC_2mim][Cl]$	1-hydroxyethyl-3-methylimidazolium chloride
$[C_7H_7mim][Cl]$	1-benzyl-3-methylimidazolium chloride
$[C_2mim][Br]$	1-ethyl-3-methylimidazolium bromide
$[C_4mim][Br]$	1-butyl-3-methylimidazolium bromide
$[C_2mim][CH_3CO_2]$	1-ethyl-3-methylimidazolium acetate
$[C_4mim][CH_3CO_2]$	1-butyl-3-methylimidazolium acetate
$[C_2mim][CH_3SO_3]$	1-ethyl-3-methylimidazolium methanesulfonate
$[C_4mim][CH_3SO_3]$	1-butyl-3-methylimidazolium methanesulfonate
$[C_2mim][CF_3SO_3]$	1-ethyl-3-methylimidazolium trifluoromethanesulfonate
$[C_4mim][CF_3SO_3]$	1-butyl-3-methyl-imidazolium trifluoromethanesulfonate
$[C_2mim][MeSO_4]$	1-ethyl-3-methylimidazolium methylsulfate
$[C_2mim][EtSO_4]$	1-ethyl-3-methylimidazolium ethylsulfate
$[C_4mim][N(CN)_2]$	1-butyl-3-methylimidazolium dicyanamide
$[C_4mim][HSO_4]$	1-butyl-3-methylimidazolium hydrogenosulfate
$[C_4mim][TFA]$	1-butyl-3-methylimidazolium trifluoroacetate

List of Tables

List of Figures

1

General Introduction

1.1. General Context

Ionic Liquids (ILs) are ionic compounds that belong to the molten salts group, often denominated by RTILs (Room Temperature Ionic Liquids). They are usually formed by large organic cations and organic or inorganic anions, allowing them to remain liquid at or near room temperature and at atmospheric pressure, since they don't have an ordered crystalline structure. Unlike molecular liquids, the ionic nature of these liquids results in a unique combination of properties for most ILs, namely their high thermal stability, large liquidus range, high ionic conductivity, negligible vapor pressure, non-flammability and a high solvating capacity for organic, inorganic and organometallic compounds. Indeed, these properties have determined their high potential to be exploited as "green solvents" in the past several years[1, 2]. In addition, the huge number of possible combinations between cations and anions allows the possibility of tuning ILs, which can be designed for a particular application or to show a specific set of intrinsic properties, thus they are also commonly described as "designer solvents"[3].

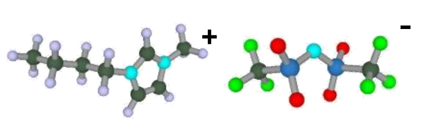

Figure 1. Example of a common IL, 1-butyl-3-methylimidazolium bis(trifluormethylsulfonyl)imide.

Besides the existence of over six hundred of common solvents used nowadays in industry, ILs are an innovative proposal. In the environmental field and with the intent of diminishing the air pollution, ILs show low vapor pressures and can substitute the typical and commonly used volatile organic compounds (VOCs). This is the main reason by which ILs are designated as "green solvents". However, the fact of showing negligible vapor pressure is not enough to assure that these compounds are in fact "green". Properties such as toxicity and biodegrability must be accessed before such assumptions.

In the past years it was believed that ILs did not evaporate, but recently Earle et al.[1] showed that with high temperature and low pressure it is possible to distillate ILs and to separate mixtures composed by different ILs using fractional distillation. Nevertheless, although distillable, this group of researchers[1] concluded that the vapor pressure of the ILs stays negligible at environmental conditions of pressure and temperature.

ILs were first discovered, almost occasionally, in 1914, during the 1st World War, by Paul Walden when testing new explosives for the substitution of nitroglycerin[4]. By the neutralization of ethylamine with concentrated nitric acid it was possible to synthesize what was considered the first RTIL: ethylammonium nitrate with a melting point of 12 ºC[4]. Some years after, ILs appeared again in the 2nd World War, in 1948, and applied in mixtures of aluminum chloride (III) and 1-ethylpyridinium bromide for the electrodeposition of aluminum[5, 6]. Nevertheless, only in the recent past, stable ionic liquids were developed and the research in the ILs field increased exponentially, as it can be seen in Figure 2.

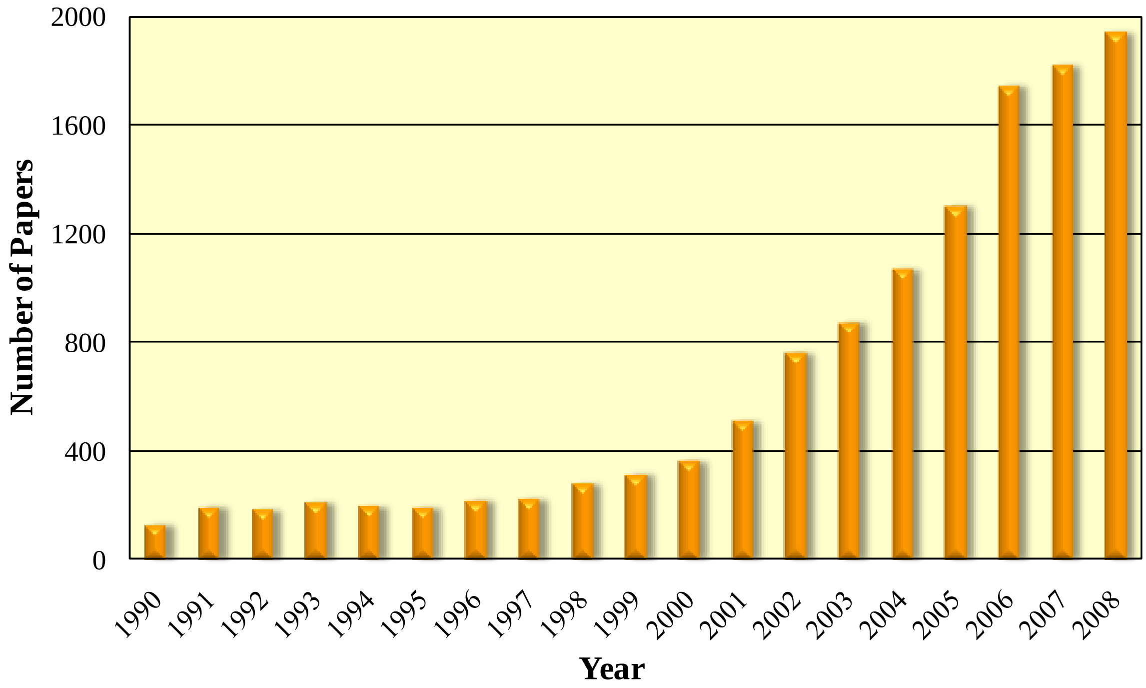

Figure 2. Number of papers published per year concerning ILs. Values taken from IsiWeb of Knowledge in 2nd of May, 2009.

Nowadays ILs show a diverse and huge number of applications such as in organic chemistry for homogeneous catalysis[7], Heck reaction[8, 9] or Suzuki reaction[10]. Besides the organic chemistry, they can also be used as solvents in inorganic synthesis[11], biocatalysis[7] and polymerization[12]. Moreover, ILs have furthermore shown potential for the separation of gases, for example to remove water or CO from natural gas[13], liquids such as substituted-benzene derivatives[14] and in the extraction of small impurities, like in the removing of traces of naphthalene or even ethanol[15]. In addition, ILs can be applied in engineering processes, as heat transfer fluids, azeotrope-breaking liquids and lubricants, as well as new materials such as electrolytes for the electrochemical industry, liquid crystals, supported IL membranes (SILMs), Gas Chromatography (GC) columns, plasticizers, surfactants, antimicrobial and embalming agents, anticorrosion coatings and electropolishing agents[16].

1.2. Scope and Objectives

ILs have a unique combination of intrinsic properties that produces an increasing interest on the research of these fluids as environmentally friendly solvents. Although ILs cannot vaporize leading to air pollution, they show a non negligible miscibility with water that may be the cause of some environmental aquatic risks. It is thus important to know the mutual solubilities between ILs and water before their industrial applications. In this work mutual solubilities with water of hydrophobic, yet hygroscopic, imidazolium and pyridinium based-ILs in combination with the anions bis(trifluoromethylsulfonyl)imide and hexafluorophosphate, were measured. The effect of the ILs structural combinations, as well as the influence of several factors, namely cation side alkyl chain length, the number of cation substitutions, the cation family, structural isomers and the anion identity in these mutual solubilities are analyzed and discussed. QSPR (Quantitative Structure Property Relationship), a correlation method based only on molecular descriptors, was applied to describe the mutual solubilities of water and ILs.

Finally, extractive fermentation using aqueous biphasic systems (ABS) is a promising separation process since it provides a non-denaturing environment for biomolecules and improves the stability of cells. Due to environmental concerns and toxicity issues related with common VOCs, ILs are being currently investigated for extraction purposes. In this work, a wide range of imidazolium-based ILs was studied aiming at obtaining new insights regarding their ability towards the formation of ABS and their capacity towards the extraction of biomolecules. Ternary phase diagrams (and respective tie-lines) formed by these hydrophilic ILs, water and the inorganic salt K_3PO_4, were measured and are reported. In addition, the extraction capacity of the studied ABS was evaluated through their application to the extraction of an essential amino acid, L-tryptophan.

2

ILs + H_2O Binary Systems

2.1. Introduction

The knowledge of ILs and water mutual solubilities is of significant importance in the evaluation of their environmental risk. Although ILs are generally referred to as "green" solvents, studies about their toxicity and biodegradability are still scarce. In fact, while they cannot contribute to air pollution due to their negligible vapor pressures, some of them show a non negligible solubility in water, thus leading to environmental problems. Once in the environment, the IL ecotoxicity can be directly linked to their lipophilicity[17-20]. Since biological membranes can be regarded as non polar interfaces, the ILs toxicity in the aquatic species is driven by the ions ability to disrupt this membrane by an hydrophobic-ionic adsorption phenomenon at the cell-membrane interface[21]. Therefore, hydrophobic ILs tend to accumulate in biological membranes and thus the toxicity will increase with their hydrophobic character. The knowledge of the ILs and water mutual solubilities can provide not only a way to evaluate their dispersion on the ecosystem, but also their effect upon the individual microorganisms.

The quantification of the amount of water in the IL-rich phase is also important as it significantly affects their pure physical properties such as viscosities, densities and surface tensions[22-24]. Water may also act as a co-solvent, for example increasing the mutual solubilities between alcohols and ILs, or as an anti-solvent, reducing the solubility of gases in ILs[25-28]. The presence of water can also affect the rates and selectivity of reactions involving or carried in ILs[29].

Despite the importance in the knowledge of the mutual solubilities between ILs and water, only few publications reporting experimental values are available[26, 30-35] and only one overview of the mutual solubilities between water and imidazolium-based ILs has been published so far[36]. Therefore, in this work, a rigorous and systematic experimental study of the mutual solubilites between ILs and water from (288.15 to 318.15) K, at atmospheric pressure, was conducted for imidazolium and pyridinium-based cations and bis(trifluoromethylsulfonyl)imide and hexafluorophosphate-based anions composing ILs. The main goal of this study is to determine the impact of the ILs structural modifications, such as the cation family, the cation alkyl chain length, the number of substitutions at the cation, and the anion identity influence in their liquid-liquid phase behavior with water.

2.2. Experimental Section

2.2.1. Materials

The mutual solubilities with water were studied for the following ILs: 1-methyl-3-propylimidazolium hexafluorophosphate, [C_3mim][PF_6], 1-butyl-3-methylimidazolium hexafluorophosphate, [C_4mim][PF_6], 1-methyl-3-propylpyridinium hexafluorophosphate, [C_3mpy][PF_6], 1,3-dimethylimidazolium bis(trifluoromethylsulfonyl)imide, [C_1mim][Tf_2N], 1,3-diethylimidazolium bis(trifluoromethylsulfonyl)imide, [C_2C_2im][Tf_2N], and 1-butyl-2,3-dimethylimidazolium bis(trifluoromethylsulfonyl)imide, [C_4C_1mim][Tf_2N]. The ILs molecular structures are shown in Figure 3.

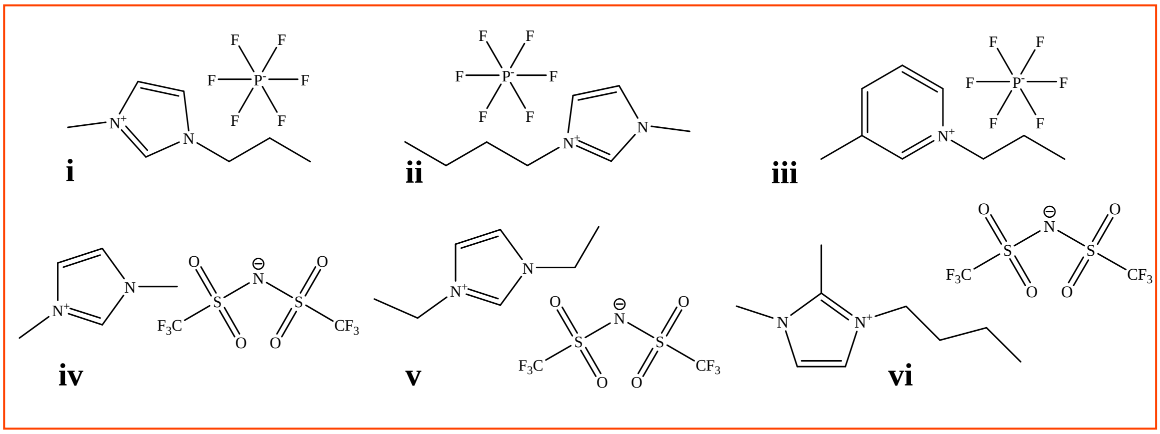

Figure 3. Chemical structure of the ILs studied: (i) [C_3mim][PF_6]; (ii) [C_3mim][PF_6]; (iii) [C_3mpy][PF_6]; (iv) [C_1mim][Tf_2N]; (v) [C_2C_2im][Tf_2N]; (vi) [C_4C_1mim][Tf_2N].

All ILs were acquired at IoLiTec with the exception of [C_1mim][Tf_2N] that was synthesized in our lab (*cf.* Appendix A), and all had mass fraction purities > 99 %. To reduce the water and volatile compounds content to negligible values, ILs individual samples were dried under constant stirring at vacuum (0.1 Pa) and moderate temperature (*circa* 350 K), for a minimum of 48 h. After this procedure, the purity of each ionic liquid was further checked by ^{1}H, ^{13}C and ^{19}F NMR (*cf.* Appendix A).

The water used was double distilled, passed by a reverse osmosis system and further treated with a MilliQ plus 185 water purification apparatus. It had a resistivity of 18.2 MΩ·cm, a TOC lower than 5 μg·L^{-1} and it was free of particles greater than 0.22 μm. The analyte used for the coulometric Karl-Fischer titration was Hydranal® - Coulomat AG from Riedel-de Haën.

2.2.2. Experimental Procedure.

The measurements of mutual solubilities between water and ILs were carried out at temperatures from (288.15 to 318.15) K and at atmospheric pressure. In the case of the water solubility in [C_3mpy][PF_6] the temperature range was from (303.15 to 318.15) K due to the high melting point of this IL. The IL and the water phases were initially vigorously agitated and allowed to reach the saturation equilibrium by the separation of both phases in 22 mL glass vials for at least 48 h. This period proved to be the minimum time required to guarantee a complete separation of the two phases, once the measurements made later did not revealed a significant variation from the ones measured with 48 h, and that no further variations in mole fraction solubilities occurred.

The temperature was maintained by keeping the glass vials containing the phases in equilibrium, inside an aluminum block specially designed for the purpose, which was then placed in an isolated air bath capable of maintaining the temperature within ± 0.01 K. The temperature control was achieved with a PID temperature controller driven by a calibrated Pt100 (class 1/10) temperature sensor inserted in the aluminum block. In order to reach temperatures below room temperature, a Julabo circulator, model F25-HD, was coupled to the overall oven system allowing the passage of a thermostatized fluid flux around the aluminum block.

Figure 4. Karl Fischer coulometric titrator.

The solubility of water in the IL-rich phase was determined using a Metrohm 831 Karl-Fischer (KF) coulometer (Figure 4) and the solubility of ILs in the water-rich phase was determined by UV-spectroscopy using a SHIMADZU UV-1700 Pharma-Spec Spectrometer (Figure 5), at a wavelength of 211 nm, using calibration curves previously established (*cf.* Appendix A). These wavelengths were found to be the maximum UV absorption lengths for the imidazolium-based cations studied. Both rich-phases were sampled at each temperature from the equilibrium vials using glass syringes, maintained dry and at the same temperature of the

Figure 5. UV Spectrometer.

measurements. For the IL-rich phase, samples of ≈ (0.1 to 0.2) g were taken and directly injected in the KF coulometric titrator while for the water-rich phase, samples of ≈ (0.3 to 1.0) g were taken and diluted by a factor ranging from (1:50 to 1:1000) (v:v) in ultra pure water, depending on the solubility of the IL under study. The high precision and accuracy of this method can be linked not only to the gravimetric procedure but also to the dilutions of the samples of the water-rich phase, avoiding phase split when working at temperatures different from room temperature. The mutual solubilities results at each individual temperature are an average of at least five independent measurements.

2.3. Results and Discussion

2.3.1. Mutual Solubilities Results.

The experimental solubility results here measured are compared with the available literature data[30, 32, 34, 37-40] in Figure 6.

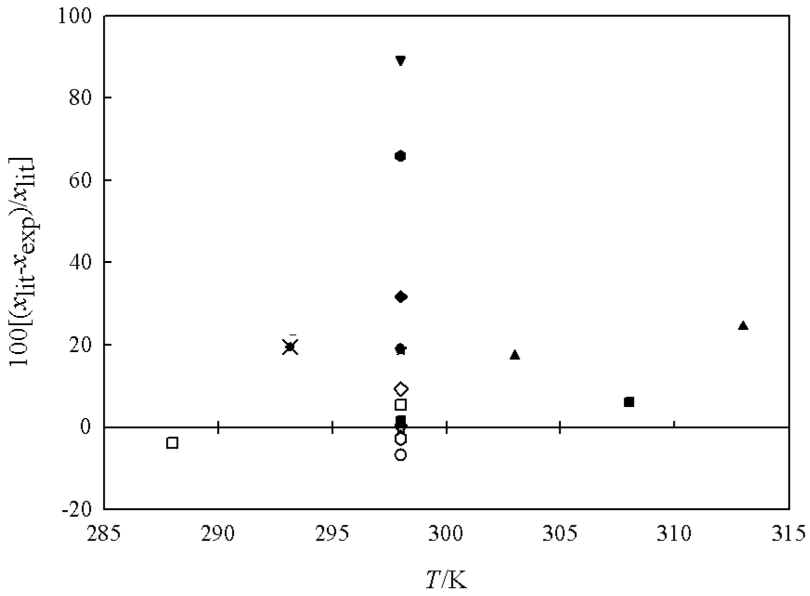

Figure 6. Relative deviations between the experimental mole fraction solubility of water in ILs (empty symbols) and ILs in water (full symbols) obtained in this work (x_{exp}) and those reported in the literature (x_{lit}) as a function of temperature: ◊, [C_8mim][PF_6], Fadeev et al.[38]; ▽, [C_4mim][PF_6], McFarlane et al.[32]; ✫ ,[C_4mim][PF_6], Anthony et al.[30]; ○, [C_8mim][PF_6], Anthony et al.[30]; △, [C_4mim][PF_6], Wong et al.[34]; □, [C_4mim][PF_6], Najdanovic-Visak et al.[39]; -, [C_4mim][PF_6], Alfassi et al.[37]; +, [C_4mim][PF_6], Shvedene et al.[40]; ×, [C_4C_1mim][PF_6], Shvedene et al.[40].

There are large differences among different authors, especially in the water-rich side, which can be directly related to the accuracy in the measurements of very low solubilities. In the IL-rich side, smaller relative deviations exist between different authors, which can be linked to the larger solubilities in this phase.

The experimental solubility data measured, and the respective expanded uncertainty with 95 % level of confidence, are shown in Table 1 and 2.

Table 1. Experimental mole fraction solubility of water in ILs and respective expanded uncertainty with 95 % level of confidence, x_w, as a function of temperature.

IL	$[C_3mim][PF_6]$	$[C_4mim][PF_6]$	$[C_3mpy][PF_6]$	$[C_3mpy][Tf_2N]$[41]	$[C_1mim][Tf_2N]$	$[C_2mim][Tf_2N]$[35]
T / K	x_w	x_w	x_w	x_w	x_w	x_w
288.15	0.2437 ± 0.0040	0.1964 ± 0.0033	---	0.2059 ± 0.0029	0.2984 ± 0.0048	0.2755 ± 0.0013
293.15	0.2709 ± 0.0024	0.2094 ± 0.0007	---	0.2259 ± 0.0091	0.3209 ± 0.0047	0.2869 ± 0.0020
298.15	0.2925 ± 0.0022	0.2289 ± 0.0032	---	0.2362 ± 0.0088	0.3399 ± 0.0096	0.2982 ± 0.0023
303.15	0.3168 ± 0.0063	0.2497 ± 0.0052	0.2949 ± 0.0050	0.2566 ± 0.0094	0.3616 ± 0.0027	0.3119 ± 0.0018
308.15	0.3461 ± 0.0007	0.2670 ± 0.0048	0.3248 ± 0.0021	0.2697 ± 0.0063	0.3799 ± 0.0014	0.3280 ± 0.0009
313.15	0.3769 ± 0.0071	0.2881 ± 0.0051	0.3516 ± 0.0087	0.2918 ± 0.0023	0.4080 ± 0.0143	0.3446 ± 0.0004
318.15	0.4050 ± 0.0041	0.3033 ± 0.0045	0.3772 ± 0.0062	0.3102 ± 0.0127	0.4346 ± 0.0164	0.3603 ± 0.0012
IL	$[C_3mim][Tf_2N]$[35]	$[C_4mim][Tf_2N]$[35]	$[C_5mim][Tf_2N]$[35]	$[C_2C_2im][Tf_2N]$	$[C_4C_1mim][Tf_2N]$	
T / K	x_w	x_w	x_w	x_w	x_w	
288.15	0.2502 ± 0.0011	0.2307 ± 0.0008	0.2052 ± 0.0011	0.2413 ± 0.0106	0.1682 ± 0.0034	
293.15	0.2581 ± 0.0009	0.2443 ± 0.0015	0.2127 ± 0.0011	0.2615 ± 0.0028	0.1826 ± 0.0043	
298.15	0.2715 ± 0.0016	0.2568 ± 0.0014	0.2211 ± 0.0013	0.2772 ± 0.0011	0.1912 ± 0.0036	
303.15	0.2861 ± 0.0024	0.2715 ± 0.0017	0.2324 ± 0.0010	0.2942 ± 0.0020	0.2120 ± 0.0009	
308.15	0.3013 ± 0.0018	0.2853 ± 0.0017	0.2449 ± 0.00033	0.3054 ± 0.0060	0.2289 ± 0.0035	
313.15	0.3172 ± 0.0012	0.2989 ± 0.0009	0.2570 ± 0.0022	0.3296 ± 0.0069	0.2439 ± 0.0059	
318.15	0.3324 ± 0.0018	0.3136 ± 0.0023	0.2669 ± 0.0019	0.3507 ± 0.0026	0.2632 ± 0.0014	

Table 2. Experimental mole fraction solubility of water in ILs and respective expanded uncertainty with 95 % level of confidence, x_{IL}, as a function of temperature.

IL	$[C_4mim][PF_6]$	$[C_1mim][Tf_2N]$	$[C_2mim][Tf_2N]$[35]	$[C_3mim][Tf_2N]$[35]
T / K	$10^3\ x_{IL}$	$10^3\ x_{IL}$	$10^4\ x_{IL}$	$10^4\ x_{IL}$
288.15	1.010 ± 0.007	1.218 ± 0.021	7.657 ± 0.091	5.147 ± 0.418
293.15	1.110 ± 0.002	1.281 ± 0.009	8.025 ± 0.192	5.270 ± 0.013
298.15	1.210 ± 0.001	1.343 ± 0.011	8.380 ± 0.133	5.399 ± 0.008
303.15	1.286 ± 0.001	1.452 ± 0.007	8.750 ± 0.022	5.682 ± 0.004
308.15	1.430 ± 0.004	1.516 ± 0.020	9.325 ± 0.189	6.042 ± 0.085
313.15	1.581 ± 0.002	1.612 ± 0.017	9.848 ± 0.056	6.493 ± 0.042
318.15	1.759 ± 0.002	1.829 ± 0.062	10.535 ± 0.045	7.010 ± 0.066
IL	$[C_4mim][Tf_2N]$[35]	$[C_5mim][Tf_2N]$[35]	$[C_2C_2im][Tf_2N]$	$[C_4C_1mim][Tf_2N]$
T / K	$10^4\ x_{IL}$	$10^4\ x_{IL}$	$10^4\ x_{IL}$	$10^4\ x_{IL}$
288.15	2.861 ± 0.010	1.843 ± 0.056	5.052 ± 0.109	2.036 ± 0.061
293.15	2.916 ± 0.037	1.883 ± 0.219	5.128 ± 0.079	2.025 ± 0.092
298.15	3.067 ± 0.012	1.956 ± 0.018	5.177 ± 0.018	2.101 ± 0.038
303.15	3.179 ± 0.018	2.011 ± 0.011	5.600 ± 0.093	2.181 ± 0.089
308.15	3.439 ± 0.042	2.183 ±0.029	5.930 ± 0.132	2.376 ± 0.018
313.15	3.944 ± 0.014	2.318 ± 0.059	6.279 ± 0.154	2.467 ± 0.086
318.15	4.702 ± 0.029	2.534 ± 0.015	6.802 ± 0.210	2.705 ± 0.035

In general terms, it can be observed that, for all the studied ILs, the miscibility of both phases increases with temperature. Note that all the studied ILs are known as "hydrophobic", but the water solubility results indicate that they are substantially "hygroscopic". The mole fraction solubility of ILs in water ranges from 10^{-3} to 10^{-4} and the water in ILs is in the order of 10^{-1}. Thus, while the water-rich phase can be considered almost as a pure phase with the dissolved IL at infinite dilution, the IL-rich phase cannot be considered as a near pure IL phase. The results obtained for all the studied ILs show a large difference in the mole fraction solubilities of water in ILs, ranging from 0.168 for the $[C_4C_1mim][Tf_2N]$ to 0.485 for $[C_1mim][Tf_2N]$. Comparing the anions it is possible to establish that their hydrophobicity increases from $[PF_6]^-$ to $[Tf_2N]^-$ both in the IL and water rich-phases, as shown in Figure 7.

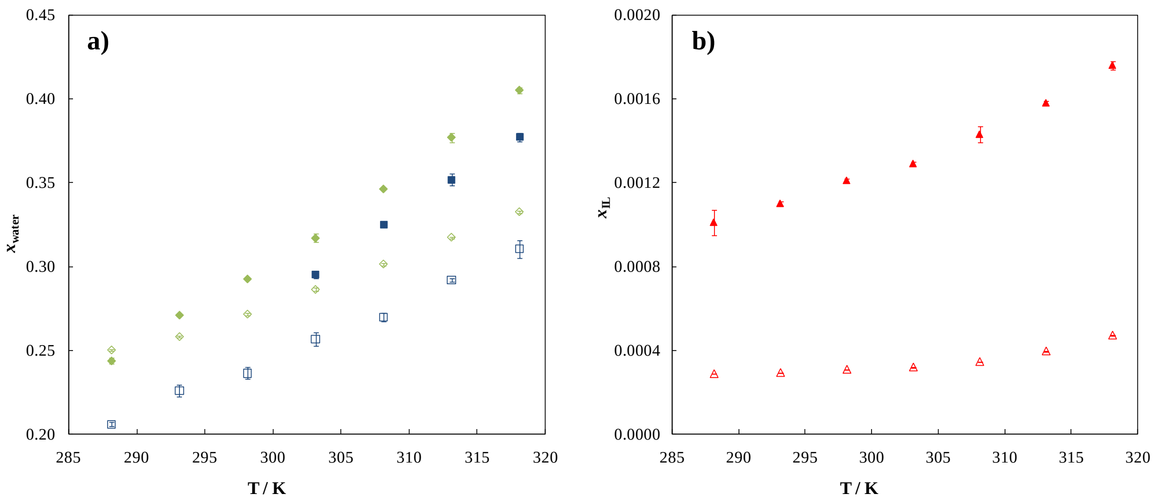

Figure 7. Anion influence in the water, a), and ILs, b), mutual solubilities: ♦, $[C_3mim][PF_6]$; ■, $[C_3mpy][PF_6]$; ◊, $[C_3mim][Tf_2N]$[35]; □, $[C_3mpy][Tf_2N]$[41]; ▲, $[C_4mim][PF_6]$; △, $[C_4mim][Tf_2N]$[35].

Figure 8 shows the results for the cation family influence in the solubility of water in ILs.

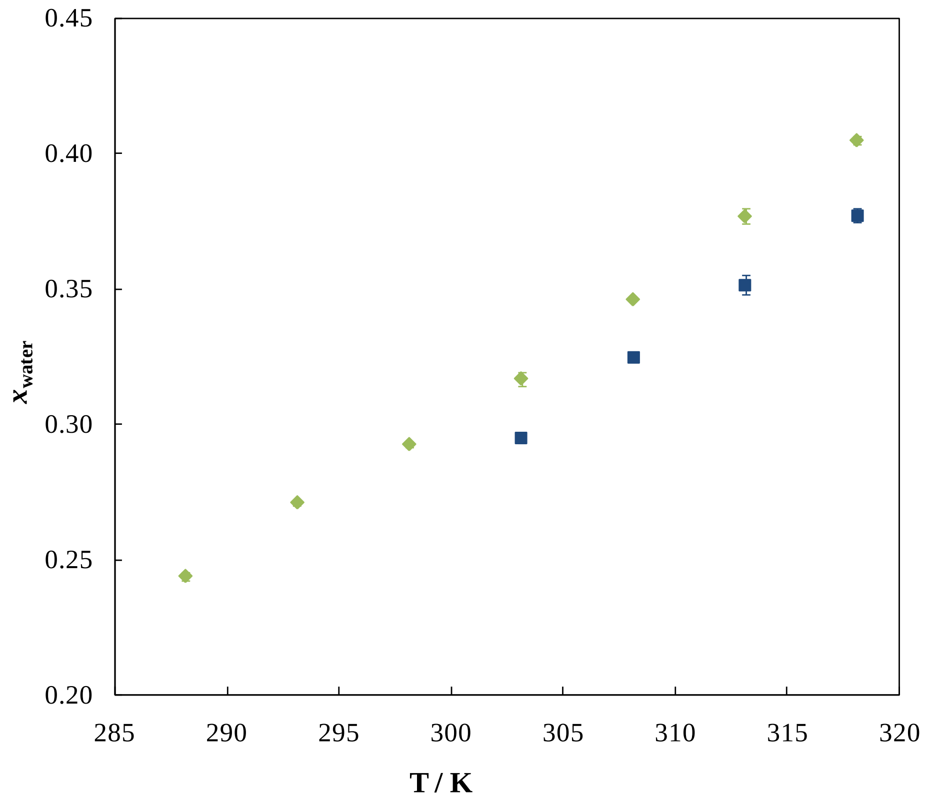

Figure 8. Influence of the cation family for the water solubility in ILs: ♦, $[C_3mim][PF_6]$; ■, $[C_3mpy][PF_6]$.

From the analysis of Figure 8, it is clear that the solubility of water in ILs increases from pyridinium to imidazolium-based ILs. When comparing with literature data[41], the cations imidazolium and pyridinium have an aromatic character so that their solubility of water and vice-versa are higher when compared to the pyrrolidinium and piperidinium-based ILs, once they have the possibility of interacting OH···π or O···π with water[41].

The influence of the alkyl side chain length at the cation is shown in Figure 9.

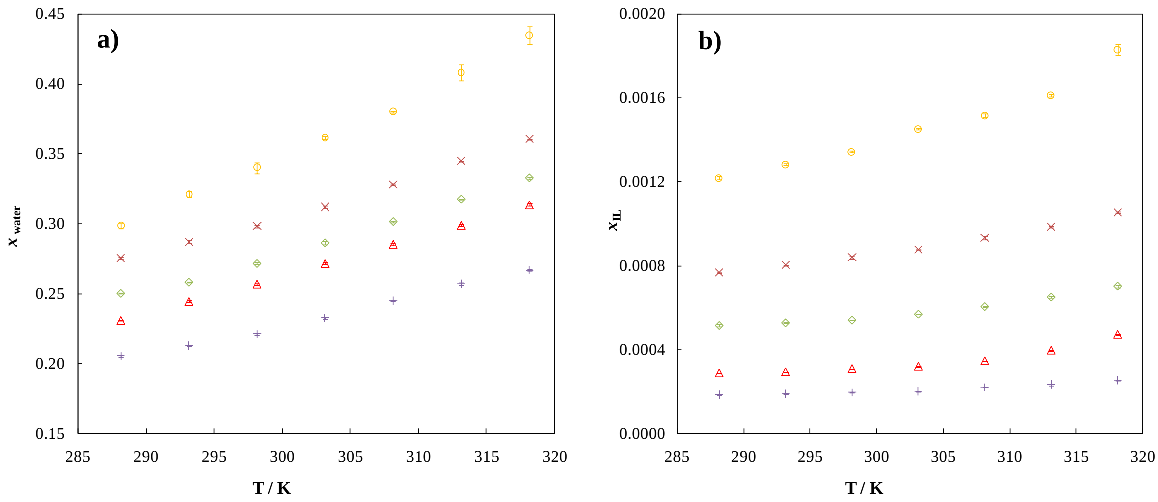

Figure 9. Cation alkyl chain length influence in the water, a), and ILs, b), mutual solubilities: ○, $[C_1mim][Tf_2N]$; ×, $[C_2mim][Tf_2N]$[35]; ◊, $[C_3mim][Tf_2N]$[35]; △, $[C_4mim][Tf_2N]$[35]; +, $[C_5mim][Tf_2N]$[35].

When analyzing Figure 9, increasing the IL alkyl chain length it decreases the solubility of water in ILs and vice-versa. Indeed, these results are consistent with the experimental data previously reported[35, 41].

The difference in the mutual solubilities between water and different ILs isomers ($[C_2C_2im][Tf_2N]$, $[C_3mim][Tf_2N]$, $[C_4C_1mim][Tf_2N]$ and $[C_5mim][Tf_2N]$) is shown in Figure 10.

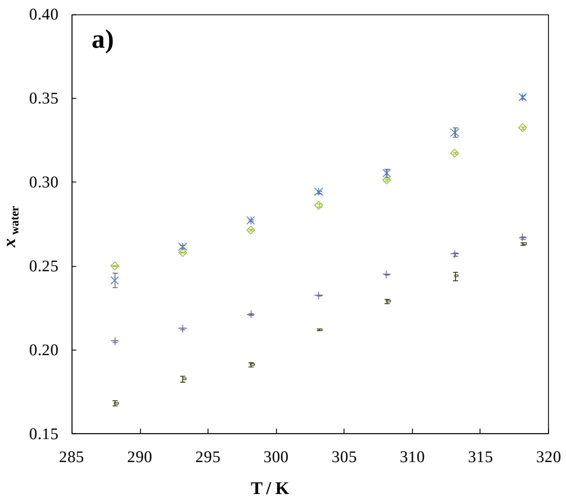

Figure 10. Isomers influence in the water, a), and ILs, b), mutual solubilities: ✳, $[C_2C_2mim][Tf_2N]$; ◇, $[C_3mim][Tf_2N]$[35]; +, $[C_5mim][Tf_2N]$[35]; –, $[C_4C_1mim][Tf_2N]$.

By the inspection of the previous figure, the tendency of the solubility of water in ILs follows the trend $[C_2C_2im]$ > $[C_3mim]$ > $[C_5mim][Tf_2N]$ > $[C_4C_1mim]$. On the other hand, the solubility of ILs in water show the tendency $[C_3mim]$ > $[C_2C_2im]$ > $[C_4C_1mim]$ > $[C_5mim][Tf_2N]$. This trend leads to the conclusion that the substitution of the most acidic hydrogen in the imidazolium ring by a methyl group decreases the water solubility in IL and increases the solubility of the IL in water. On the other hand, keeping the number of substitutions at the cation, $[C_2C_2im][Tf_2N]$ and $[C_3mim][Tf_2N]$, the increase of one of the alkyl chains decreases the solubility of water in IL.

2.3.2. Temperature Dependence of Water in ILs Solubility.

The equation that follows (Eq. 1) proved to accurately correlate the experimental solubility data of water in ILs,

$$\ln x_w = A_1 + \frac{B_1}{T} \tag{1}$$

where x_w is the mole fraction solubility of the water in IL, T is the temperature in K and A_1 and B_1 are fitting parameters that are shown in Table 3. The proposed correlation shows a relative maximum average deviation from experimental mole fraction data (δ) of 3 %. In Figure 11 is shown the fitting of Eq.1 to the experimental data.

Table 3. Fitting parameters for the mole fraction solubility of water in ILs, as a function of temperature, using Eq. 1.

IL	A_1	B_1 / K	Adj $R^{2(a)}$	δ / (%)
$[C_3mim][PF_6]$	3.94	-1541	0.9988	1.01
$[C_4mim][PF_6]$	2.92	-1261	0.9967	1.94
$[C_3mpy][PF_6]$	3.99	-1579	0.9947	0.66
$[C_3mpy][Tf_2N]$[41]	2.68	-1227	0.9950	1.49
$[C_1mim][Tf_2N]$	2.54	-1040	0.9975	1.23
$[C_2mim][Tf_2N]$[35]	1.57	-827	0.9939	0.91
$[C_3mim][Tf_2N]$[35]	1.71	-896	0.9929	1.40
$[C_4mim][Tf_2N]$[35]	1.72	-936	0.9998	0.25
$[C_5mim][Tf_2N]$[35]	1.29	-831	0.9930	1.11
$[C_2C_2im][Tf_2N]$	2.41	-1101	0.9935	1.88
$[C_4C_1mim][Tf_2N]$	2.99	-1376	0.9939	2.53

[(a)]Adjusted R^2

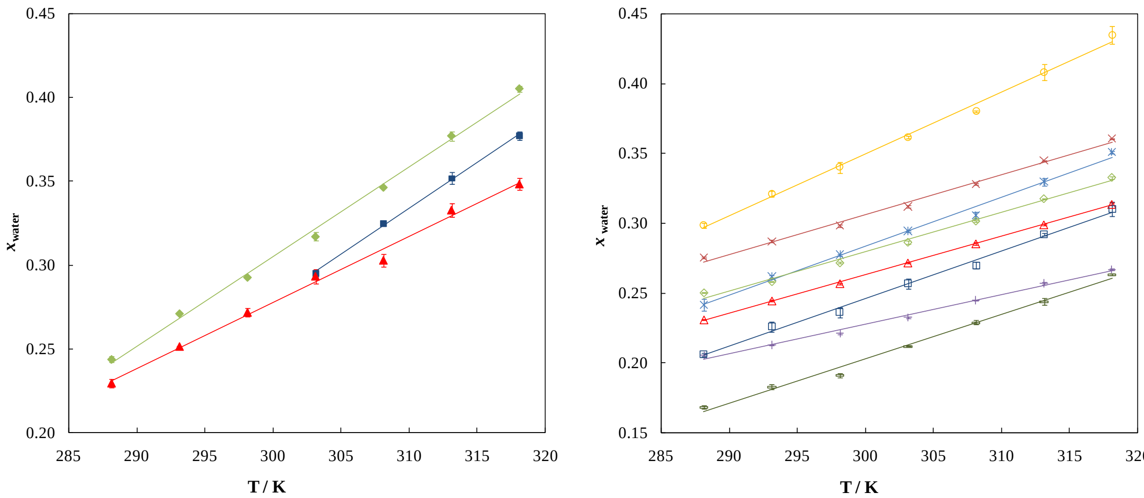

Figure 11. Experimental solubility values adjusted with Eq. 1: ♦, $[C_3mim][PF_6]$; ■, $[C_3mpy][PF_6]$; ▲, $[C_4mim][PF_6]$; ○, $[C_1mim][Tf_2N]$; ×, $[C_2mim][Tf_2N]$[35]; ✳, $[C_2C_2mim][Tf_2N]$; ◇, $[C_3mim][Tf_2N]$[35]; △, $[C_4mim][Tf_2N]$[35]; □, $[C_3mpy][Tf_2N]$[41]; +, $[C_5mim][Tf_2N]$[35]; –, $[C_4C_1mim][Tf_2N]$.

2.3.3. Temperature Dependence of ILs in Water Solubility.

The model for experimental solubility of ILs in water data was carried out using Eq. 2 that showed to be capable of describing the temperature dependence of the solubility of organics in water,

$$\ln x_{\mathrm{IL}} = C_1 + \frac{D_1}{T} + E_1 \ln T \qquad (2)$$

where x_{IL} is the mole fraction solubility of the IL in water, T is the absolute temperature in K and C_1, D_1 and E_1 are fitting parameters that are shown in Table 4. The proposed correlations showed a relative maximum deviation from experimental mole fraction data (δ) of 2 %. In Figure 12 it is shown the fitting of Eq. 2 to the experimental data.

Table 4. Fitting parameters for the mole fraction solubility of ILs in water as a function of temperature, using Eq. 2.

IL	C_1	D_1 / K	E_1	Adj $R^{2(a)}$	δ / (%)
[C_4mim][PF_6]	-198	7208	29	0.9976	1.38
[C_1mim][Tf_2N]	-272	10988	40	0.9836	2.50
[C_2mim][Tf_2N][35]	-166	6365	24	0.9986	0.54
[C_3mim][Tf_2N][35]	-351	14700	52	0.9989	0.51
[C_4mim][Tf_2N][35]	-873	37782	130	0.9870	2.91
[C_5mim][Tf_2N][35]	-375	15725	55	0.9943	1.27
[C_2C_2im][Tf_2N]	-355	14858	52	0.9857	2.16
[C_4C_1mim][Tf_2N]	-393	16583	58	0.9837	2.14

[(a)]Adjusted R^2

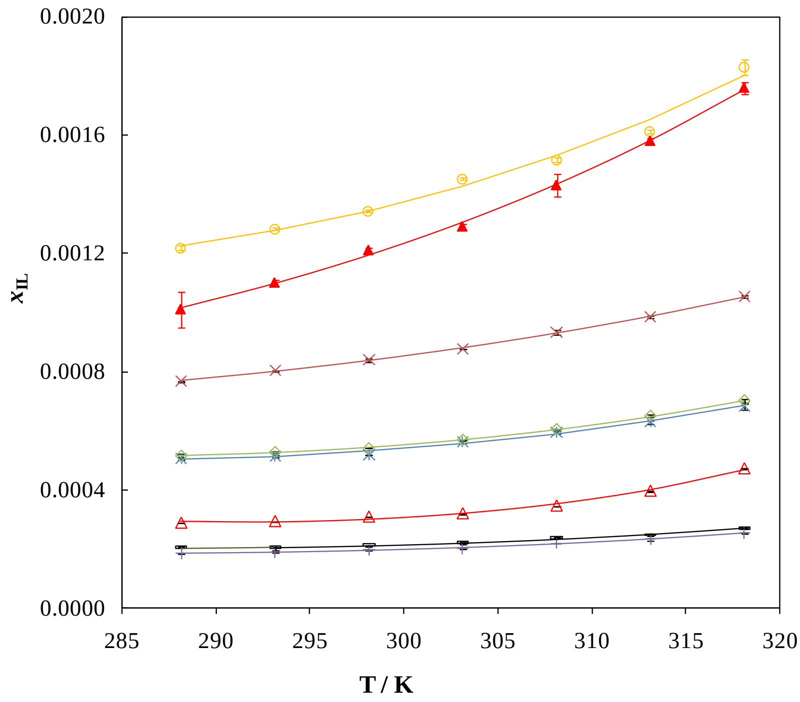

Figure 12. Experimental solubility values adjusted with Eq. 2: ○, [C_1mim][Tf_2N]; ▲, [C_4mim][PF_6]; ×, [C_2mim][Tf_2N][35]; ◊, [C_3mim][Tf_2N][35]; ✳, [C_2C_2mim][Tf_2N]; △, [C_4mim][Tf_2N][35]; –, [C_4C_1mim][Tf_2N]; +, [C_5mim][Tf_2N][35].

2.4. Conclusions

New data for mutual solubilities between water and hydrophobic imidazolium and pyridinium-based cations in combination with bis(trifluoromethylsulfonyl)imide and hexafluorophosphate-based anions in the temperature range between (288.15 and 318.15) K, and at atmospheric pressure, were determined. The hydrophobic tendency of the cation family increases from imidazolium to pyridinium-based ILs and with the alkyl chain length increase within the same cation family. Furthermore, the inclusion of a third methyl group replacing the most acidic hydrogen at the imidazolium cation showed to have different impacts in both rich-phases, which was addressed by the relative influence of the hydrogen-bonding capacity in both phases. The anion hydrophobic tendency increases from hexafluorophosphate to bis(trifluoromethylsulfonyl)imide-based ILs. Moreover, the discussed amphiphilic character of the studied salts can be used to fine tune the ILs mutual solubilities with water and to control their ecotoxicity impact.

3

QSPR Modelling of ILs + H_2O Binary Systems

3.1. Introduction

Quantitative Structure-Activity Relationships (QSAR) and Quantitative Structure-Property Relationships (QSPR) are methods for the direct prediction of compound's properties based on its molecular structure. These models correlate experimental data with specific parameters, named molecular descriptors, derived from the compound's 3D structure. Using these models it is possible to predict properties of new and hypothetical molecules, not yet synthesised. QSAR/QSPR models are especially apt to the development of new drugs, conception of new molecules, molecular modelling and resolution of new problems related with chemical engineering. QSAR deals mainly with biological/chemical activity while QSPR with physical and chemical properties.

In 1868 the first publication on the quantitative relation of physiological properties with the chemical structure appeared[42]. In the 20th century, during the 60's, there was an important progress in this field with the development of a linear free energy relationship (LFER). These studies, along with the development of computers, allowed the appearance of new and more complex descriptors[43].

These models can be used as predictive instruments for the estimation of physical-chemical properties, identifying the most favourable compounds, thus orienting the synthesis and reducing the number of compounds to be synthesized. They can also be used as diagnostic instruments, giving the possible information about types of interaction forces, in the receptor nature, in the mechanism of action and in detection of exceptions that may occur. These models show however some limitations, since they are not accurate to describe some specific interactions between molecules, such as hydrogen bonding[43].

For QSPR studies a quantitative description of the molecular structure is required, that is obtained by parameters and descriptors. A parameter describes a molecular property and is obtained from a regression model using an estimator, while a descriptor is known as a term, index or a parameter that transmits structural information.

There have been studies of biological and physical-chemical properties such as solubility of aqueous solutions, vapour pressure, partioning coefficients, among others, by this approach[44-50]. Recently, QSPR studies have been used in correlations and prediction of various properties of ILs such as melting points of quaternary ammonium, imidazolium and pyridinium-based ILs[51], conductivities and viscosities[52].

The main goal of this work is, using the data gathered at Path's laboratories and found in literature, to create a model to describe mutual solubilities of some ILs and water.

3.2. Experimental database

The mutual solubilities between water and 26 different ILs were studied: several found in literature (1-hexyl-3-methylimidazolium hexafluorophosphate, $[C_6mim][PF_6]$, 1-methyl-3-octylimidazolium hexafluorophosphate, $[C_8mim][PF_6]$, 1-butyl-2,3-dimethylimidazolium hexafluorophosphate, $[C_4C_1mim][PF_6]$, 1-ethyl-3-methylimidazolium bis(trifluoromethylsulfonyl)imide, $[C_2mim][Tf_2N]$, 1-methyl-3-propylimidazolium bis(trifluoromethylsulfonyl)imide, $[C_3mim][Tf_2N]$, 1-butyl-3-methylimidazolium bis(trifluoromethylsulfonyl)imide, $[C_4mim][Tf_2N]$, 1-methyl-3-pentylimidazolium bis(trifluoromethylsulfonyl)imide, $[C_5mim][Tf_2N]$, 1-hexyl-3-methylimidazolium bis(trifluoromethylsulfonyl)imide, $[C_6mim][Tf_2N]$, 1-heptyl-3-methylimidazolium bis(trifluoromethylsulfonyl)imide, $[C_7mim][Tf_2N]$, 1-methyl-3-octylimidazolium bis(trifluoromethylsulfonyl)imide, $[C_8mim][Tf_2N]$, 1-methyl-3-propylpyridinium bis(trifluoromethylsulfonyl)imide, $[C_3mpy][Tf_2N]$, 1-methyl-1-propylpyrrolidinium bis(trifluoromethylsulfonyl)imide, $[C_3mpyr][Tf_2N]$, 1-butyl-1-methylpyrrolidinium bis(trifluoromethylsulfonyl)imide $[C_4mpyr][Tf_2N]$ and 1-methyl-1-propylpiperidinium bis(trifluoromethylsulfonyl)imide, $[C_3mpip][Tf_2N]$)[35, 36, 41], others reported in this thesis in Chapter 2 (1-methyl-3-propylimidazolium hexafluorophosphate, $[C_3mim][PF_6]$, 1-butyl-3-methylimidazolium hexafluorophosphate, $[C_4mim][PF_6]$, 1-methyl-3-propylpyridinium hexafluorophosphate, $[C_3mpy][PF_6]$, 1,3-dimethylimidazolium bis(trifluoromethylsulfonyl)imide, $[C_1mim][Tf_2N]$, 1,3-diethylimidazolium bis(trifluoromethylsulfonyl)imide $[C_2C_2im][Tf_2N]$, 1-butyl-2,3-dimethylimidazolium bis(trifluoromethylsulfonyl)imide, $[C_4C_1mim][Tf_2N]$) and some data not yet reported (1-decyl-3-methylimidazolium bis(trifluoromethylsulfonyl)imide, $[C_{10}mim][Tf_2N]$, 1-butyl-3-methylpyridinium bis(trifluoromethylsulfonyl)imide, $[C_4mpy][Tf_2N]$, 1-butyl-4-methylpyridinium bis(trifluoromethylsulfonyl)imide, $[4\text{-}C_4mpy][Tf_2N]$, butylpyridinium bis(trifluoromethylsulfonyl)imide, $[C_4py][Tf_2N]$, hexylpyridinium bis(trifluoromethylsulfonyl)imide, $[C_6py][Tf_2N]$, octylpyridinium bis(trifluoromethylsulfonyl)imide, $[C_8py][Tf_2N]$).

3.3. Methodology

The structures of each cation and anion of the ILs were drawn using ChemDraw Ultra 9.0-2004. After that, the file was transformed in a Mol2 file, so that it could be used in Dragon®, version 5.3 - 2005, to calculate de molecular descriptors for each individual ion.
In order to correlate the property with descriptors, a equation type

$$ln\ x = a + b\ \Delta_1 + c\ \Delta_2 + d\ \Delta_3 \quad (3)$$

where x is the molar fraction of water in IL or IL in water; a, b, c and d are coefficients and Δ_1 is the cavity term, Δ_2 is a polarizability descriptor and Δ_3 is the descriptor related with hydrogen bonding, was used based on LSER (Linear Solvation Energy Relationship). Among the 1664 descriptors calculated by Dragon® were chosen the most similar to the ones above. This narrows the possibility to 30 descriptors. All of these 30 descriptors were correlated with the property x, and the most correlated ones were chosen. All the others that were correlated with those were excluded. Then, a model was made only with one descriptor at the time, and afterwards the model was improved by the addition of new descriptors. This improved model was tested and if the prediction improved the added descriptor was retained, if not it was excluded. Models were fitted for mutual solubilities at 303 K.

3.4. Results and Discussion

For the cations, the followed models were tested for a common anion ($[TF_2N]$).

$$ln\ x = a + b\ \mathrm{Sp} \quad (4)$$

$$ln\ x = a + b\ \mathrm{Sv} \quad (5)$$

$$ln\ x = a + b\ \mathrm{Sp} + c\ \mathrm{Sv} \quad (6)$$

where Sp is the sum of atomic polarizabilities and Sv is the sum of atomic van der Waals volumes, both scaled on Carbon atom, both belonging to constitutional descriptors.
Once the model was fitted for the cations, a descriptor to take into account the contribution of the anion was introduced into the model. The descriptor chosen was Jhetp (Balaban-type index from polarizability weighted distance matrix, topological descriptors).
The final relationship described in Eq. 7 was used in all calculations.

$$\ln x = m_0 + m_1 \times \mathrm{Sp\ (cation)} + m_2 \times \mathrm{Sv\ (cation)} + m_3 \times \mathrm{Jhept\ (anion)} \quad (7)$$

Table 5 shows the descriptors used in this model and the experimental data and predicted values from the studied model for mutual solubilities of water and ILs and respective relative deviation (δ).

The 26 ILs were divided into 2 sets: 17 in a training set and 9 in a test set, chosen randomly.

Table 5. Used descriptors, experimental data and predicted values for mutual solubilities of water and ILs

	IL		Descriptors			Experimental	Predicted	δ / %	Experimental	Predicted	δ / %
	Cation	Anion	Sp	Sv	Jhetp	Data (ln x_w)	Value (ln x_w)		Data (ln x_{IL})	Value (ln x_{IL})	
Training Set	[C_4mim]	[PF_6]	14.96	13.87	2.908	-1.228	-1.228	0.0	-6.656	-6.496	2.4
	[C_6mim][35]		18.48	17.07		-1.386	-1.376	0.8	-7.667	-7.660	0.1
	[C_8mim][35]		22.01	20.26		-1.528	-1.528	0.0	-8.835	-8.835	0.0
	[C_3mpy]		14.95	13.88		-1.221	-1.224	0.2	-6.220	-6.486	4.3
	[C_1mim]	[Tf_2N]	9.68	9.08	3.932	-1.017	-1.080	6.1	-6.535	-6.324	3.2
	[C_3mim][35]		13.20	12.28		-1.251	-1.228	1.9	-7.473	-7.488	0.2
	[C_4mim][35]		14.96	13.87		-1.304	-1.304	0.0	-8.054	-8.074	0.2
	[C_6mim][35]		18.48	17.07		-1.520	-1.452	4.5	-9.238	-9.238	0.0
	[C_7mim][35]		20.24	18.67		-1.570	-1.526	2.8	-9.849	-9.820	0.3
	[C_{10}mim][a]		25.53	23.46		-1.604	-1.752	9.2	---	---	---
	[C_2C_2im]		13.20	12.28		-1.224	-1.228	0.4	-7.488	-7.488	0.0
	[C_3mpy][41]		14.95	13.88		-1.347	-1.300	3.5	-7.850	-8.063	2.7
	[4-C_4mpy][a]		16.72	15.48		-1.336	-1.376	3.0	---	---	---
	[C_4py][a]		14.95	13.88		-1.312	-1.300	0.9	---	---	---
	[C_8py][a]		22.00	20.27		-1.510	-1.600	6.0	---	---	---
	[C_3mpip][41]		17.24	15.67		-1.487	-1.448	2.7	---	---	---
	[C_3mpyr][41]		15.48	14.08		-1.370	-1.372	0.1	---	---	---
Test Set	[C_3mim]	[PF_6]	13.20	12.28	2.908	-1.149	-1.152	0.2	-5.969	-5.910	1.0
	[C_4C_1mim][35]		16.72	15.47		-1.519	-1.302	**14.3**	-7.042	-7.078	0.5
	[C_2mim][35]	[Tf_2N]	11.44	10.68	3.932	-1.165	-1.154	1.0	-7.041	-6.906	1.92
	[C_5mim][35]		16.72	15.47		-1.459	-1.378	5.6	-8.512	-8.656	1.7
	[C_8mim][35]		22.01	20.26		-1.479	-1.604	8.5	-10.246	-10.412	1.6
	[C_4C_1mim]		16.72	15.47		-1.552	-1.378	**11.2**	-8.430	-8.656	2.7
	[C_4mpy][a]		16.72	15.48		-1.454	-1.376	5.4	---	---	---
	[C_6py][a]		18.48	17.08		-1.402	-1.450	3.5	---	---	---
	[C_4mpyr][41]		17.24	15.67		-1.457	-1.448	0.6	---	---	---

[a] Data not yet reported

In Figure 13 is shown the plots of predicted *vs*. experimental data for all ILs studied in this work.

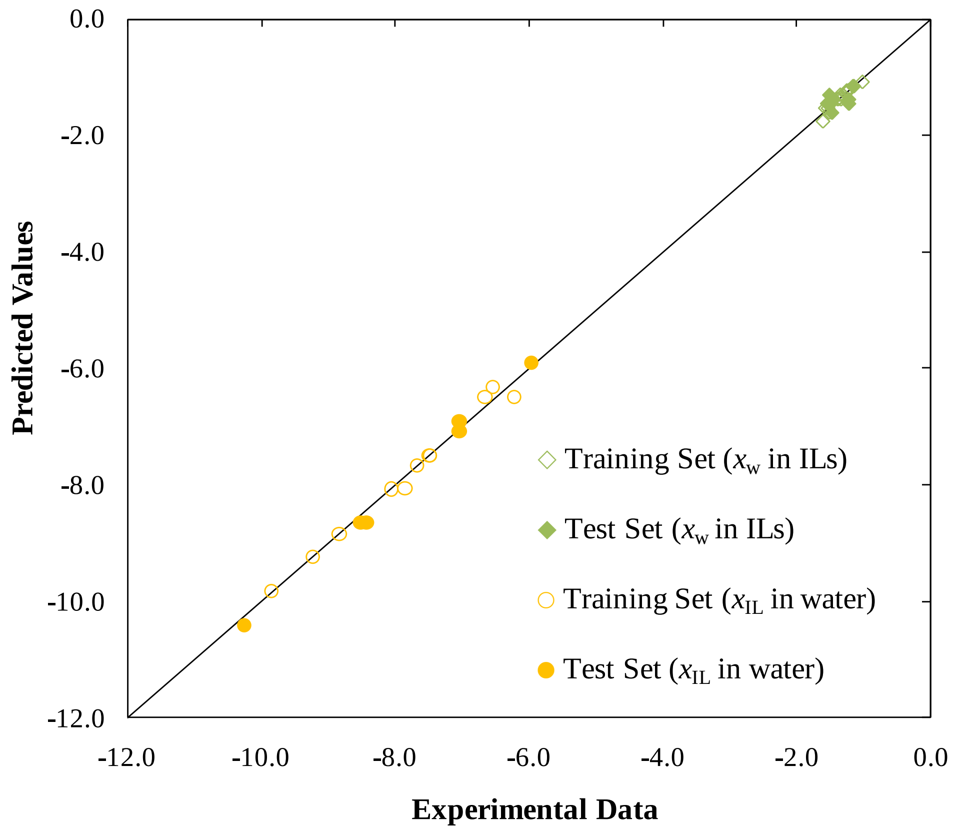

Figure 13. Predicted values and experimental data: ◇, ◆ Solubility of water in ILs; ○, ● Solubility of ILs in water.

The proposed model shows average deviations for the predicted values of the water solubility in ILs and ILs solubility in water of 4 % and 1 %, respectively. Furthermore, higher deviations for the trisubstituted ILs are shown in water solubility in ILs, compared to the monosubstituted and disubstituted ILs. However, for solubility of the trisubstituted ILs in water the deviations are lower. From the analysis of Table 5, it is possible to see that the predicted value for both phases for $[C_4C_1mim][Tf_2N]$ is equal to $[C_5mim][Tf_2N]$. In the previous Chapter of this thesis it was shown that the behaviour of $[C_4C_1mim][Tf_2N]$ is different for the aqueous-rich phase and IL-rich phase. This model predicted the same behaviour for both phases which resulted in a higher deviation for solubility of water in this IL.

3.5. Conclusions

It was possible to built a model to predict the mutual solubilities of water and ILs. For that purpose 26 different ILs were used based on the LSER Model. With exception for water solubility in [C_4C_1mim]-based ILs the deviation of the predicted value to the experimental data is inferior to 10 %. This model could be an interesting tool to predict mutual solubilities of water and ILs not yet synthesized.

4

ILs + H_2O + K_3PO_4 Ternary Systems

4.1. Introduction

The efficiency and viability of any biotechnological process depends largely on downstream processing which ensures the purity and quality of the biomolecules and represents about 60 % to 90 % of the cost of the final product[53]. Many metabolites and/or bioproducts show narrow tolerance limits of pH, ionic strength, temperature, osmotic pressure and surface charges; thus, the extraction and isolation techniques must be specific and compatible with the product[54]. Conventional techniques used for product recovery from biotechnological processes are usually expensive and present low yields[55]. Therefore, there have been considerable efforts from the industrial and academic communities to develop cost-effective separation techniques[56], such as liquid-liquid extraction in aqueous biphasic systems (ABS). These systems are formed when two mutually incompatible - though both miscible with water - polymer/polymer, polymer/salt or salt/salt systems are employed. Above a critical concentration of those components, spontaneous phase separation takes place, and the extraction of biomolecules can be achieved by the manipulation of the affinity of the specific compound for each of the aqueous-rich phases.

The first suggestion that ILs could be used to prepare ABS was reported by Gutowski et al.[57] and the potential advantages of factual IL-based ABS have motivated previous studies on the interactions between water and ILs, and between ILs and salts in aqueous solutions towards achieving a deeper understanding of the molecular phenomena governing the IL-based ABS scenario[22, 35, 36, 41]. In spite of the scattered results that have been reported concerning IL-based ABS, there are still many gaps in the ILs characterization and a general picture of the situation that would allow the finest selection of the IL is still lacking. Research regarding the use of IL-based ABS has been so far mostly centred on the influence of several inorganic salts on the phase diagrams[56-60] (where the ions influence follows the well known Hofmeister series)[58] or in the use of carbohydrates for IL-based ABS formation[61-64]. Surprisingly, one of the most interesting practical issues - the evaluation of the extraction ability of those IL-based ABS - was seldom studied. Only testosterone, epitestosterone, penicillin G and opium alkaloids were previously used as partitioning solutes[65-67]. No reports concerning the extraction of aminoacids or even proteins using ILs-based ABS were found in the literature.

In this work we individually evaluated the IL cation and anion influence in promoting IL-based ABS maintaining the same inorganic salt (K_3PO_4). Different phase diagrams (binodal curves and tie-lines) for systems of hydrophilic ILs + K_3PO_4 + water, at 298 K and atmospheric pressure, were determined. The binodal curves were fitted to a three-parameter equation and the tie-lines were estimated using the Merchuck et al. approach[68]. The selected ILs combination allowed the study of the cation alkyl chain length, the number of alkyl groups at the cation, the type of functional groups at the cation and the anion identity impact in their ABS promotion capability. In addition, the ABS here investigated were characterized according to their extractive potential of aminoacids, where L-tryptophan (Figure 14) was selected as a model biomolecule. Aminoacids are important compounds of several biotechnological processes and the development of methods for their separation and purification is still a main problem.

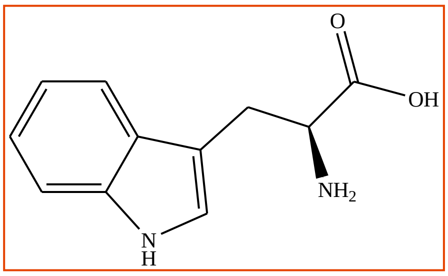

Figure 14. Chemical structure of L-tryptophan.

4.2. Experimental Section

4.2.1. Materials

The ABS studied in this work were established by using an aqueous solution of K_3PO_4 ≥ 98 w/w % pure from Sigma and different aqueous solutions of hydrophilic ILs. The ILs studied were imidazolium chloride, [im][Cl], methylimidazolium chloride, [C_1im][Cl], ethylimidazolium chloride, [C_2im][Cl], 1,3-dimethylimidazolium chloride, [C_1mim][Cl], 1-ethyl-3-methylimidazolium chloride, [C_2mim][Cl], 1-butyl-3-methylimidazolium chloride, [C_4mim][Cl], 1-hexyl-3-methylimidazolium chloride, [C_6mim][Cl], 1-allyl-3-methylimidazolium chloride, [amim][Cl], 1-hydroxyethyl-3-methylimidazolium chloride, [OHC_2mim][Cl], and 1-benzyl-3-methylimidazolium chloride, [C_7H_7mim][Cl]; 1-ethyl-3-methylimidazolium bromide, [C_2mim][Br], 1-ethyl-3-methylimidazolium acetate, [C_2mim][CH_3CO_2], 1-ethyl-3-methylimidazolium methylsulfate, [C_2mim][$MeSO_4$], 1-ethyl-3-methylimidazolium ethylsulfate, [C_2mim][$EtSO_4$], 1-ethyl-3-methylimidazolium methanesulfonate, [C_2mim][CH_3SO_3], 1-ethyl-3-methylimidazolium trifluoromethanesulfonate, $[C_2mim][CF_3SO_3]$, 1-butyl-3-methylimidazolium bromide, $[C_4mim][Br]$, 1-butyl-3-methylimidazolium acetate, $[C_4mim][CH_3CO_2]$, 1-butyl-3-methylimidazolium dicyanamide, $[C_4mim][N(CN)_2]$, 1-butyl-3-methylimidazolium methanesulfonate, $[C_4mim][CH_3SO_3]$, 1-butyl-3-methylimidazolium hydrogenosulfate, $[C_4mim][HSO_4]$, 1-butyl-3-methyl-imidazolium trifluoromethanesulfonate, $[C_4mim][CF_3SO_3]$ and 1-butyl-3-methylimidazolium trifluoroacetate, $[C_4mim][TFA]$. The ILs molecular structures are shown in Figure 15. All ILs used in this work were acquired at Iolitec with the exception of $[C_1mim][Cl]$ that was synthesized in our lab (*cf.* Appendix B) and $[C_4mim][TFA]$ that was acquired at Solchemar. To reduce the water and volatile compounds content to negligible values, ILs individual samples were dried under constant stirring at moderate vacuum and temperature ($\approx$ 353 K) for a minimum of 48 h. After this procedure, the purity of each ionic liquid was further checked by ^{1}H, ^{13}C and ^{19}F (whenever possible) NMR spectra and found to be > 99 w/w % for all samples (*cf.* Appendix B). The water used was ultra-pure water, double distilled, passed by a reverse osmosis system and further treated with a Milli-Q plus 185 water purification apparatus. The L-tryptophan with a purity > 99.0 w/w % was from Fluka.

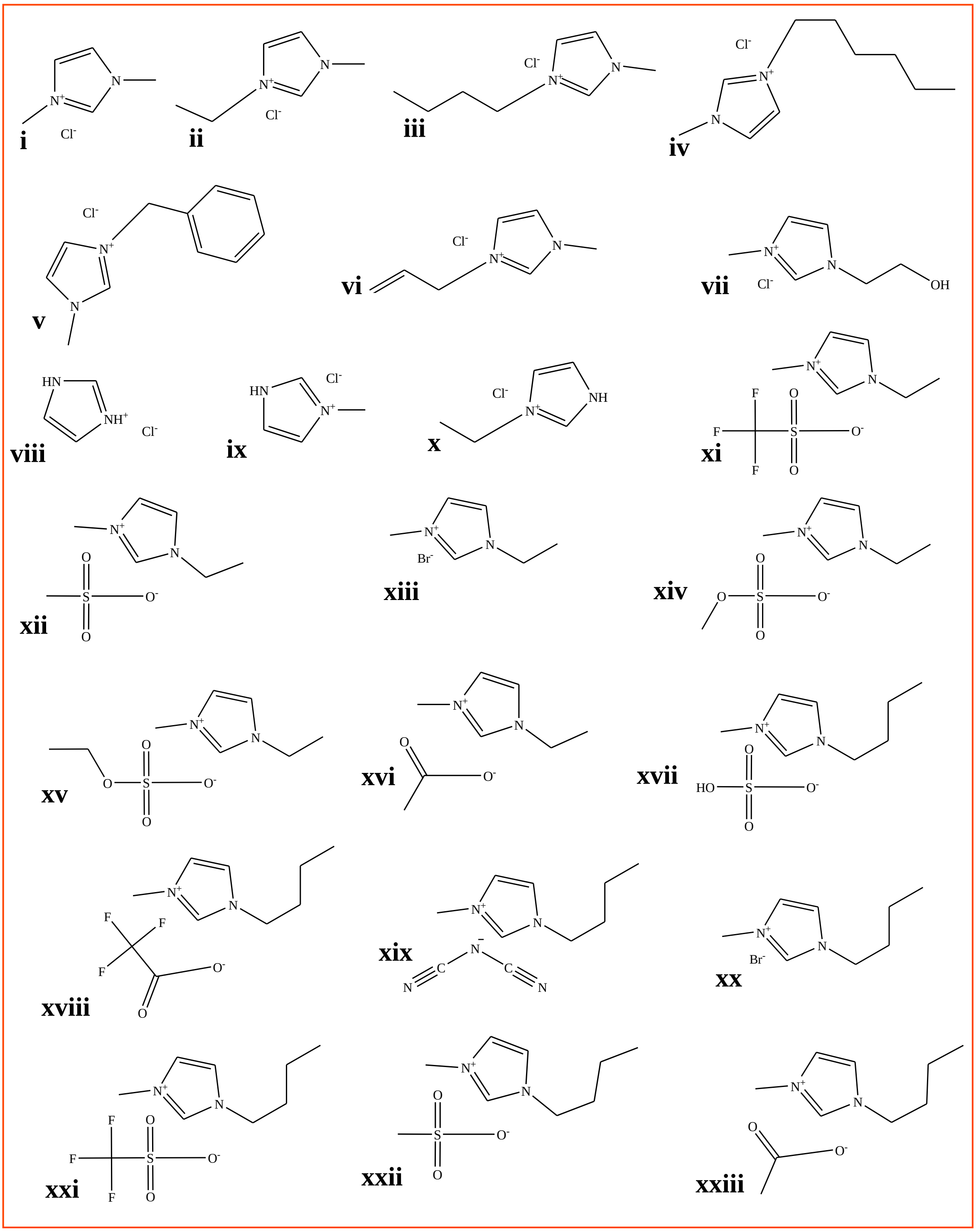

Figure 15. Chemical structure of the ILs studied: (i) [C_1mim][Cl]; (ii) [C_2mim][Cl]; (iii) [C_4mim][Cl]; (iv) [C_6mim][Cl]; (v) [C_7H_7mim][Cl]; (vi) [amim][Cl]; (vii) [OHC_2mim][Cl]; (viii) [im][Cl]; (ix) [C_1im][Cl]; (x) [C_2im][Cl]; (xi) [C_2mim][CF_3SO_3]; (xii) [C2mim][CH_3SO_3]; (xiii) [C_2mim][Br]; (xiv) [C_2mim][$MeSO_4$]; (xv) [C_2mim][$EtSO_4$]; (xvi) [C_2mim][CH_3CO_2] ; (xvii) [C_4mim][HSO_4]; (xviii) [C_4mim][TFA]; (xix) [C_4mim][$N(CN)_2$]; (xx) [C_4mim][Br]; (xxi) [C_4mim][CF_3SO_3]; (xxii) [C_4mim][CH_3SO_3]; (xxiii) [C_4mim][CH_3CO_2].

4.2.2. Phase Diagrams and Tie-Lines

The phase diagram binodals were determined through the cloud point titration method[69, 70] at 298 K (± 1 K), as shown in Figure 16. The experimental procedure adopted was validated with the phase diagram obtained for the [C_4mim][Cl] IL + water + K_3PO_4 ternary system against literature data[71]. Aqueous solutions of K_3PO_4 at 40 w/w % and aqueous solutions of the different hydrophilic ILs at variable concentrations were prepared and used for the phase diagrams binodal determination. Repetitive drop-wise addition of the aqueous inorganic salt solution to the aqueous solution of IL was carried until the detection of a cloudy solution, followed by the drop-wise addition of ultra-pure water until the detection of a monophasic region (clear and limpid solution). Drop-wise additions were carried under constant stirring. The ternary system compositions were determined by the weight quantification of all components added within an uncertainty of $\pm 10^{-4}$ g.

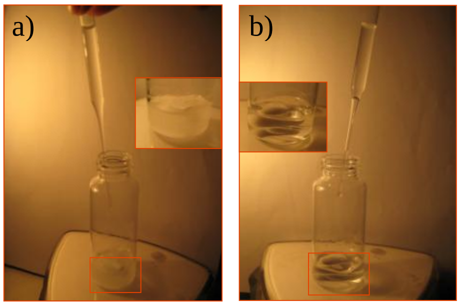

Figure 16. Experimental determination of the binodal curve for the aqueous systems IL-K_3PO_4: a) addition of K_3PO_4 for the cloud point detection; b) addition of water for the clean point detection.

The tie-lines (TLs) were determined by a gravimetric method described by Merchuck et al.[68]. For the TLs determination a mixture at the biphasic region was prepared, vigorously stirred and allowed to reach the equilibrium by the separation of both phases for 24 h at 298 K using small ampoules (*ca*. 10 mL) especially designed for the purpose. After the separation step, both top and bottom phases were weighed. Each individual TL was determined by application of the lever rule to the relationship between the top mass phase composition and the overall system composition[68].

Figure 17. Experimental determination of the TLs

For that purpose the experimental binodal curves were fitted using Eq. 5[68],

$$Y = A\exp\left[\left(BX^{0.5}\right)-\left(CX^{3}\right)\right] \qquad (5)$$

where Y and X, are respectively, the IL and salt weight percentages, and A, B and C are constants obtained by the regression.

For the determination of TLs was solved the following system of four equations (Eq. 6, 7, 8 and 9) and four unknown values (Y_T, Y_B, X_T and X_B):

$$\begin{cases} Y_T = A\exp\left[\left(BX_T^{\ 0.5}\right)-\left(CX_T^{\ 3}\right)\right] & (6) \\ Y_B = A\exp\left[\left(BX_B^{\ 0.5}\right)-\left(CX_B^{\ 3}\right)\right] & (7) \\ Y_T = \dfrac{Y_M}{\alpha'} - \left(\dfrac{1-\alpha'}{\alpha'}\right)Y_B & (8) \\ X_T = \dfrac{X_M}{\alpha'} - \left(\dfrac{1-\alpha'}{\alpha'}\right)X_B & (9) \end{cases}$$

The subscript letters *T*, *B* and *M* represent respectively the top, the bottom and the mixture phase. The parameter α' is the ratio between the top mass and the total mass of the mixture. The solution of the referred system gives the concentration of the IL and salt in the top and bottom phases. For calculation of the tie-line length (TLL) was used Eq. 10

$$TLL = \sqrt{(X_T - X_B)^2 + (Y_T - Y_B)^2} \qquad (10)$$

4.2.3. Partitioning of L-tryptophan

The partition coefficients of L-tryptophan, K_{Trp}, are defined as the ratio of the concentration of L-tryptophan in the IL and in the K_3PO_4 aqueous-rich phases and as described by Eq. 11,

$$K_{\mathrm{Trp}} = \frac{[\mathrm{Trp}]_{\mathrm{IL}}}{[\mathrm{Trp}]_{\mathrm{K_3PO_4}}} \qquad (11)$$

where $[\mathrm{Trp}]_{\mathrm{IL}}$ and $[\mathrm{Trp}]_{\mathrm{K_3PO_4}}$ are the concentration of L-tryptophan in the IL and in the K_3PO_4 aqueous-rich phases, respectively.

A mixture in the biphasic region was selected and used to evaluate the L-tryptophan partitioning. For this purpose aqueous solutions of L-tryptophan with a concentration of approximately 0.78 $g{\cdot}dm^{-3}$ were used. The biphasic solution was left to equilibrate for 12 h (a time period established in previous optimizing experiments) to achieve a complete L-tryptophan partitioning between the two phases. The aminoacid quantification, in both phases, was carried by UV spectroscopy using a SHIMADZU UV-1700, Pharma-Spec Spectrometer, at a wavelength of 279 nm and using calibration curves previously established (*cf.* Appendix B). Moreover, both phases were weighted and the corresponding TLs obtained as previously described.

4.3. Results and Discussion

4.3.1. Phase Diagrams and Tie-Lines

Since ILs are ionic by nature, the IL-based ABS are more complex than typical polyethylene glycol-based ABS due to the possibility of ion exchange and/or ion-pairing between both salt phases. Bridges et al.[58] have shown that there is ion partition between both phases yet maintaining electroneutrality. However, the overall deviations observed are small enough to be considered as a source of error in the cloud point titration (as determined by radioanalitycal results) and thus yielding a satisfactory representation of the ions concentration present at any TL.

The experimental phase diagrams at 298 K and at atmospheric pressure for each IL + K_3PO_4 + H_2O system are shown in Figure 18, Figure 19, 21 and Figure 22 in molality units for a detailed understanding of the ILs impact on the ABS formation (*cf.* Appendix B with the experimental weight fraction data). Figure 18 and 19 show the influence of the cation while Figures 21 and 22 show the anion influence. Figure 18 shows the binodal curve for the ILs [amim][Cl], [OHC$_2$mim][Cl], [C$_7$H$_7$mim][Cl], [C$_6$mim][Cl], [C$_4$mim][Cl], [C$_2$mim][Cl] and [C$_1$mim][Cl].

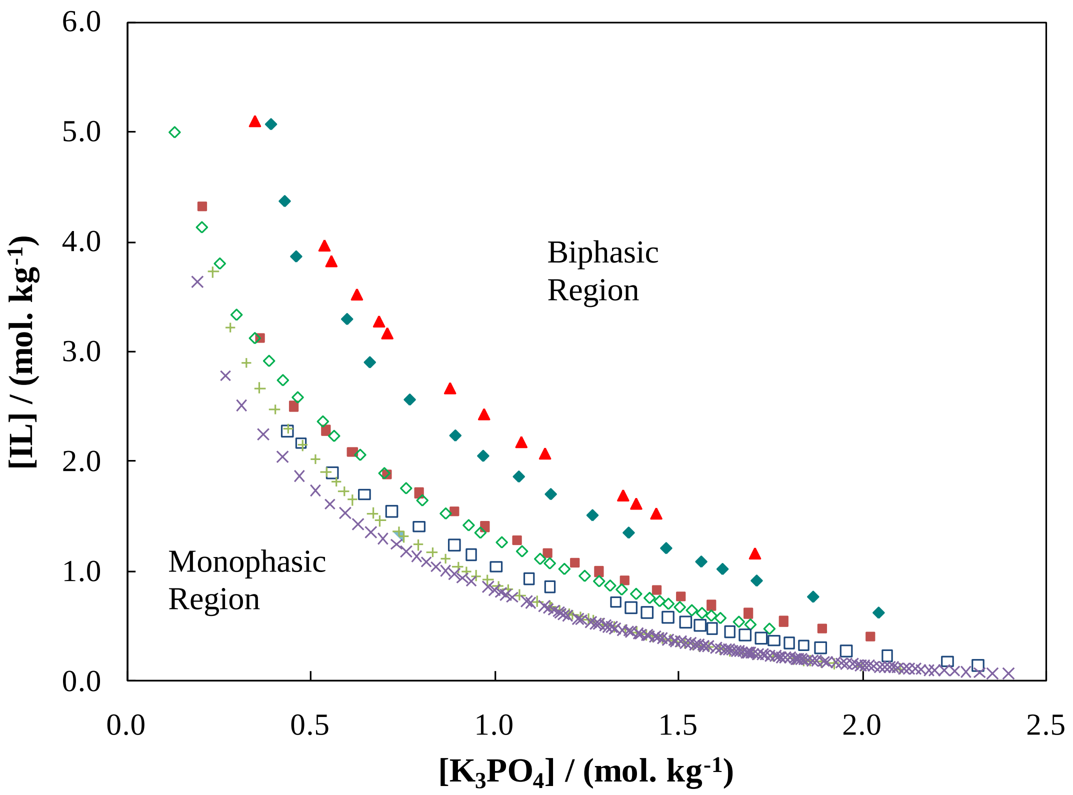

Figure 18. Phase diagram for the di-substituted imidazolium-based ternary systems composed by IL + K_3PO_4 + H_2O at 298 K: ♦, [C_1mim][Cl]; ■, [C_2mim][Cl]; □, [C_4mim][Cl]; ×, [C_6mim][Cl]; +, [C_7H_7mim][Cl]; ◊, [amim][Cl]; ▲, [OHC_2mim][Cl].

The observation of Figure 18 indicates that the larger the cation alkyl chain the greater it is the IL ability for ABS formation. It is well known that the cation alkyl chain length increase leads to the increase of the IL hydrophobic nature and therefore to a poorer affinity for water[57]. The higher the IL affinity for water and/or the IL hydrophilic nature the less effective is the IL in promoting ABS. Moreover, the presence of a terminal hydroxyl group at the alkyl chain leads to a large decrease in the ABS promoting ability due to the higher hydrophilicity of the IL when compared with the [C_2mim][Cl]. Also the presence of a double bond at the propyl chain of the imidazolium cation ([amim][Cl]) or the presence of a benzyl group ([C_7H_7mim][Cl]) as a substituent group decreases the ABS formation ability, although in a less pronounced way.

When a second electrolyte is added to a non-electrolyte or electrolyte aqueous solution, the solubility of the solute usually decreases as a consequence of the salting-out effect. In general, ILs with lower water solubility require less salt to promote the two phases separation resulting in a binodal curve closer to the axis and in a larger biphasic region. The results here obtained show that the ability of the ILs for ABS formation follows the order: [C_6mim][Cl] > [C_7H_7mim][Cl] > [C_4mim][Cl] > [C_2mim][Cl] ≈ [amim][Cl] > [C_1mim][Cl] > [OHC_2mim][Cl].

Figure 19 illustrates the experimental binodal curves obtained for the mono- and un-substituted imidazolium chlorides [C_2im][Cl], [C_1im][Cl] and [im][Cl].

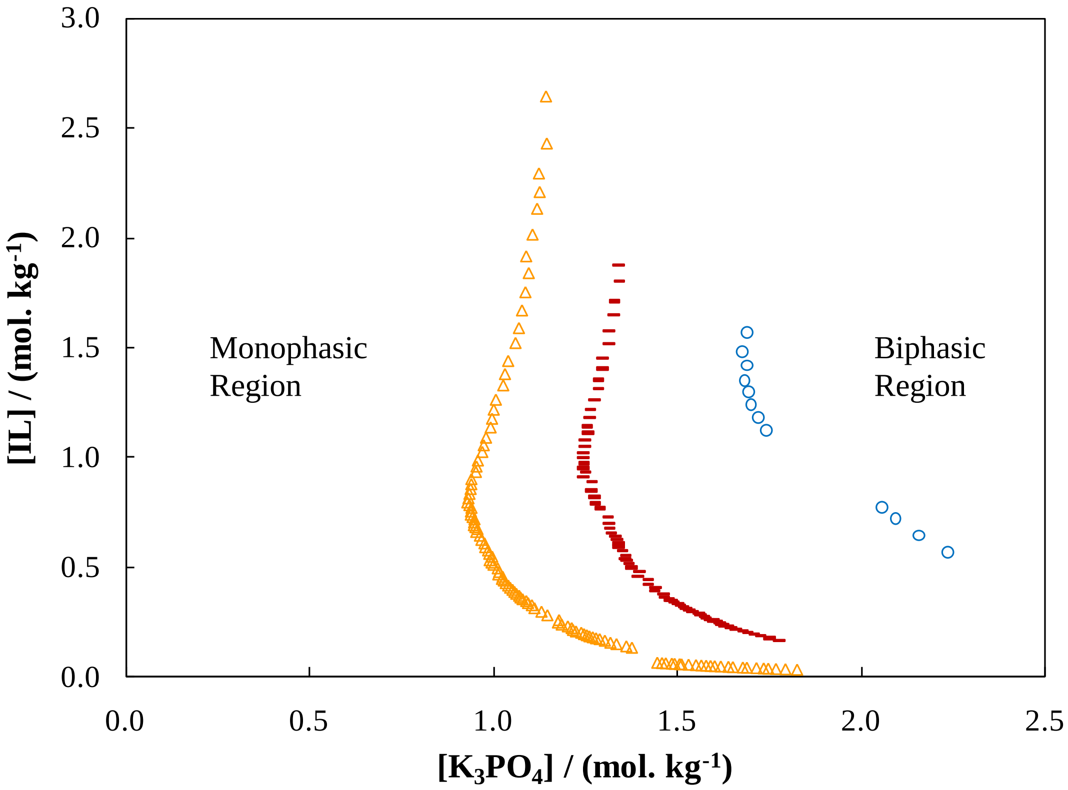

Figure 19. Phase diagram for the un- and mono-substituted imidazolium-based ternary systems composed by IL + K_3PO_4 + H_2O at 298 K: ○, [im][Cl]; ‾, [C_1im][Cl] and △, [C_2im][Cl].

These systems reveal an "atypical" behaviour for ABS involving ILs not previously reported. The asymmetrical behaviour of these aqueous biphasic systems has been previously observed for ABS of polyethylene glycol (PEG) and low weight polysaccharides[72, 73] and they may constitute an interesting approach for product separations. For the same K_3PO_4 molality two monophasic and one biphasic regions are present and thus the system can be moved between the various phases by simple variation of the IL concentration. Comparing the three ILs the ABS forming ability ranks from [C_2im][Cl] > [C_1im][Cl] > [im][Cl]. The number of alkyl substituents and again the alkyl chain length increase leads to a higher ABS inducing capacity. Curiously, comparing the results reported in Figure 18 and 19 and depicted in Figure 20, there are specific ranges of concentration where the monosubstituted imidazolium-based ILs are more effective in promoting phase separation than their di-substituted analogues.

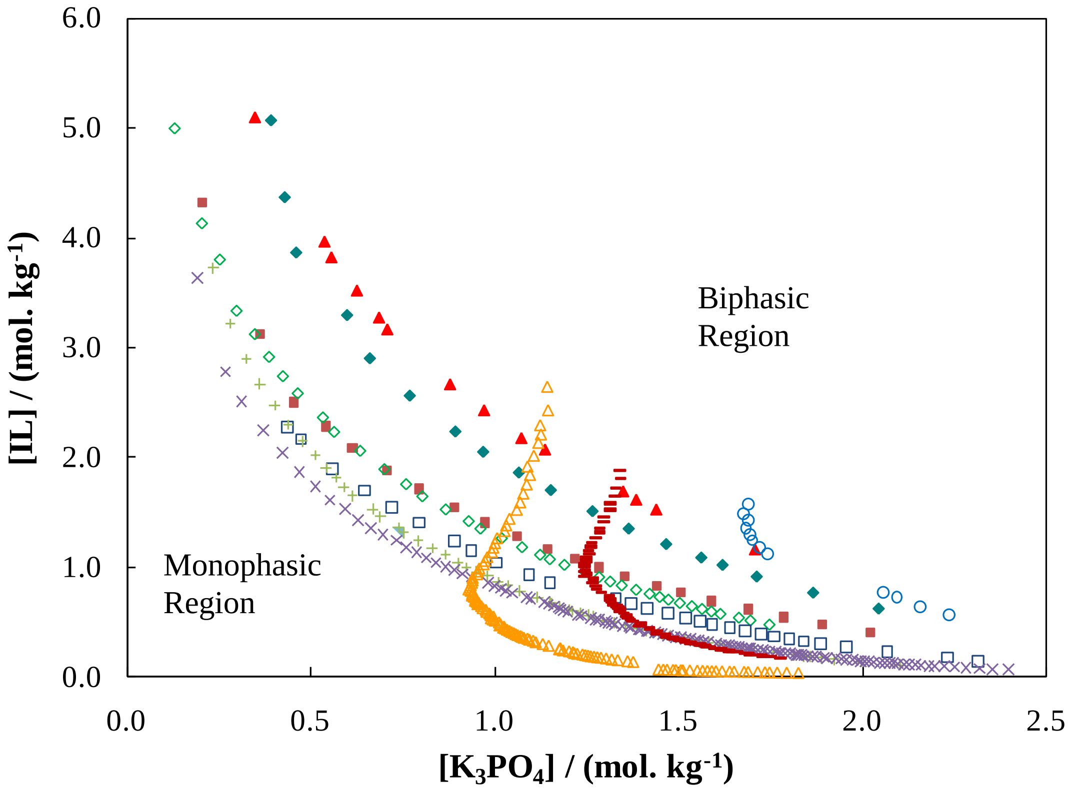

Figure 20. Phase diagram for the un-, mono- and di-substituted imidazolium-based ternary systems composed by IL + K_3PO_4 + H_2O at 298 K: ○, [im][Cl]; ▬, [C_1im][Cl] and △, [C_2im][Cl]; ♦, [C_1mim][Cl]; ■, [C_2mim][Cl]; □, [C_4mim][Cl]; ×, [C_6mim][Cl]; +, [C_7H_7mim][Cl]; ◊, [amim][Cl]; ▲, [OHC_2mim][Cl].

Figure 21 shows the binodal curves for [C_2mim][[Cl]], [C_2mim][Br], [C_2mim[CH_3SO_3], [C_2mim][CH_3CO_2], [C_2mim][$MeSO_4$], [C_2mim][$EtSO_4$] and [C_2mim][CF_3SO_3].

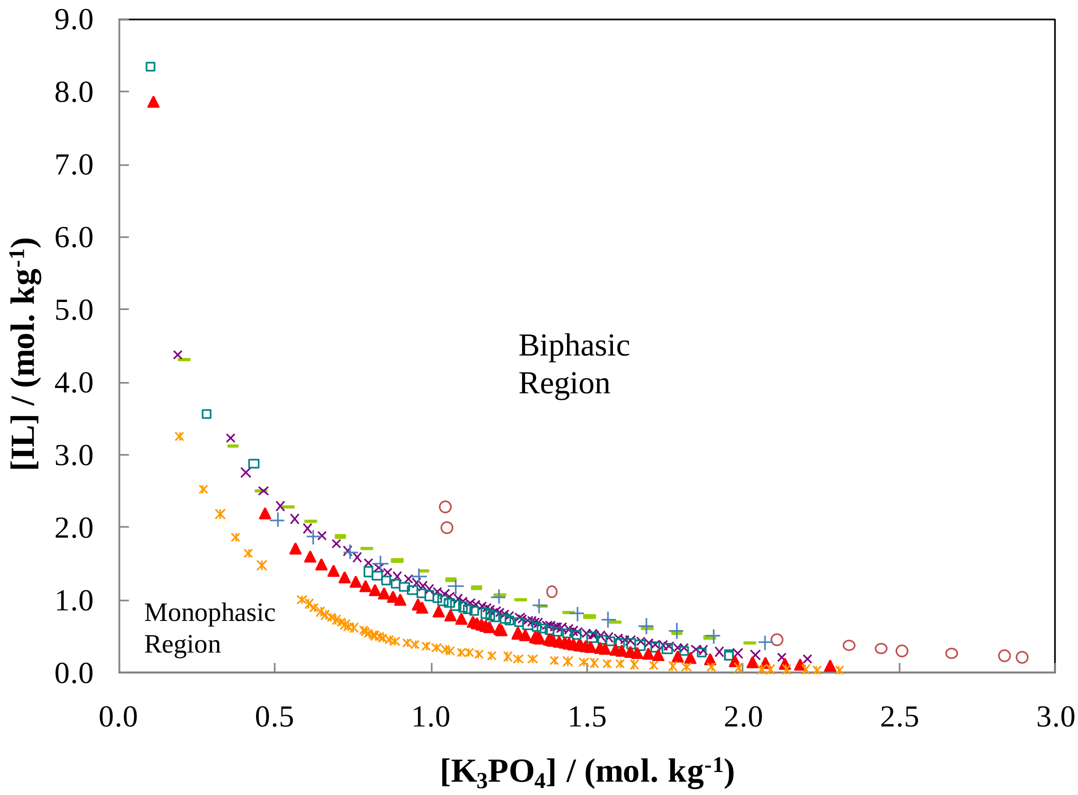

Figure 21. Phase diagrams for [C_2mim]-based ternary systems composed by IL + K_3PO_4 + H_2O at 298 K: ✳, [C_2mim][CF_3SO_3]; ▲, [C_2mim][$EtSO_4$]; +, [C_2mim][CH_3CO_2]; □, [C_2mim][$MeSO_4$]; ×, [C_2mim][Br]; –, [C_2mim][Cl]; ○, [C_2mim][CH_3SO_3].

Figure 22 shows the binodal curves for [C_4mim][Cl], [C_4mim][Br], [C_4mim][CH_3SO_3], [C_4mim][CH_3CO_2], [C_4mim][HSO_4], [C_4mim][$N(CN)_2$], [C_4mim][TFA] and [C_4mim][CF_3SO_3].

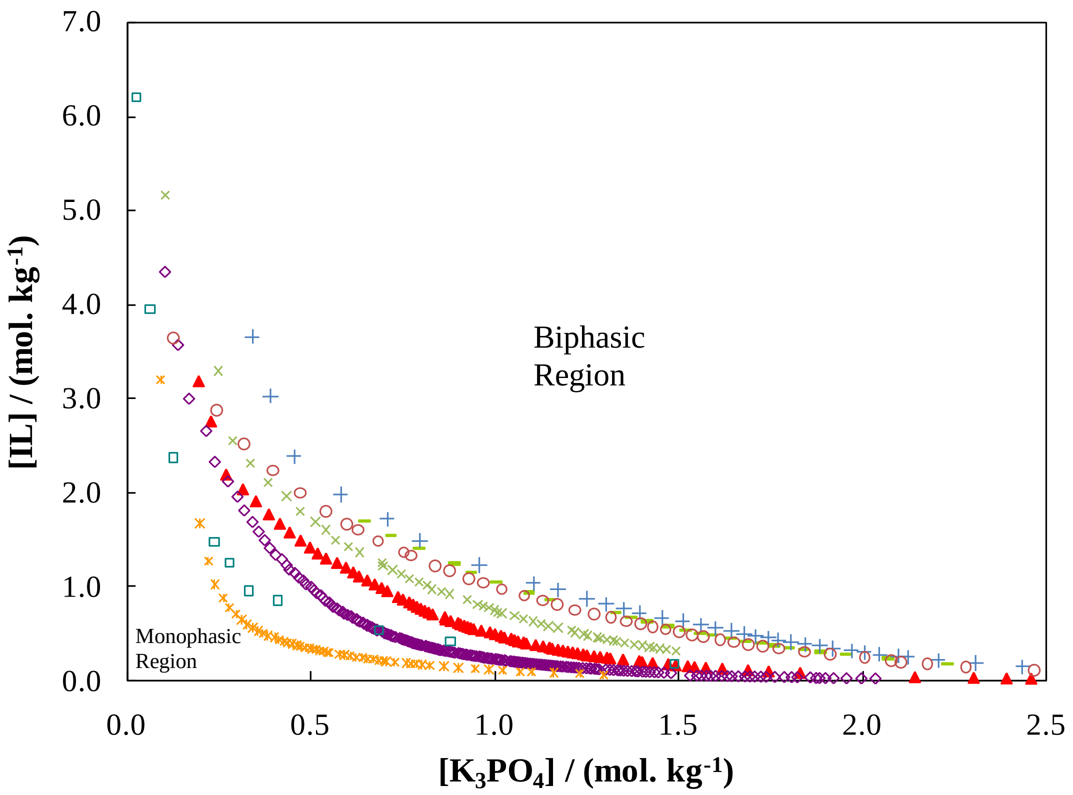

Figure 22. Phase diagrams for $[C_4mim]$-based ternary systems composed by IL + K_3PO_4 + H_2O at 298 K: ✳, $[C_4mim][CF_3SO_3]$; ◊, $[C_4mim][N(CN)_2]$; □, $[C_4mim][HSO_4]$; ▲, $[C_4mim][TFA]$; ×, $[C_4mim][Br]$; ○, $[C_4mim][CH_3SO_3]$; ‾, $[C_4mim][Cl]$; +, $[C_4mim][CH_3CO_2]$.

The results obtained show that the ability of ILs for ABS formation follows the order: $[C_2mim][CF_3SO_3]$ > $[C_2mim][EtSO_4]$ > $[C_2mim][MeSO_4]$ > $[C_2mim][Br]$ > $[C_2mim][Cl]$ ≅ $[C_2mim][CH_3CO_2]$ > $[C_2mim][CH_3SO_3]$ and $[C_4mim][CF_3SO_3]$ > $[C_4mim][N(CN)_2]$ > $[C_4mim][HSO_4]$ > $[C_4mim][TFA]$ > $[C_4mim][Br]$ > $[C_4mim][Cl]$ ≅ $[C_4mim][CH_3CO_2]$ ≅ $[C_4mim][CH_3SO_3]$.

In PEG-based ABS the salt anion has the major impact on the polymer solubility and hence in the ABS phase diagrams, while the cation has a minor (though sizeable) effect[74]. For the ILs, it is here shown that the IL cation has a huge influence in the phase diagrams behaviour allowing the IL-based ABS to be tailored to meet the specific requirements of a particular separation.

The salting-out effect is usually explained based on the ordering of bulk water and on the ability of the ions to decrease the water structure by a simple hydration phenomena. Recent works are converging upon to the idea that interactions between the IL ions and the inorganic salt ions may be present, and are mainly responsible for the salting-in or salting-out phenomena[75, 76]. Salting-out inducing ions act mainly through an entropic effect resulting from the formation of water-ion hydration complexes while the salting-in inducing ions directly interact with the hydrophobic moieties of the IL. The ions specific effects seem to be dominated by the ion-ion *versus* ion-water interactions through a complex interplay of factors, and not by the water-structure modification as classically accepted[77]. Keeping in mind that PO_4^{3-} is a high charge density ion (salting-out inducing ion), and that this ion was used in all the ternary systems evaluated, it is possible to assess the IL anions inducing character. According to Figure 21 and 22, the closer to the axis is located the binodal curve, the larger the IL anion salting-in inducing behaviour - that is the lower the density charge of the IL anions.

Studies regarding the ILs polarity provide useful information on the IL cations and anions solvation at the molecular level. The introduction of empirical solvent polarity scales, based on solvent interactions with a reference solute, has lead to a rank on the compounds[78]. Frequently used polarity scales, based on solvatochromic probes, are the Reichardt $E_T(30)$ scale and the Kamlet-Taft's solvent parameters[79, 80]. In fact, the polarities of imidazolium-based ILs were found to be similar to that of short chain alcohols[81]. A review regarding the polarity of ILs was recently published by Reichardt[82]. It should, nevertheless, be kept in mind that the solvent parameters are dependent on the molecule probe employed[79], and particularly relevant for these nano-structured fluids.

Table 6 reports the hydrogen bond basicity (β) and hydrogen bond acidity (α) of [C_4mim]-based ILs using the solvatochromic probe $[Fe(phen)_2(CN)_2]ClO_4$[83].

Table 6. Hydrogen Bond Acidity (α) and Hydrogen Bond Basicity (β) of [C_4mim]-Based ILs with the Solvatochromic Probe [Fe(phen)$_2$(CN)$_2$]ClO_4[83].

IL Anion	α [83]	β [83]
[Cl]	0.32	0.95
[Br]	0.36	0.87
[CH_3CO_2]	0.36	0.85
[CH_3SO_3]	0.36	0.85
[$MeSO_4$]	0.39	0.75
[TFA]	0.43	0.74
[$N(CN)_2$]	0.44	0.64
[CF_3SO_3]	0.50	0.57
[BF_4]	0.52	0.55
[PF_6]	0.54	0.44
[$(CF_3SO_2)_2N$]	0.55	0.42

The value of α decreases with increasing hydrogen bond accepting strength of the IL anion. The ABS studied concern electrolyte solutions in aqueous medium and reflect the competition between the inorganic salt and the IL ions for the creation of water-ion hydration complexes. Therefore, the ability of a specific anion to be preferentially hydrated, largely depends on the anion’s hydrogen bonding accepting ability, and thus the ABS formation ability strongly depends on anion’s hydrogen bonding basicity. This fact was observed for the sequence studied of ILs anions in promoting ABS (Table 6). It is here obvious that the compilation of an accurate and extensive polarity scale of ILs is of main significance, allowing the prediction of their behaviour in aqueous systems, before carrying extensive experimental measurements of phase diagrams of main importance will be the compilation of a polarity scale regarding the IL cation (not found in the available literature).

The experimental binodal curves were fitted to the empirical relationship described by Eq. 5[68] (*cf.* Appendix B). The regression parameters and the tie-line equations obtained for each ternary system, as well as the tie-line lengths (TLLs), are reported in Table 7 and 8, respectively.

Table 7. Correlation parameters used in Eq. 5 to describe the binodals.

IL + K_3PO_4 + water system	*A*	*B*	10^5 *C*	Adj $R^{2(a)}$
[C_1mim][Cl]	109.9	-0.3735	1.990	0.9954
[C_2mim][Cl]	78.25	-0.3389	2.697	0.9964
[C_4mim][Cl]	72.64	-0.3185	4.070	0.9994
[C_6mim][Cl]	84.02	-0.3563	5.462	0.9997
[C_7H_7mim][Cl]	94.67	-0.3545	6.128	0.9999
[amim][Cl]	72.00	-0.2924	4.088	0.9998
[OHC_2mim][Cl]	103.7	-0.3067	1.004	0.9835
[C_2mim][Br]	85.60	-0.3134	4.684	0.9992
[C_2mim][CH_3SO_3]	1476	-0.9004	0.5903	0.9957
[C_2mim][CH_3CO_2]	56.51	-0.2346	3.022	0.9998
[C_2mim][$MeSO_4$]	99.34	-0.3374	4.693	0.9993
[C_2mim][$EtSO_4$]	91.81	-0.3320	5.740	0.9995
[C_2mim][CF_3SO_3]	149.2	-0.5684	9.496	0.9938
[C_4mim][Br]	95.90	-0.3912	5.197	0.9987
[C_4mim][CH_3SO_3]	70.24	-0.2539	4.489	0.9997
[C_4mim][CH_3CO_2]	109.4	-0.3832	3.126	0.9950
[C_4mim][HSO_4]	94.08	-0.6021	0.8797	0.9973
[C_4mim][$N(CN)_2$]	190.7	-0.8344	1.000	0.9573
[C_4mim][TFA]	92.30	-0.3790	9.897	0.9981
[C_4mim][CF_3SO_3]	182.8	-0.9676	1.000	0.9970

$^{(a)}$Adjusted R^2

Table 8. Experimental data for the Tie Lines (TLs) and tie line length (TLL).

IL	Weight fraction composition / %		TL equation IL (wt %) = *a* + *b*·K_3PO_4 (wt %)		TLL
	IL	K_3PO_4	*a*	*b*	
[C_1mim][Cl]	25.20	16.54	47.48	-1.347	31.75
[C_2mim][Cl]	26.30	14.93	42.79	-1.104	47.03
	24.88	20.85	49.83	-1.196	59.46
[C_4mim][Cl]	15.75	22.67	42.27	-1.170	45.97
	17.69	21.54	42.91	-1.171	47.67
	21.36	23.04	51.40	-1.304	61.20
[C_6mim][Cl]	10.78	26.04	45.65	-1.340	47.79
	15.16	25.33	52.62	-1.479	58.32
[C_7H_7mim][Cl]	20.17	20.05	53.86	-1.680	52.78
	17.56	26.09	60.57	-1.648	66.29
[amim][Cl]	26.64	16.60	47.32	-1.246	53.95
	26.80	21.20	52.85	-1.229	65.40
[OHC_2mim][Cl]	41.17	15.36	86.86	-2.976	66.66
[C_2mim][Br]	15.31	26.21	60.39	-1.720	64.07
[C_2mim][CH_3CO_2]	30.01	15.16	44.20	-0.9356	62.04
	24.94	14.96	38.31	-0.8940	49.18
[C_2mim][$MeSO_4$]	20.31	24.94	61.58	-1.655	65.19
	33.23	12.81	59.70	-1.644	61.82
[C_2mim][$EtSO_4$]	14.89	25.16	58.16	-1.720	59.99
	20.24	21.17	56.62	-1.718	56.80
	24.21	25.13	61.64	-1.490	70.84
[C_2mim][CF_3SO_3]	20.00	22.47	78.70	-2.613	79.59
	25.07	14.93	69.22	-2.958	61.84
[C_4mim][Br]	21.09	29.55	69.95	-1.653	24.54
	24.41	19.90	58.90	-1.733	62.34
[C_4mim][CH_3SO_3]	30.33	14.86	49.34	-1.280	56.20
	25.03	14.96	43.66	-1.245	38.91
[C_4mim][$N(CN)_2$]	19.89	22.65	69.98	-2.211	71.44
	24.86	15.86	64.42	-2.446	61.84
	15.19	20.12	64.97	-2.528	61.87
[C_4mim][TFA]	15.24	20.39	59.58	-2.174	59.03
	19.90	24.65	70.35	-2.047	76.77
[C_4mim][CF_3SO_3]	25.00	15.35	69.78	-2.917	68.83
	25.08	14.96	69.68	-2.982	68.37

The TLs representation is shown in Figure 23 for the ternary system [C_4mim][Cl] + K_3PO_4 + water as an example measured in this work. For shorter TLLs, the TLs are approximately parallel while for longer TLLs the tie-lines slopes start to deviate. These deviations in the TLs slopes are in agreement with literature[84] and are related with the fact that the K_3PO_4-rich phase is increasingly free of IL at longer TLLs.

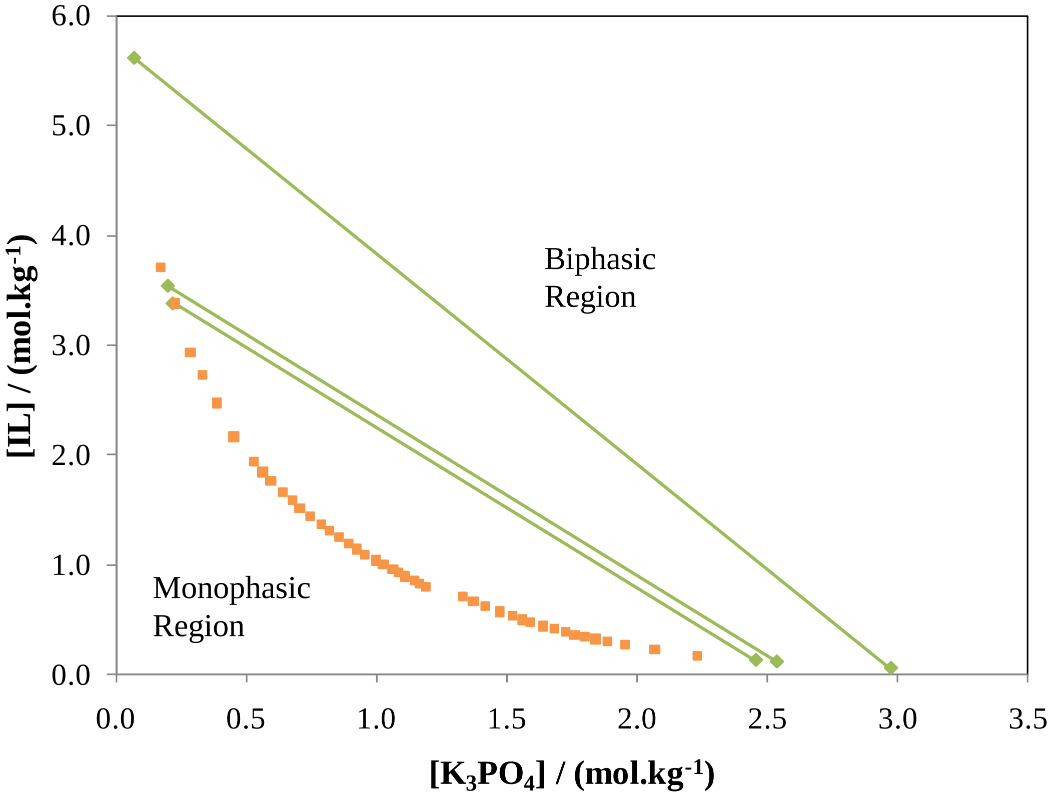

Figure 23. Phase diagram for the [C_4mim][Cl] + K_3PO_4 + water ternary system at 298 K: ■, binodal curve data; ♦, TL data.

4.3.2. Partitioning of L-tryptophan in ABS

Amino acids are the constituents of proteins. The partitioning studies of such biomolecules in ABS have great significance, not only regarding their purification, but also with the aim of extending them to proteins and enzymes. The success of the extractive potential of ABS depends on the ability to manipulate phase properties to obtain the appropriate partition coefficients and selectivity for the biomolecule of interest. There are several approaches to manipulate a particular solute partitioning: (i) adjust the system by applying different salts and/or ILs controlling thus the solute’ affinity; (ii) change the system composition by changing either the concentration of salt and IL; (iii) introduction of additional co-solvents, anti-solvents or amphiphilic structures to the overall system.

As shown in Table 9, the partition coefficients of L-tryptophan (K_{Trp}) in IL-based ABS are substantially higher than in usual PEG-polysaccharide systems (with $K_{Trp} \approx 1$)[85] or PEG-inorganic salts systems (with $K_{Trp} \approx 1$ to 7)[86]. The IL-based ABS are thus far more efficient for L-tryptophan separation than conventional ABS. Table 9 also shows the composition of the ternary system employed for the L-tryptophan partition studies as well as the corresponding TLs and TLLs.

Table 9. Weight fraction composition and partition coefficients of L-tryptophan in ILs-ABS systems.

IL	Weight fraction composition / %		TL equation IL (wt %) = *a* + *b*·K_3PO_4 (wt %)		TLL	K_{Trp}
	IL	K_3PO_4	*a*	*b*		
[amim][Cl]	26.91	15.91	47.20	-1.275	52.53	124 ± 5
[C_7H_7mim][Cl]	25.11	18.30	56.62	-1.722	57.62	78.4 ± 0.5
[OHC_2mim][Cl]	40.57	16.05	87.17	-2.904	68.38	73.1 ± 0.8
[C_2mim][Cl]	25.90	14.90	42.36	-1.105	45.73	59.2 ± 0.4
[C_4mim][Cl]	25.35	15.97	43.46	-1.149	50.03	36.6 ± 0.6
[C_1im][Cl]	15.36	30.53	---	---	---	21.3 ± 0.3
[im][Cl]	15.24	32.80	---	---	---	14.2 ± 0.4
[C_2mim][CH_3CO_2]	24.94	14.96	38.31	-0.8940	49.18	16.4 ± 0.8
[C_2mim][$MeSO_4$]	24.98	14.94	49.80	-1.661	28.89	4.5 ± 0.9
[C_2mim][$EtSO_4$]	24.97	15.06	48.90	-1.589	39.86	6.0 ± 0.5
[C_2mim][CF_3SO_3]	24.87	16.35	75.49	-3.095	70.66	17.5 ± 0.8
[C_4mim][Br]	25.82	15.17	51.60	-1.699	48.36	35.6 ± 0.8
[C_4mim][CH_3SO_3]	25.03	14.96	43.66	-1.245	38.91	10.4 ± 0.4
[C_4mim][$N(CN)_2$]	24.40	16.82	67.35	-2.553	64.90	45.1 ± 0.9
[C_4mim][TFA]	25.13	15.22	57.90	-2.154	56.16	36.1 ± 0.7
[C_4mim][CF_3SO_3]	25.08	16.18	76.12	-3.154	75.39	16.6 ± 0.6

During the partitioning of L-tryptophan between the two phases there are several competing interactions between the IL, the inorganic salt, the L-tryptophan and water. There may occur hydrogen-bonding interactions, $\pi\cdots\pi$ interactions, as well as electrostatic interactions. In general, the results indicate that K_{Trp} increases with the IL cation hydrophilic nature and thus the main interactions between the IL cation and the aminoacid determining the L-tryptophan partitioning are hydrophobic and hydrogen-bonding type interactions. The cation influence of the ILs studied in L-tryptophan partition coefficient follows the rank [amim][Cl] > [OHC$_2$mim][Cl] > [C$_2$mim][Cl] > [C$_4$mim][Cl] > [C$_7$H$_7$mim][Cl] > [C$_1$im][Cl] > [im][Cl]. The highest partition coefficient occurs for the [amim][Cl] followed by [OHC$_2$mim][Cl] due to the presence of a double bound and a hydroxyl group at one of the alkyl side chains, respectively. Increasing the IL cation alkyl chain decreases the L-tryptophan partitioning in the di-substituted imidazolium-based ILs. The mono- and un-substituted imidazolium-based ILs present the lower partition coefficients for the L-tryptophan that could result from the decrease of the hydrophobic interactions existence between them. Evaluating the anion capability to extract L-tryptophan, the K_{Trp} follow the rank: [C$_2$mim][Cl] > [C$_2$mim][CF$_3$SO$_3$] ≅ [C$_2$mim][CH$_3$CO$_2$] > [C$_2$mim][EtSO$_4$] ≅ [C$_2$mim][MeSO$_4$] and [C$_4$mim][N(CN)$_2$] > [C$_4$mim][Cl] ≅ [C$_4$mim][TFA] ≅ [C$_4$mim][Br] > [C$_4$mim][CF$_3$SO$_3$] > [C$_4$mim][CH$_3$SO$_3$]. L-tryptophan partitions preferentially for IL-rich phases composed by halogenated ions such as [Cl] or [Br] or to the most hydrophobic anions, i.e., anions with higher hydrogen bonding accepting strength (β), such as [N(CN)$_2$] and fluoride-based anions. Indeed, these partition coefficients seem to closely follow the Hofmeister series[87]. Salting-in inducing IL ions tend to increase the solute partition coefficient while the salting-out inducing IL ions tend to decrease it.

Comparing the cation and the anion influence on partition coefficients of L-tryptophan, the influence of the IL imidazolium-based cation on the extraction capacity of ABS seems to be more important than the influence of the anion. Indeed, in the study of the cation influence the K_{Trp} was found to vary between 10 and 120 (at approximately the same compositions of IL plus inorganic salt). The presence of benzyl groups and double bounds at the imidazolium side alkyl chain substantially increased such partition coefficients. Besides the $\pi\cdots\pi$ stacking, the possibility of solute-IL hydrogen-bonding seems to rule the partition behaviour.

Wang and co-workers[88] reported the extraction of aminoacids from an aqueous phase using hydrophobic water immiscible ILs. The results obtained in this work show that the magnitudes of L-tryptophan partition coefficients using IL-based ABS can be as much as 1000 times larger than using water immiscible ILs. Indeed our results show that nearly complete extraction of L-tryptophan can be achieved in a single step extraction procedure. Besides the higher hydrophilic ILs affinity for L-tryptophan another factor should be taken into account. In ILs-ABS the presence of an inorganic salt also leads to the aminoacid salting-out from the aqueous phase, further enhancing the distribution ratio of L-tryptophan. This was previously shown by Fan et al.[89] with the extraction of endocrine-disrupting phenols by the use of hydrophobic ILs in the absence and presence of inorganic salts. Nevertheless the high partition coefficients obtained with IL-based ABS for the extraction of L-tryptophan show that these systems may be a successful and a clean approach for biomolecules separation and purification in biotechnological processes.

4.4. Conclusions

The problems of using traditional solvents for the separation of biomolecules in biotechnological processes are pressing the exploration of ILs as new promising extraction media. The ILs ability to form salt–salt ABS allows for hydrophilic ILs to be used in liquid-liquid extractions and new phase equilibrium data for systems involving hydrophilic imidazolium-based ILs + K_3PO_4 + water were presented.

The tunability of IL-based ABS systems was demonstrated by the evaluation of the IL cation and anion influence in promoting ABS. The results showed that IL-based ABS can be obtained over a large range of concentrations both for ILs and the inorganic salt. The results obtained indicated that the IL cation has a major influence in the behaviour of the binodal curves and in the promotion of ABS followed by the IL anion. Increasing the alkyl chain length (for mono or di-substituted ILs) increases the phase separation ability, while the insertion of a double bond, a benzyl group or an hydroxyl group leads to the decrease of ABS promotion capability. On the other hand, the ability of imidazolium-based ILs for aqueous phase separation was shown to closely follow the hydrogen bond accepting strength decrease of the anions composing the IL. The results indicate that IL-based ABS can be obtained over a large range of concentration of both the inorganic salt and the IL, as well as such systems can be finely tuned by the change of the IL anion and/or cation.

The capacity of the IL-based aqueous biphasic systems as extraction media was remarkably demonstrated with the high L-tryptophan partitioning coefficients obtained. It was shown that depending on the nature of the IL used the partition coefficients can vary between 4 and 120. The values obtained are substantially larger than those observed with conventional polymer-based ABS and further studies regarding ILs aiming at obtaining a complete perspective of the molecular interactions controlling the solutes partition behavior is of utmost importance.

5

Final Remarks

5.1. Conclusions

In this work it was possible to evaluate the cation structure and the anion nature on mutual solubilities between water and some hydrophobic ionic liquids. In order to complement this study, it was built a model based on molecular descriptors that could predict with reasonable accuracy mutual solubilities of water and several ILs. In the other hand, with hydrophilic imidazolium-based ILs, it was possible to determine ternary systems of the kind ILs + H_2O + K_3PO_4. Based on this, the potential of these systems to extract a biomolecule (L-tryptophan) was evaluated, and showed to be highly more efficient than other systems already reported on literature, such as PEG-inorganic salts systems.

5.2. Future work

In the future the development of accurate methods for the determination of the solubility of ILs with non-aromatic in water should be carried, such as the pyrrolidinium and piperidinim-based ILs that could not be quantified by UV, while they haven't double bonds or interactions $\pi\cdots\pi$. The QSPR model should be tested for the mutual solubilities of ILs with water for others temperatures, since in this work only one temperature was evaluated (303.15 K). Others ILs, not yet synthesized, should be tested with this model in a way to avoid unnecessary synthesis. For ABS, the future work passes by the substitution of the inorganic salt by sugars and by the substitution of imidazolium-based ILs for cholines-based ILs that are substantially more benign and biodegradable ILs.

6

References

1 Earle, M.J., Esperanca, J., Gilea, M.A., Lopes, J.N.C., Rebelo, L.P.N., Magee, J.W., Seddon, K.R., and Widegren, J.A., *Nature*, 439 **2006** 831-834.

2 Rogers, R.D. and Seddon, K.R., *Science*, 302 **2003** 792-793.

3 Plechkova, N.V. and Seddon, K.R., *Chem. Soc. Rev.*, 37 **2008** 123-150.

4 Walden, P., *Bulletin de l'Académie Impériale des Sciences de St.-Pétersbourg*, 8 **1914** 405-422.

5 Hurley, F.H., US 4,446,331 **1948**

6 Wier, T.P. and Hurley, F.H., US 4,446,349 **1948**

7 Jain, N., Kumar, A., Chauhan, S., and Chauhan, S.M.S., *Tetrahedron*, 61 **2005** 1015-1060.

8 Sheldon, R., *Chem. Commun.*, **2001** 2399-2407.

9 Zhao, H., Xia, S.Q., and Ma, P.S., *J. Chem. Technol. Biotechnol.*, 80 **2005** 1089-1096.

10 Wong, H.-t., Han, S., and Livingston, A.G., *Chem. Eng. Sci.*, 61 **2006** 1338-1341.

11 Endres, F. and Welton, T., *Inorganic Synthesis*, in *Ionic Liquids in Synthesis*, T.W. Peter Wasserscheid, **2002**, Wiley-VCH Verlag GmbH & Co. KGaA: 289-318.

12 Carmichael, A.J. and Haddleton, D.M., *Polymer Synthesis in Ionic Liquids*, in *Ionic Liquids in Synthesis*, T.W. Peter Wasserscheid, **2002**, Wiley-VCH Verlag GmbH & Co. KGaA: 319-335.

13 Brennecke, J.F., Anthony, J.L., and Maginn, E.J., *Gas Solubilities in Ionic Liquids*, in *Ionic Liquids in Synthesis*, P. Wasserscheid and T. Welton, **2002**, Wiley-VCH: 81-93.

14 Huddleston, J.G., Willauer, H.D., Swatloski, R.P., Visser, A.E., and Rogers, R.D., *Chem. Commun.*, **1998** 1765-1766.

15 Joglekar, H.G., Rahman, I., and Kulkarni, B.D., *Chem. Eng. Technol.*, 30 **2007** 819-828.

16 Zhao, H., *Chem. Eng. Commun.*, 193 **2006** 1660-1677.

17 Couling, D.J., Bernot, R.J., Docherty, K.M., Dixon, J.K., and Maginn, E.J., *Green Chem.*, 8 **2006** 82-90.

18 Docherty, K.M. and Kulpa, C.F., *Green Chem.*, 7 **2005** 185-189.

19 Ranke, J., Müller, A., Bottin-Weber, U., Stock, F., Stolte, S., Arning, J., Störmann, R., and Jastorff, B., *Ecotoxicology and Environmental Safety*, 67 **2007** 430-438.

20 Zhao, D.B., Liao, Y.C., and Zhang, Z.D., *Clean-Soil Air Water*, 35 **2007** 42-48.

21 Garcia, M.T., Gathergood, N., and Scammells, P.J., *Green Chem.*, 7 **2005** 9-14.

22 Freire, M.G., Carvalho, P.J., Fernandes, A.M., Marrucho, I.M., Queimada, A.J., and Coutinho, J.A.P., *J. Colloid Interface Sci.*, 314 **2007** 621-630.

23 Gardas, R.L., Freire, M.G., Carvalho, P.J., Marrucho, I.M., Fonseca, I.M.A., Ferreira, A.G.M., and Coutinho, J.A.P., *J. Chem. Eng. Data*, 52 **2007** 80-88.

24 Seddon, K.R., Stark, A., and Torres, M.J., *Pure Appl. Chem.*, 72 **2000** 2275-2287.

25 Fu, D.B., Sun, X.W., Pu, J.J., and Zhao, S.Q., *J. Chem. Eng. Data*, 51 **2006** 371-375.

26 Huddleston, J.G., Visser, A.E., Reichert, W.M., Willauer, H.D., Broker, G.A., and Rogers, R.D., *Green Chem.*, 3 **2001** 156-164.

27 Najdanovic-Visak, V., Rebelo, L.P.N., and da Ponte, M.N., *Green Chem.*, 7 **2005** 443-450.

28 Ventura, S.P.M., Pauly, J., Daridon, J.L., Marrucho, I.M., Dias, A.M.A., and Coutinho, J.A.P., *J. Chem. Eng. Data*, 52 **2007** 1100-1102.

29 Hanke, C.G. and Lynden-Bell, R.M., *J. Phys. Chem. B*, 107 **2003** 10873-10878.

30 Anthony, J.L., Maginn, E.J., and Brennecke, J.F., *J. Phys. Chem. B*, 105 **2001** 10942-10949.

31 Crosthwaite, J.M., Aki, S., Maginn, E.J., and Brennecke, J.F., *J. Phys. Chem. B*, 108 **2004** 5113-5119.

32 McFarlane, J., Ridenour, W.B., Luo, H., Hunt, R.D., DePaoli, D.W., and Ren, R.X., *Sep. Sci. Technol.*, 40 **2005** 1245-1265.

33 Rebelo, L.P.N., Najdanovic-Visak, V., Visak, Z.P., da Ponte, M.N., Szydlowski, J., Cerdeirina, C.A., Troncoso, J., Romani, L., Esperanca, J., Guedes, H.J.R., and de Sousa, H.C., *Green Chem.*, 6 **2004** 369-381.

34 Wong, D.S.H., Chen, J.P., Chang, J.M., and Chou, C.H., *Fluid Phase Equilib.*, 194 **2002** 1089-1095.

35 Freire, M.G., Carvalho, P.J., Gardas, R.L., Marrucho, I.M., Santos, L., and Coutinho, J.A.P., *J. Phys. Chem. B*, 112 **2008** 1604-1610.

36 Freire, M.G., Santos, L., Fernandes, A.M., Coutinho, J.A.P., and Marrucho, I.M., *Fluid Phase Equilib.*, 261 **2007** 449-454.

37 Alfassi, Z.B., Huie, R.E., Milman, B.L., and Neta, P., *Anal. Bioanal. Chem.*, 377 **2003** 159-164.

38 Fadeev, A.G. and Meagher, M.M., *Chem. Commun.*, **2001** 295-296.

39 Najdanovic-Visak, V., Esperanca, J., Rebelo, L.P.N., da Ponte, M.N., Guedes, H.J.R., Seddon, K.R., and Szydlowski, J., *PCCP*, 4 **2002** 1701-1703.

40 Shvedene, N.V., Borovskaya, S.V., Sviridov, V.V., Ismailova, E.R., and Pletnev, I.V., *Anal. Bioanal.Chem.*, 381 **2005** 427-430.

41 Freire, M.G., Neves, C.M.S.S., Carvalho, P.J., Gardas, R.L., Fernandes, A.M., Marrucho, I.M., Santos, L., and Coutinho, J.A.P., *J. Phys. Chem. B*, 111 **2007** 13082-13089.

42 Crum-Brown, A. and Fraser, T.R., *Trans. R. Soc. Edinburgh*, 25 **1868-9** 151-203.

43 Grover, M., Singh, B., Bakshi, M., and Singh, S., *PSTT*, 3 **2000** 28-35.

44 Katritzky, A.R., Dobchev, D.A., Hür, E., Fara, D.C., and Karelson, M., *Bioorg. Med. Chem.*, 13 **2005** 1623-1632.

45 Katritzky, A.R., Kuanar, M., Fara, D.C., Karelson, M., Acree, J.W.E., Solov'ev, V.P., and Varnek, A., *Bioorg. Med. Chem.*, 13 **2005** 6450-6463.

46 Katritzky, A.R., Kuanar, M., Fara, D.C., Karelson, M., and Acree, W.E., *Bioorg. Med. Chem.*, 12 **2004** 4735-4748.

47 Katritzky, A.R., Kuanar, M., Slavov, S., Dobchev, D.A., Fara, D.C., Karelson, M., Acree, J.W.E., Solov'ev, V.P., and Varnek, A., *Bioorg. Med. Chem.*, 14 **2006** 4888-4917.

48 Katritzky, A.R., Mu, L., and Karelson, M., *J. Chem. Inf. Comput. Sci.*, 36 **1996** 1162-1168.

49 Katritzky, A.R., Tamm, K., Kuanar, M., Fara, D.C., Oliferenko, A., Oliferenko, P., Huddleston, J.G., and Rogers, R.D., *J. Chem. Inf. Comput. Sci.*, 44 **2004** 136-142.

50 Katritzky, A.R., Wang, Y., Sild, S., Tamm, T., and Karelson, M., *J. Chem. Inf. Comput. Sci.*, 38 **1998** 720-725.

51 Varnek, A., Kireeva, N., Tetko, I.V., Baskin, I.I., and Solov'ev, V.P., *J. Chem. Inf. Mod.*, 47 **2007** 1111-1122.

52 Bini, R., Malvaldi, M., Pitner, W.R., and Chiappe, C., *J. Phys. Org. Chem.*, 21 **2008** 622-629.

53 Kula, M.-R., Kroner, K.H., and Hustedt, H., *Purification of enzymes by liquid-liquid extraction*, in *Reaction Engineering*, **1982**, Springer Berlin / Heidelberg: 73-118.

54 Banik, R.M., Santhiagu, A., Kanari, B., Sabarinath, C., and Upadhyay, S.N., *World J. of Microbiol. Biotechnol.*, 19 **2003** 337-348.

55 Silva, M.E. and Franco, T.T., *Braz. J. Chem. Eng.*, 17 **2000** 1-17.

56 Pei, Y., Wang, J., Liu, L., Wu, K., and Zhao, Y., *J. Chem. Eng. Data*, 52 **2007** 2026-2031.

57 Gutowski, K.E., Broker, G.A., Willauer, H.D., Huddleston, J.G., Swatloski, R.P., Holbrey, J.D., and Rogers, R.D., *J. Am. Chem. Soc.*, 125 **2003** 6632-6633.

58 Bridges, N.J., Gutowski, K.E., and Rogers, R.D., *Green Chem.*, 9 **2007** 177-183.

59 Visak, Z.P., Lopes, J.N.C., and Rebelo, L.P.N., *Monatsh. Chem.*, 138 **2007** 1153-1157.

60 Zafarani-Moattar, M.T. and Hamzehzadeh, S., *J. Chem. Eng. Data*, 52 **2007** 1686-1692.

61 Wu, B., Zhang, Y.M., and Wang, H.P., *J. Phys. Chem. B*, 112 **2008** 6426-6429.

62 Wu, B., Zhang, Y.M., and Wang, H.P., *J. Chem. Eng. Data*, 53 **2008** 983-985.

63 Wu, B., Zhang, Y.M., Wang, H.P., and Yang, L.L., *J. Phys. Chem. B*, 112 **2008** 13163-13165.

64 Zhang, Y.Q., Zhang, S.J., Chen, Y.H., and Zhang, J.M., *Fluid Phase Equilib.*, 257 **2007** 173-176.

65 He, C., Li, S., Liu, H., Li, K., and Liu, F., *J. Chromatogr. A*, 1082 **2005** 143-149.

66 Li, S., He, C., Liu, H., Li, K., and Liu, F., *J. Chromatogr. B*, 826 **2005** 58-62.

67 Liu, Q.F., Yu, J., Li, W.L., Hu, X.S., Xia, H.S., Liu, H.Z., and Yang, P., *Sep. Sci. Technol.*, 41 **2006** 2849-2858.

68 Merchuk, J.C., Andrews, B.A., and Asenjo, J.A., *Journal of Chromatography B: Biomedical Sciences and Applications*, 711 **1998** 285-293.

69 Galaev, I.Y. and Mattiasson, B., *Enzyme Microb. Technol.*, 15 **1993** 354-366.

70 Willauer, H.D., Huddleston, J.G., and Rogers, R.D., *Ind. Eng. Chem. Res.*, 41 **2002** 1892-1904.

71 Deng, Y., Chen, J., and Zhang, D., *J. Chem. Eng. Data*, 52 **2007** 1332-1335.

72 Chethana, S., Rastogi, N.K., and Raghavarao, K., *Biotechnol. Lett.*, 28 **2006** 25-28.

73 Closs, C.B., Conde-Petit, B., Roberts, I.D., Tolstoguzov, V.B., and Escher, F., *Carbohydr. Polym.*, 39 **1999** 67-77.

74 Rogers, R.D. and Bauer, C.B., *Journal of Chromatography B: Biomedical Sciences and Applications*, 680 **1996** 237-241.

75 Freire, M.G., Carvalho, P.J., Silva, A.M.S., Santos, L.M.N.B.F., Rebelo, L.P.N., Marrucho, I.M., and Coutinho, J.A.P., *J. Phys. Chem. B*, 113 **2009** 202-211.

76 Tome, L.I.N., Varanda, F.R., Freire, M.G., Marrucho, I.M., and Coutinho, J.A.P., *J. Phys. Chem. B*, 113 **2009** 2815-2825.

77 Hofmeister, F., *Arch. Exp. Pathol. Pharmakol.*, XXV **1888** 1.

78 Baker, S.N., Baker, G.A., and Bright, F.V., *Green Chem.*, 4 **2002** 165-169.

79 Reichardt, C., *Chem. Rev.*, 94 **1994** 2319-2358.

80 Kamlet, M.J. and Taft, R.W., *J. Am. Chem. Soc.*, 98 **1976** 377-383.

81 Aki, S., Brennecke, J.F., and Samanta, A., *Chem. Commun.*, **2001** 413-414.

82 Reichardt, C., *Green Chem.*, 7 **2005** 339-351.

83 Lungwitz, R., Friedrich, M., Linert, W., and Spange, S., *New J. Chem.*, 32 **2008** 1493-1499.

84 Huddleston, J.G., Willauer, H.D., and Rogers, R.D., *J. Chem. Eng. Data*, 48 **2003** 1230-1236.

85 Lu, M. and Tjerneld, F., *J. Chromatogr. A*, 766 **1997** 99-108.

86 Salabat, A., Abnosi, M.H., and Motahari, A., *J. Chem. Eng. Data*, 53 **2008** 2018-2021.

87 Zhao, H., *J. Chem. Technol. Biotechnol.*, 81 **2006** 877-891.

88 Wang, J.J., Pei, Y.C., Zhao, Y., and Hu, Z.G., *Green Chem.*, 7 **2005** 196-202.

89 Fan, J., Fan, Y., Pei, Y., Wu, K., Wang, J., and Fan, M., *Sep. Purif. Technol.*, 61 **2008** 324-331.

7

List of Publications

Co-author in:

- Mara G. Freire, Catarina M. S. S. Neves, Isabel M. Marrucho, João A. P. Coutinho, Ana M. Fernandes; *Hydrolysis of Tetrafluoroborate and Hexafluorophosphate as Counter Anions in Imidazolium-Based Ionic Liquids*, **J. Phys. Chem. B** (2009) accepted.
- Sonia P. M. Ventura, Catarina M. S. S. Neves, Mara G. Freire, Isabel M. Marrucho, João A. P. Coutinho; *Evaluation of Anion Influence on the Formation and Extraction Capacity of Ionic-Liquid-Based Aqueous Biphasic Systems*, **J. Phys. Chem. B** (2009) doi:10.1021/jp903286d.
- Catarina M. S. S. Neves, Sonia P. M. Ventura, Mara G. Freire, Isabel M. Marrucho, João A. P. Coutinho; *Evaluation of Cation Influence on the Formation and Extraction Capability of Ionic-Liquid-Based Aqueous Biphasic Systems*, **J. Phys. Chem. B** 113 (2009) 5194-5199 doi:10.1021/jp900293v.
- Mara G. Freire, Catarina M. S. S. Neves, Pedro J. Carvalho, Ramesh L. Gardas, Ana M. Fernandes, Isabel M. Marrucho, Luis M. N. B. F. Santos and Joao A. P. Coutinho; *Mutual Solubilities of Water and Hydrophobic Ionic Liquids*, **J. Phys. Chem. B** 111 (45) (2007) 13082-13089 doi:10.1021/jp076271e.

Acknowledgements in:

- Pedro J. Carvalho, Víctor H. Álvarez, Bernd Schröder, Ana M. Gil, Isabel M. Marrucho, Martín Aznar, Luís M. N. B. F. Santos, João A. P. Coutinho; *Specific Solvation Interactions of CO2 on Acetate and Trifluoroacetate Imidazolium Based Ionic Liquids at High Pressures*, **J. Phys. Chem. B** 113 (2009) 6803-6812 doi:10.1021/jp901275b.
- Luciana I. N Tomé, Fatima R. Varanda, Mara G. Freire, Isabel M. Marrucho and João A. P. Coutinho; *Towards an understanding of the mutual solubilities of water and hydrophobic ionic liquids in the presence of salts: The anion effect*, **J. Phys. Chem. B** 113 (2009) 2815-2825 doi:10.1021/jp810141d.

- Mara G. Freire, Pedro J. Carvalho, Ramesh L. Gardas, Isabel M. Marrucho, Luis M. N. B. F. Santos and João A. P. Coutinho; *Mutual Solubilities of Water and the [$C_n$mim][Tf_2N] Hydrophobic Ionic Liquids*, **J. Phys. Chem. B** 112 (2008) 1604-1610 doi:10.1021/jp7097203.

Appendix A

1. Synthesis of IL

1, 3-dimethylimidazolium bis(trifluoromethylsulfonyl)imide synthesis. 1,3-dimethylimidazolium bis(triflyl)imide ($[C_1mim][Tf_2N]$) has been synthesized by means of Carbonate Based Ionic Liquid Synthesis (CBILS©), of proionic/ Sigma Aldrich[1]. 1,3-dimethylimidazolium hydrogencarbonate (the CBIL precursor as a 45.91 % solution in H_2O : Methanol (3:2)) has been treated with an exact stoichiometric amount of lithium bis(triflyl)imide (Sigma Aldrich). The precipitate of lithium carbonate formed during reaction was filtered off, and water and methanol was removed by rotary evaporation, leaving $[C_1mim][Tf_2N]$ liquid.

References

1
http://www.sigmaaldrich.com/Area_of_Interest/Chemistry/Chemical_Synthesis/Product_Highlights/CBILS.html in 14th Febuary 2008.

2. NMR Spectrum

[C_3mim][PF_6]

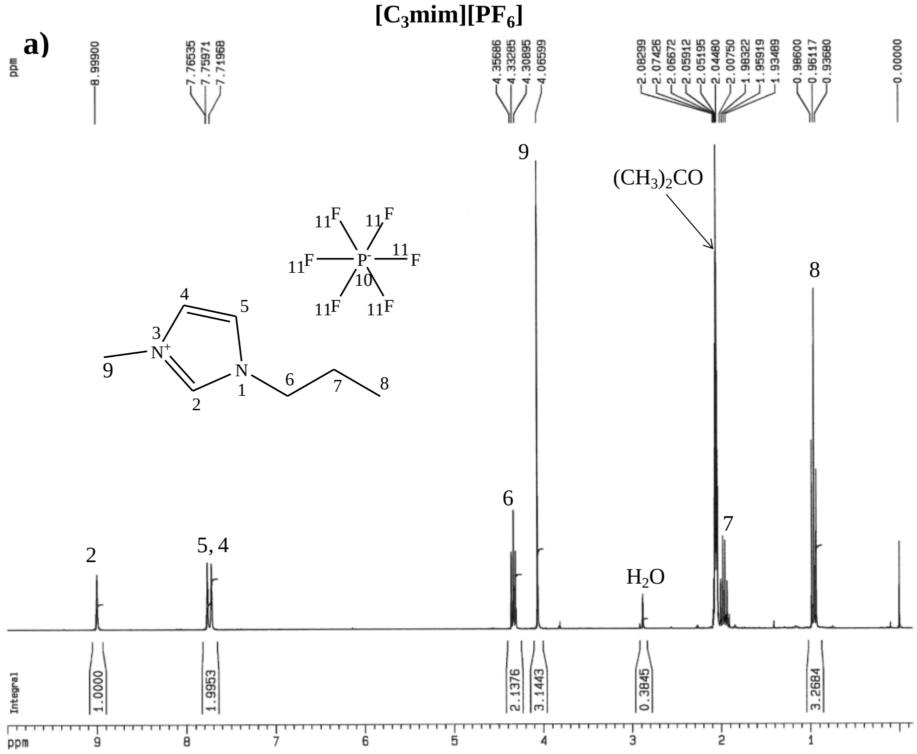

[C_3mim][PF_6]

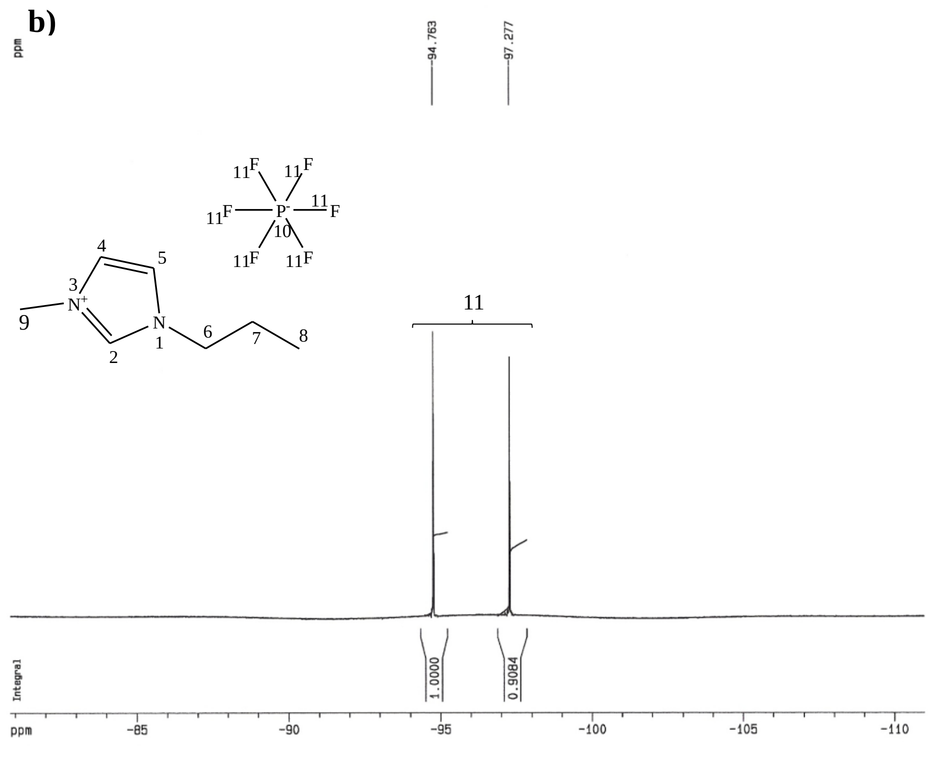

Figure A 1. NMR Spectra of [C_3mim][PF_6]: a) ^{1}H; b) ^{19}F.

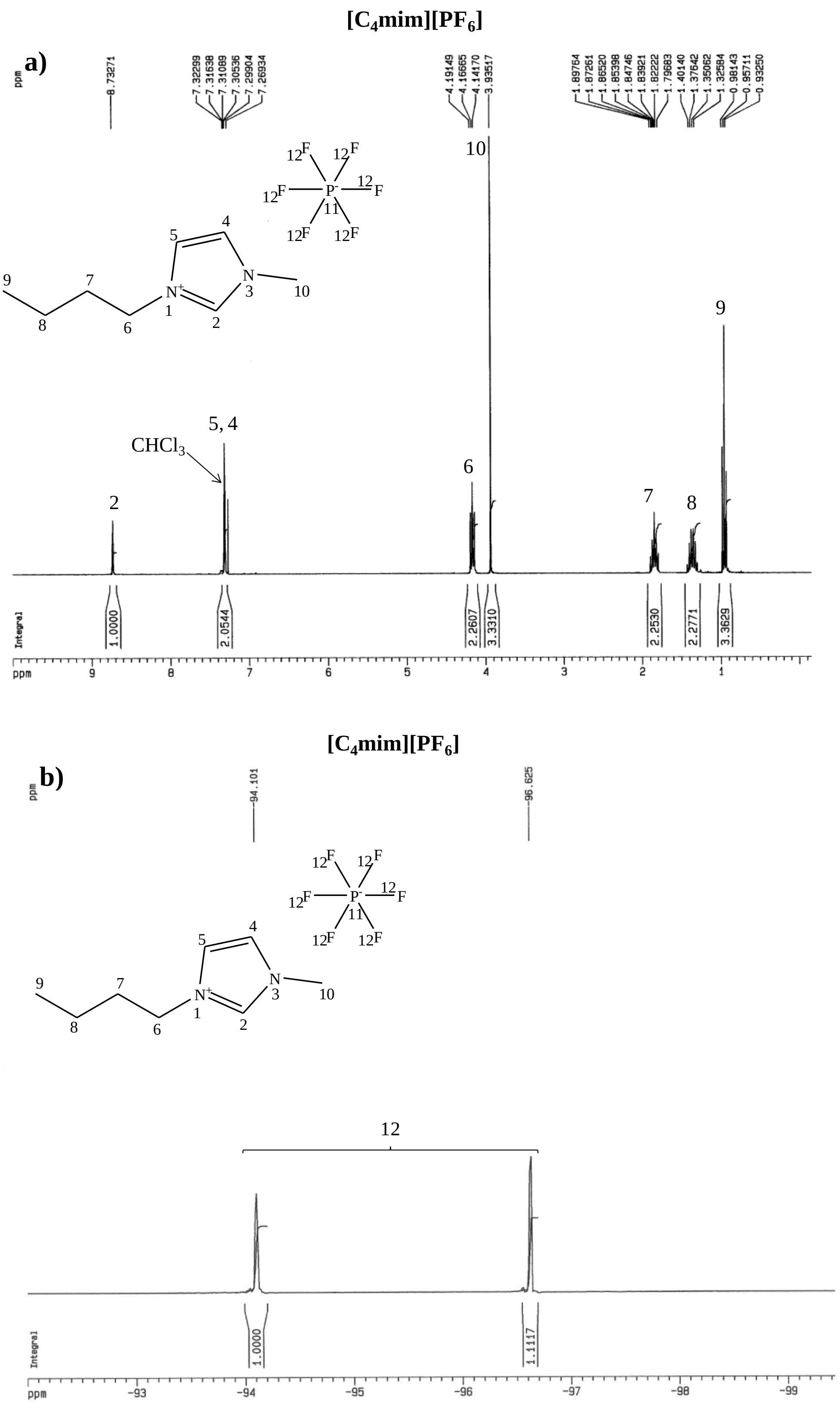

Figure A 2. NMR Spectra of [C$_4$mim][PF$_6$]: a) ^{1}H; b) ^{19}F.

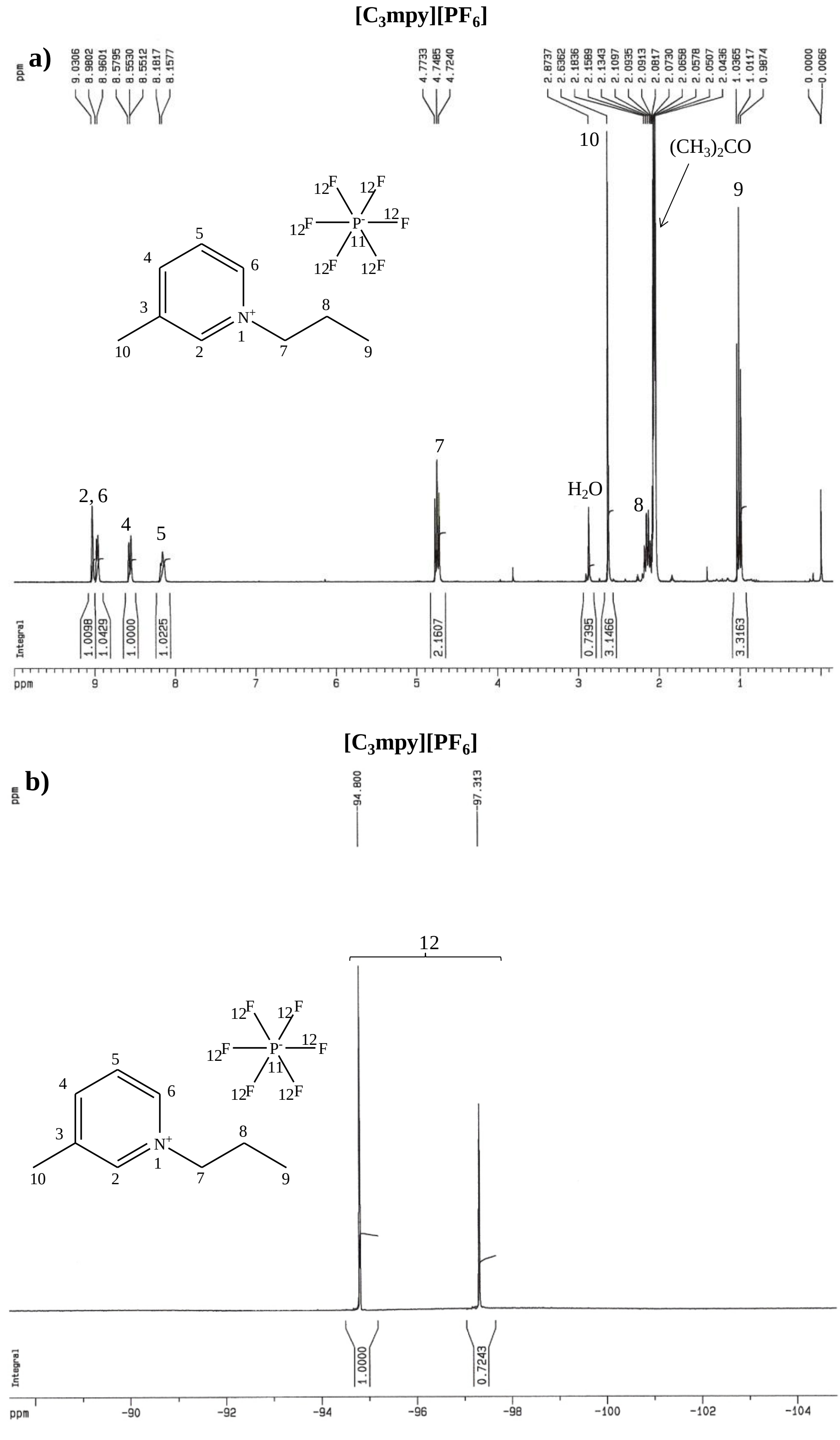

Figure A 3. NMR Spectra of [C_3mpy][Tf_2N]: a) ^1H; b) ^{19}F.

[C_1mim][Tf_2N]

a)

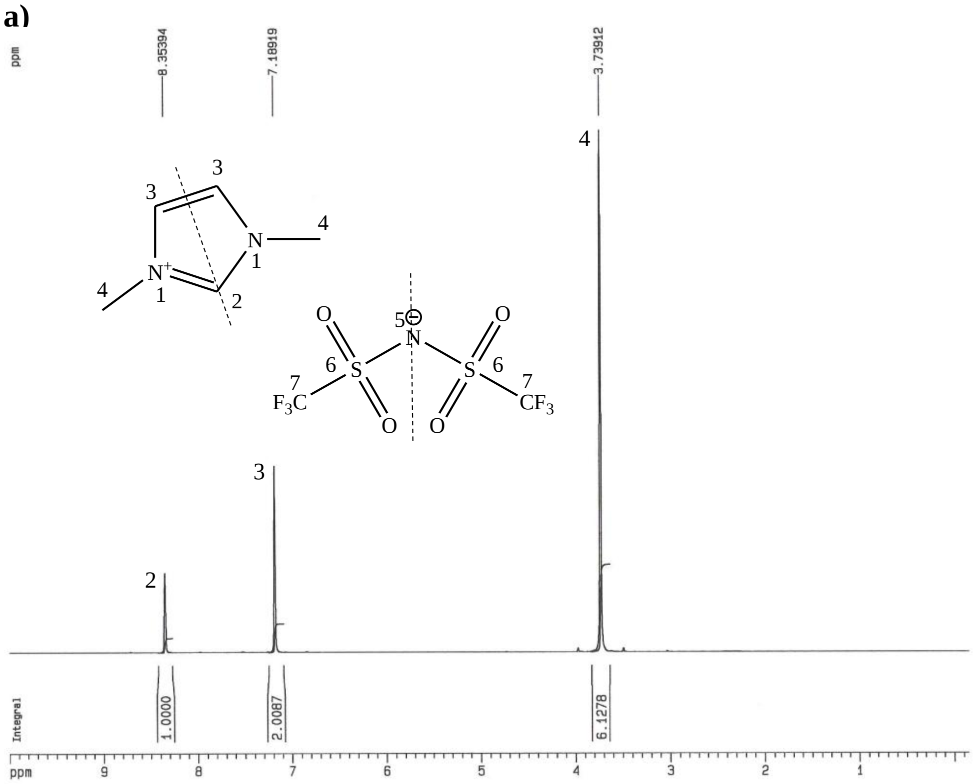

[C_1mim][Tf_2N]

b)

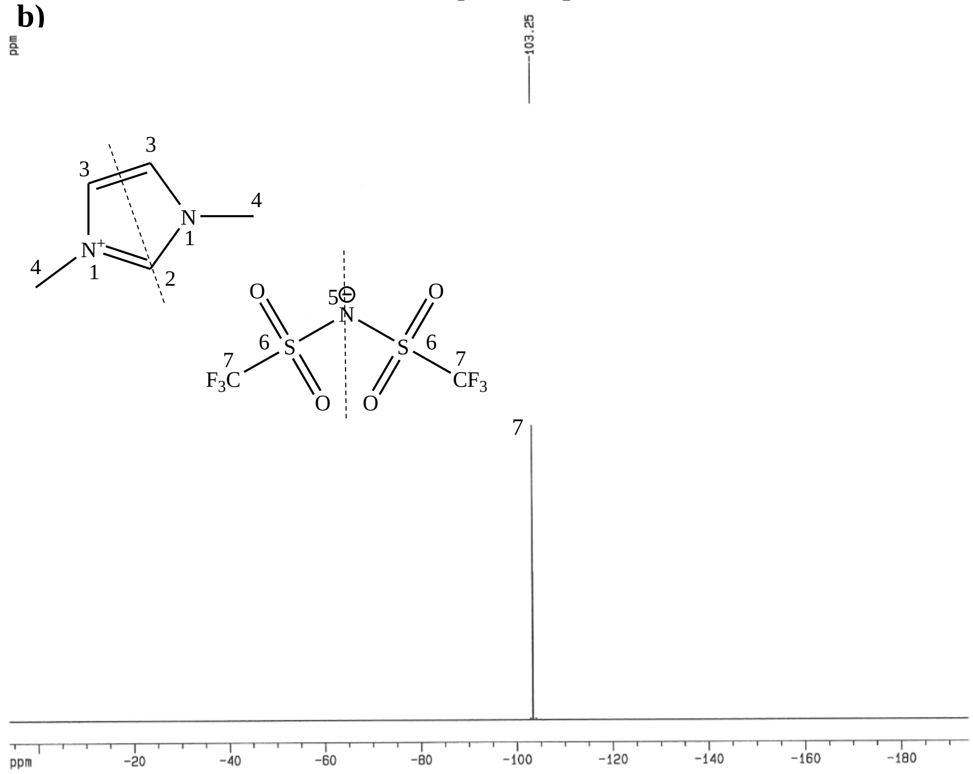

Figure A 4. NMR Spectra of [C_1mim][Tf_2N]: a) ^{1}H; b) ^{19}F.

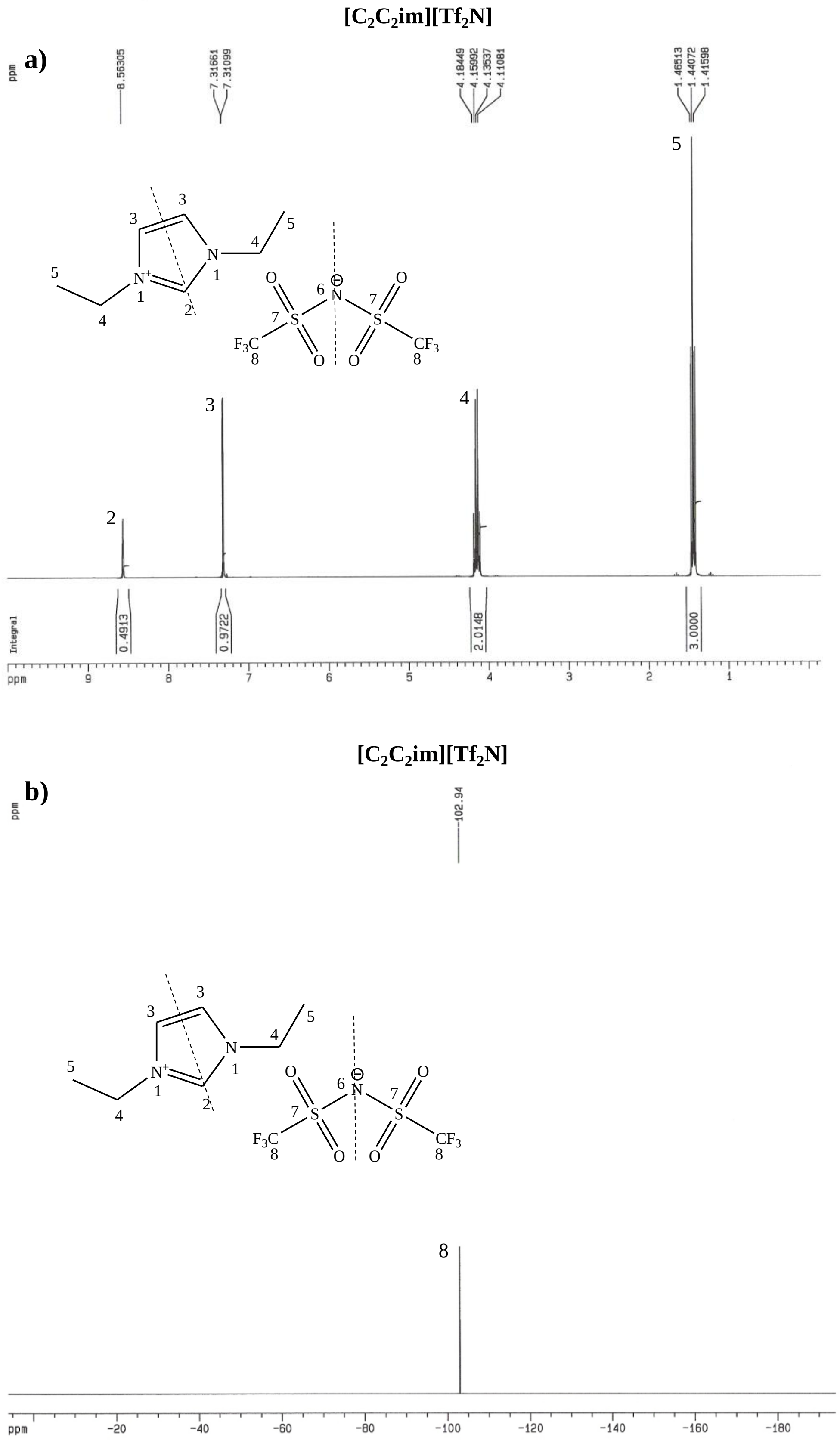

Figure A 5. NMR Spectra of $[C_2C_2im][Tf_2N]$: a) ^1H; b) ^{19}F.

[C_4C_1mim][Tf_2N]

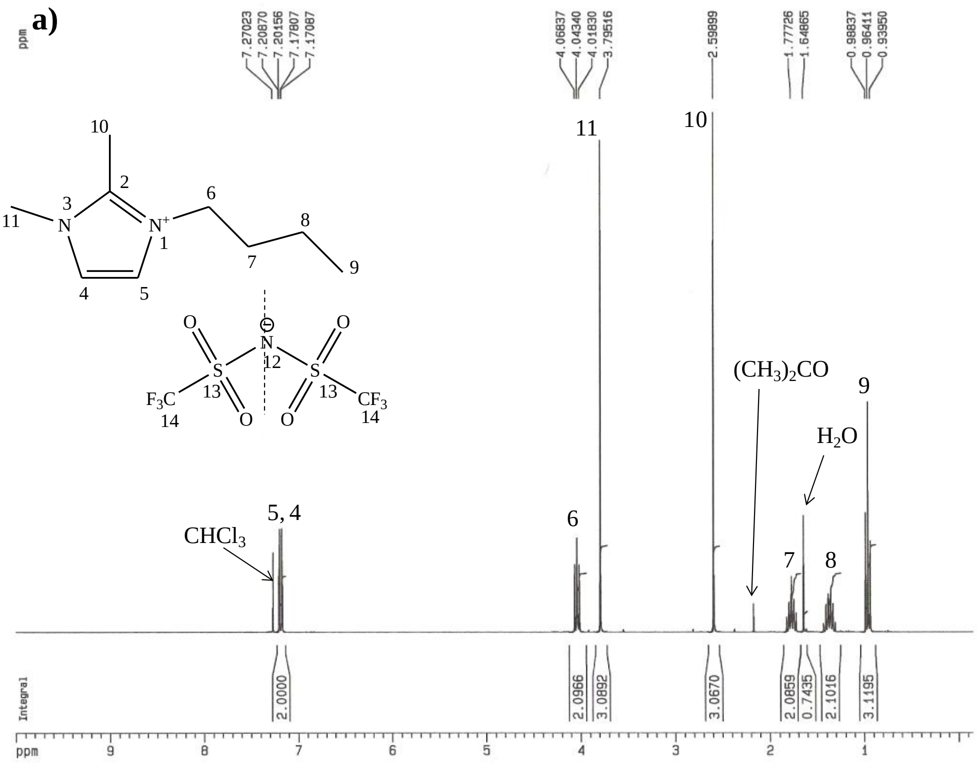

[C_4C_1mim][Tf_2N]

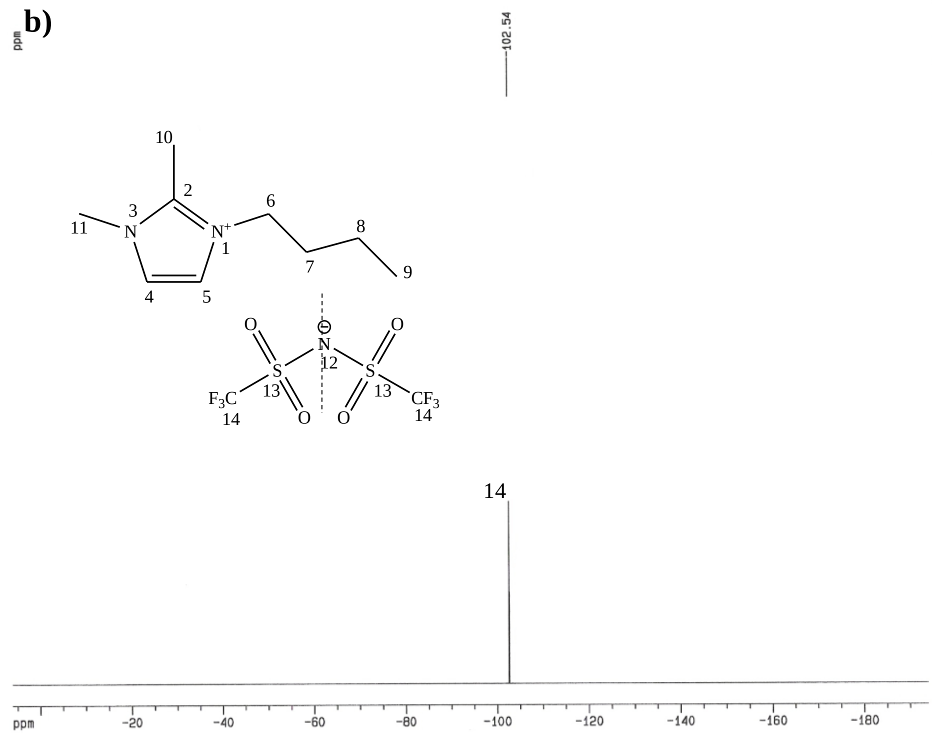

Figure A 6. NMR Spectra of [C_4C_1mim][Tf_2N]: a) ^{1}H; b) ^{19}F.

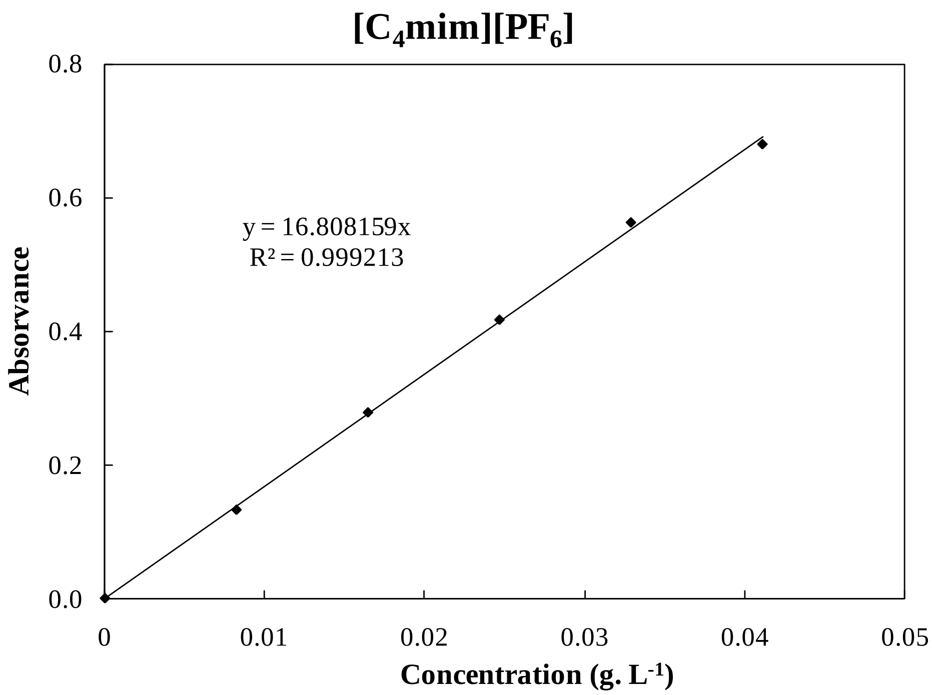

Figure A 7. Calibration curve for [C_4 mim][PF_6].

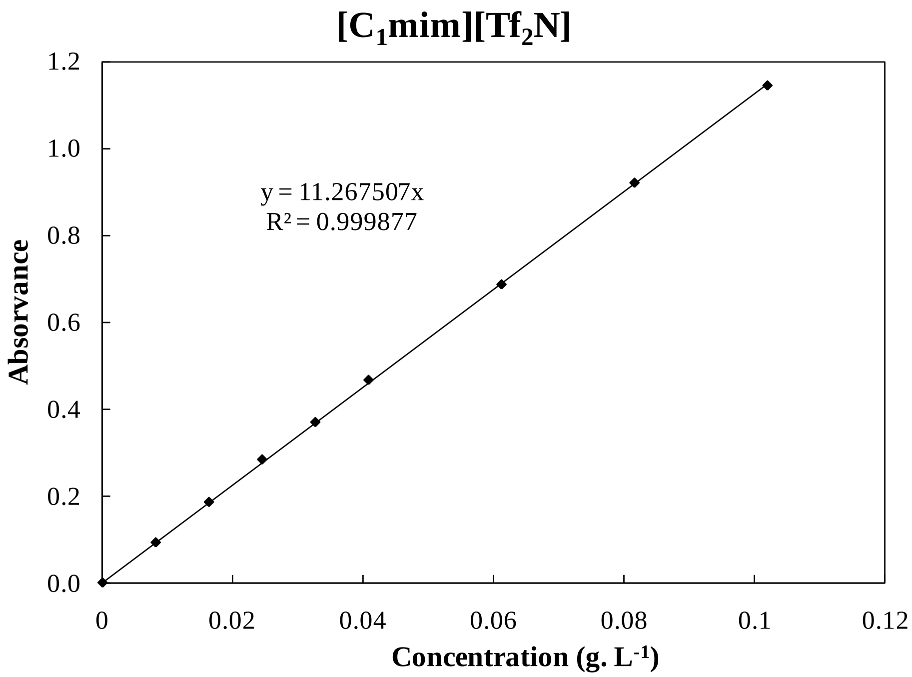

Figure A 8. Calibration curve for [C_1mim][Tf_2N].

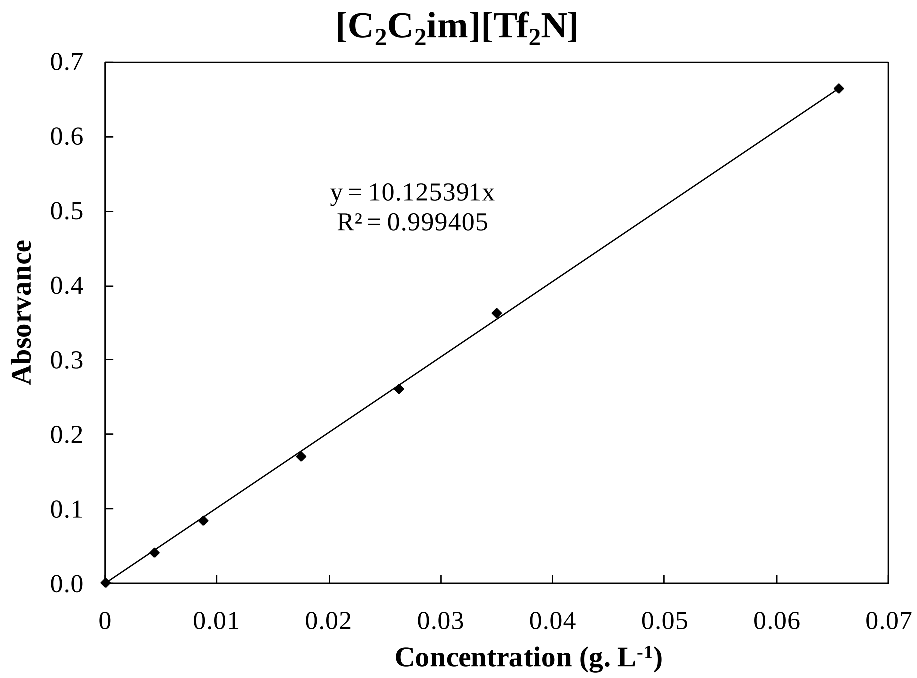

Figure A 9. Calibration curve for $[C_2C_2im][Tf_2N]$.

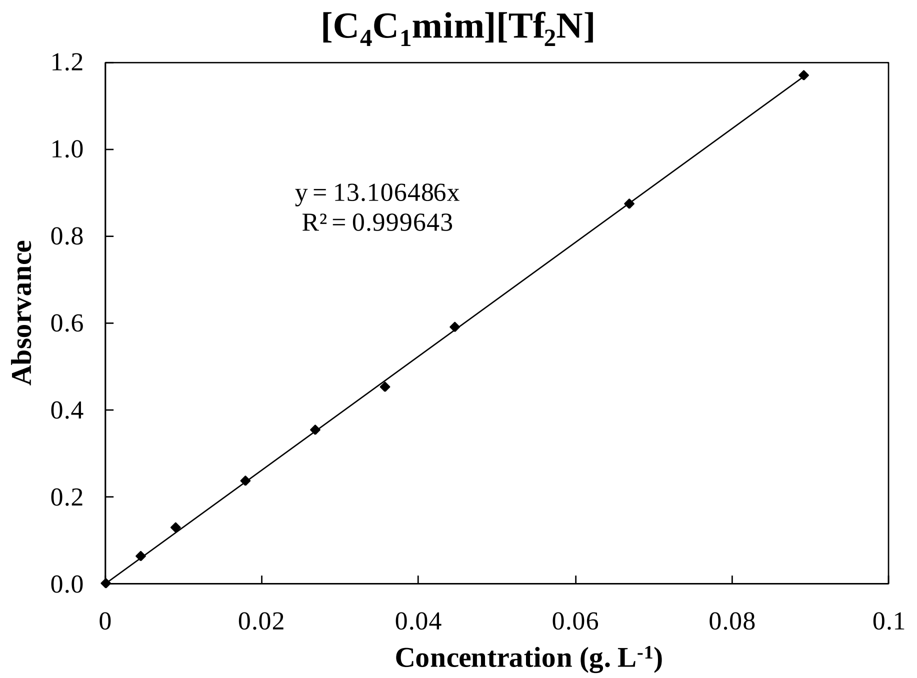

Figure A 10. Calibration curve for $[C_4\ C_1mim][Tf_2N]$.

Appendix B

1. Synthesis of IL

1,3-dimethylimidazolium chloride synthesis. 1,3-dimethylimidazolium chloride ($[C_1im]Cl$) has been synthesized by means of Carbonate Based Ionic Liquid Synthesis (CBILS©) of proionic / Sigma Aldrich.[1] 1,3-dimethylimidazolium hydrogenocarbonate (the CBIL precursor as a 45.91 % solution in H_2O : Methanol (3:2)) has been treated with an exact stoichiometric amount of hydrochloric acid (FIXANAL / Riedel-de Haën). After the evolution of CO_2 ceased, the solvents have been removed in vacuum, leaving white crystals of $[C_1im]Cl$.

References

1
http://www.sigmaaldrich.com/Area_of_Interest/Chemistry/Chemical_Synthesis/Product_H Highlight/CBILS.html in 14th February 2008.

2. NMR Spectrum

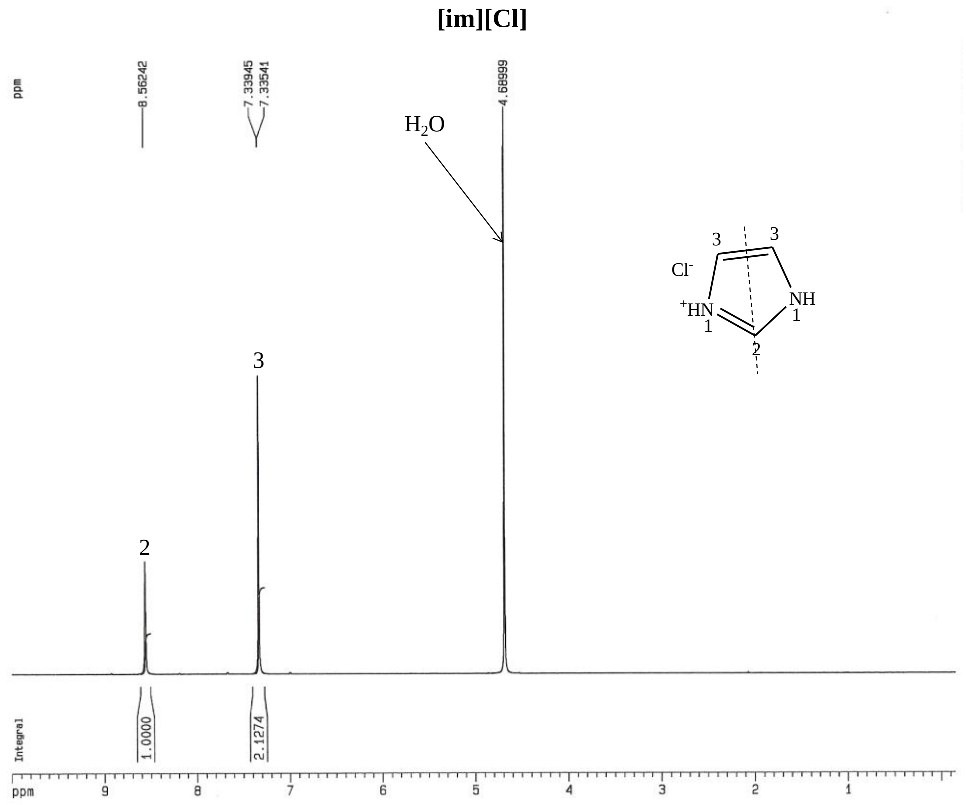

Figure B 1. ^{1}H NMR Spectra of [im][Cl].

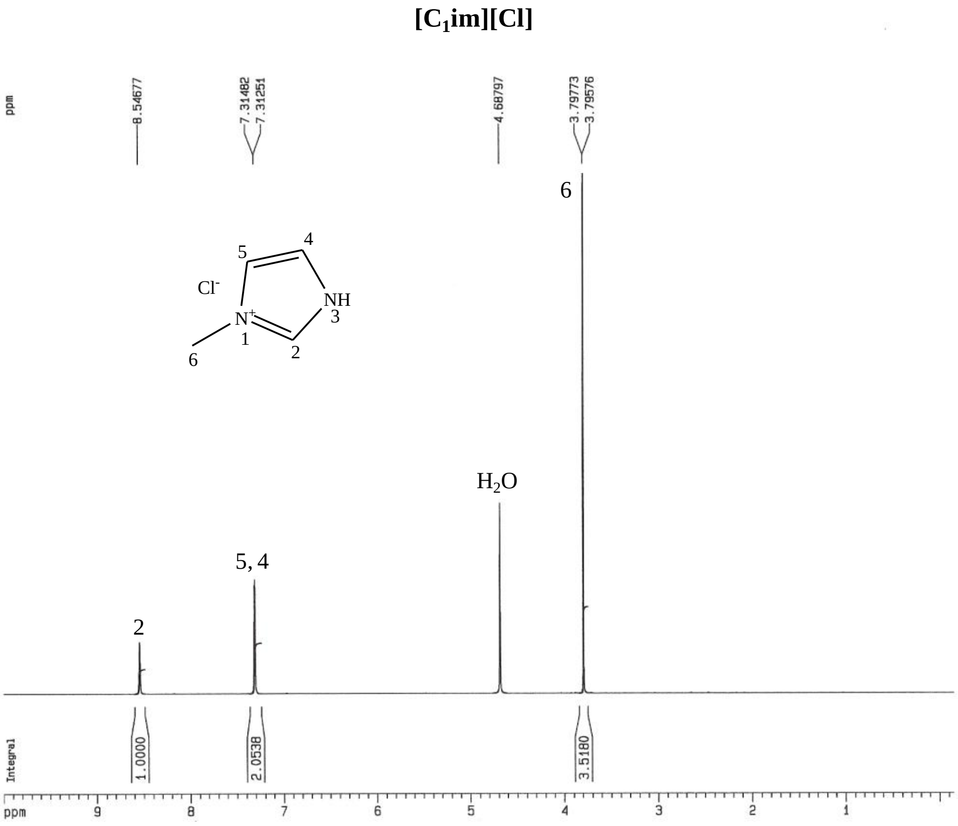

Figure B 2. [1]H NMR Spectra of $[C_1im][Cl]$.

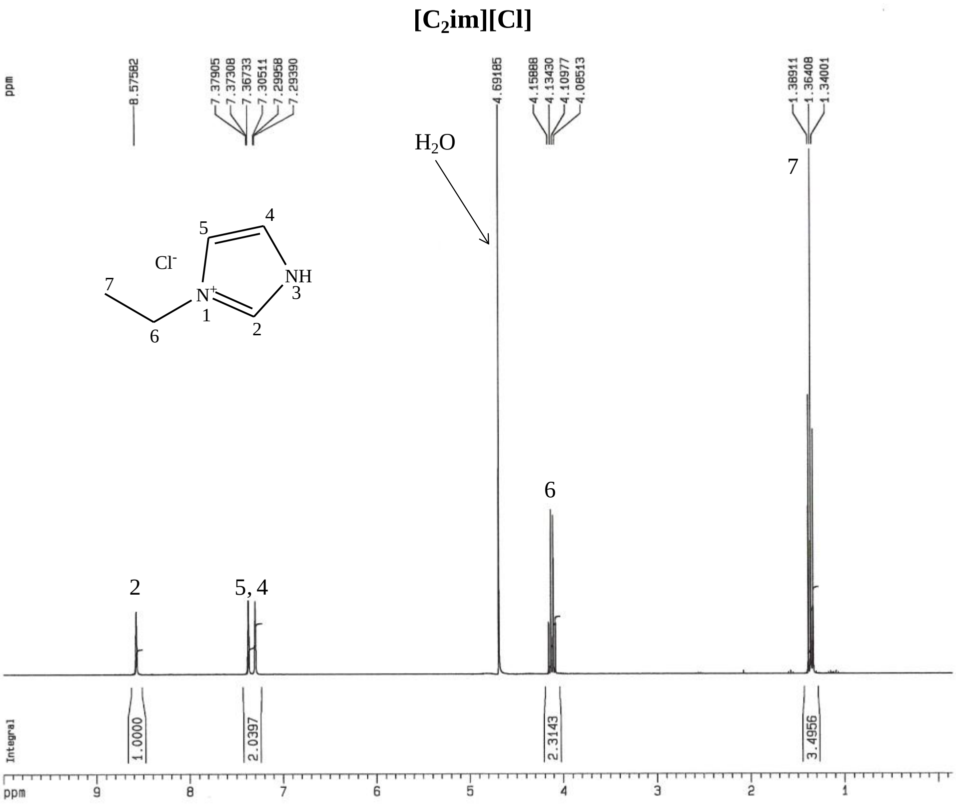

Figure B 3. [1]H NMR Spectra of $[C_2im][Cl]$.

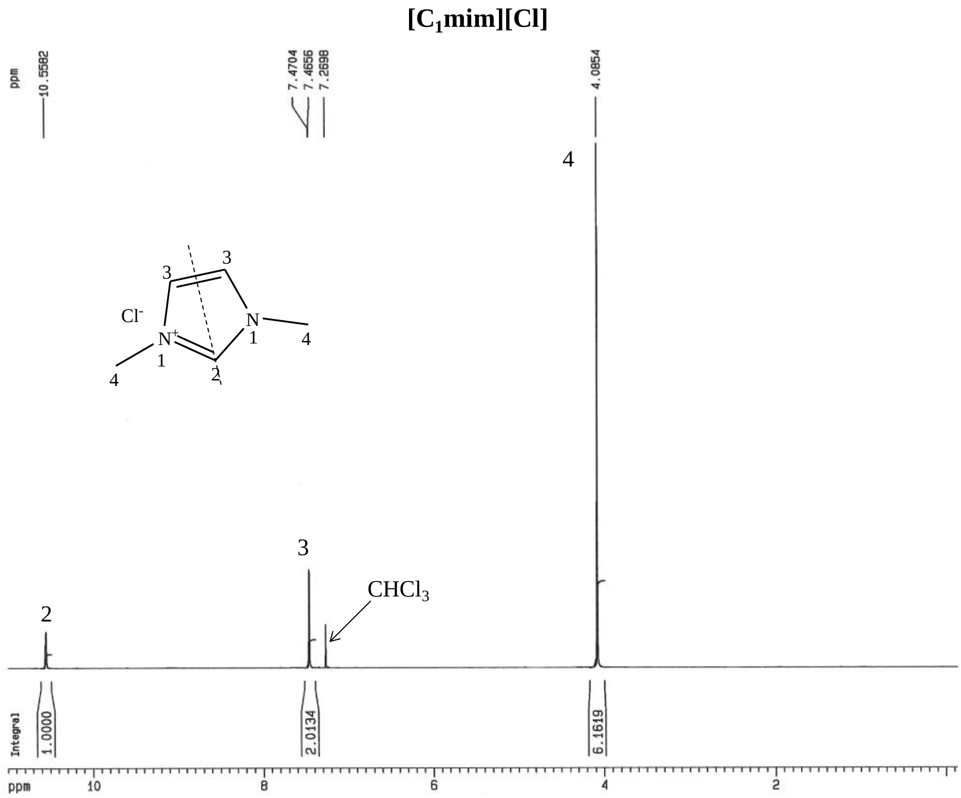

Figure B 4. ^{1}H NMR Spectra of $[C_1mim][Cl]$.

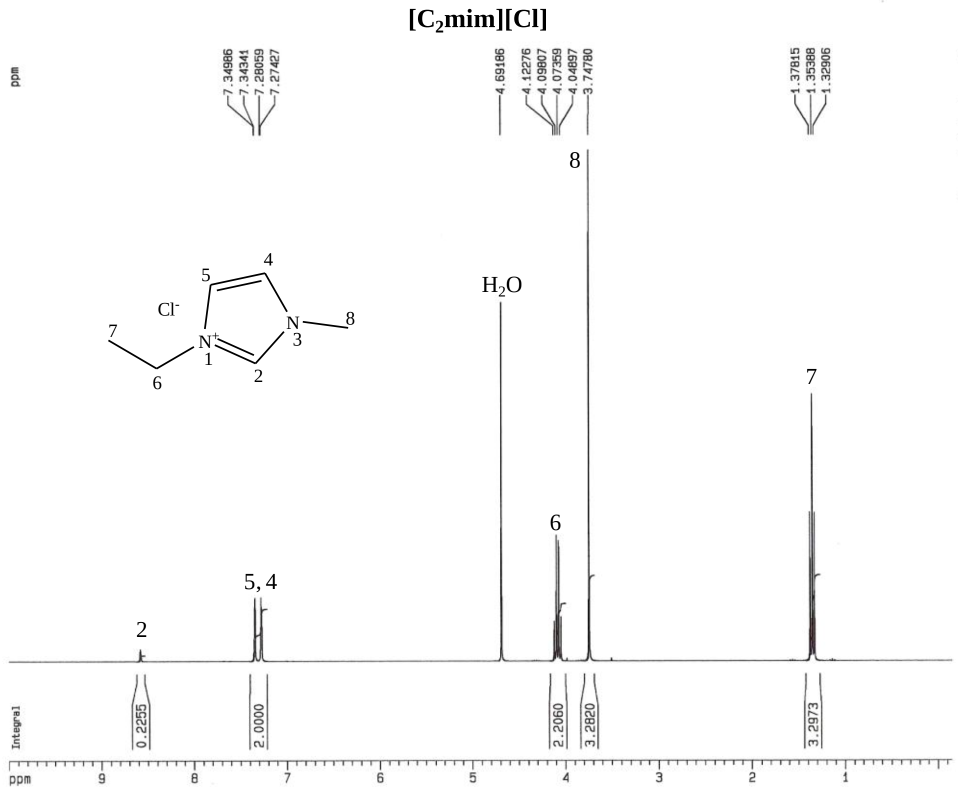

Figure B 5. ^{1}H NMR Spectra of $[C_2mim][Cl]$.

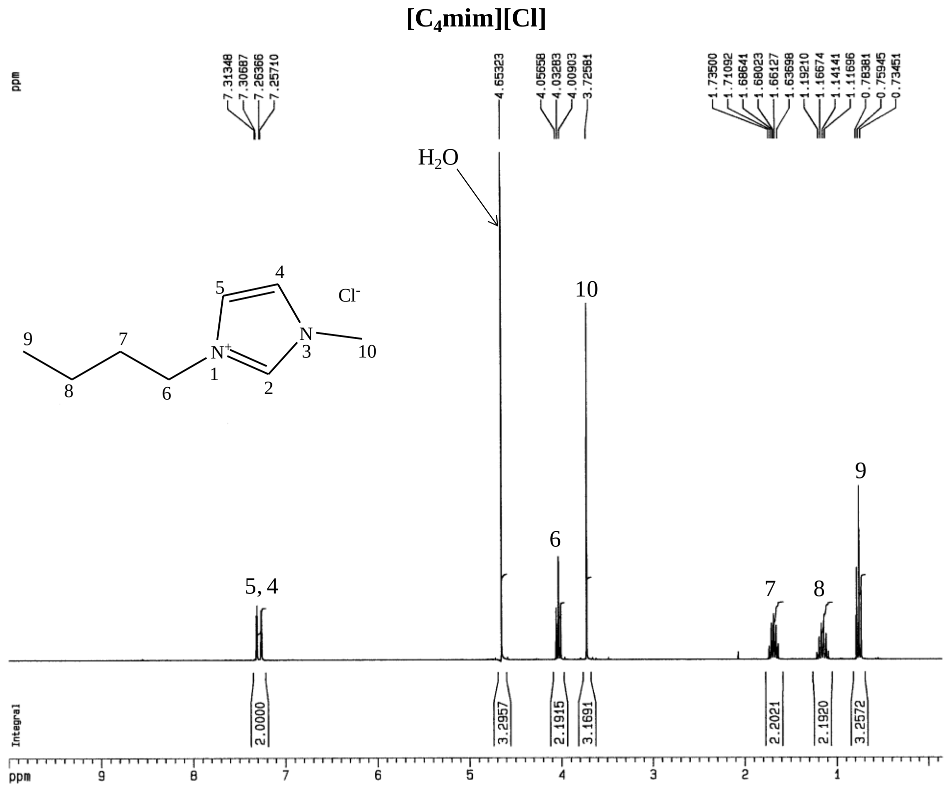

Figure B 6. ^{1}H NMR Spectra of [C$_4$mim][Cl].

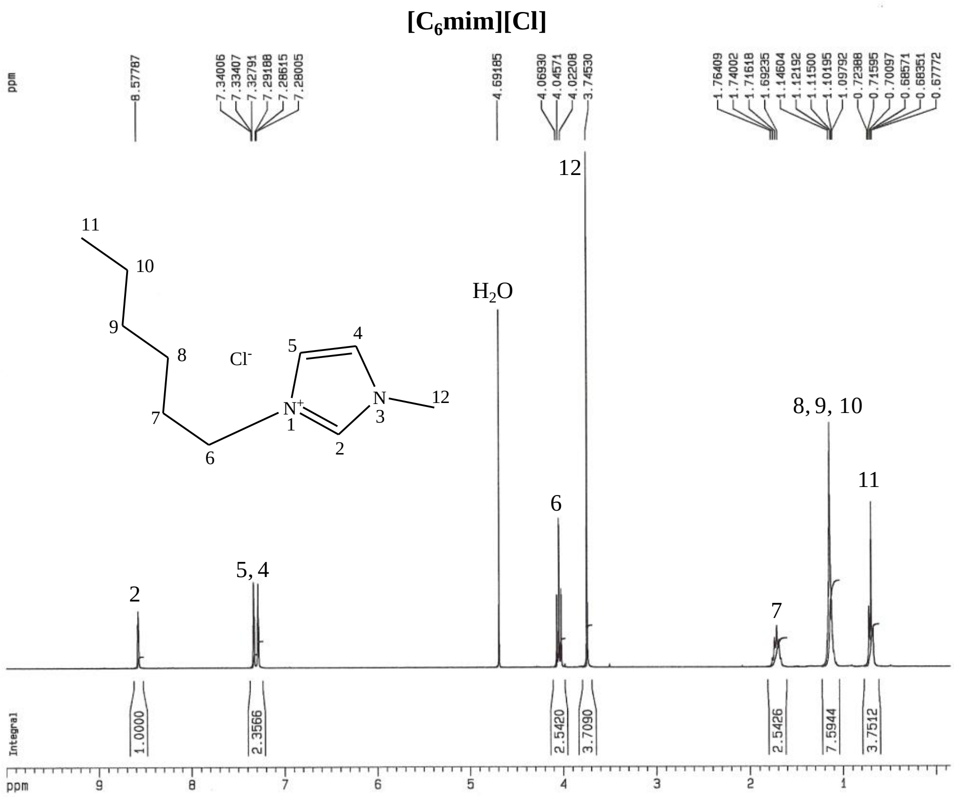

Figure B 7. ^{1}H NMR Spectra of [C$_6$mim][Cl].

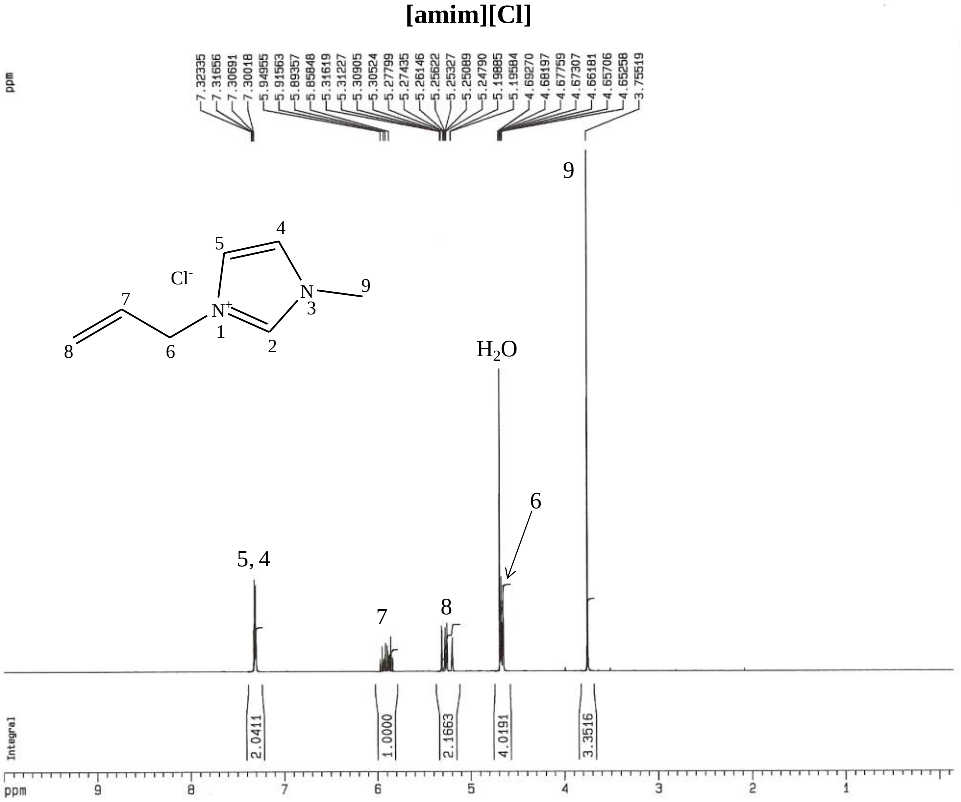

Figure B 8. ^{1}H NMR Spectra of [amim][Cl].

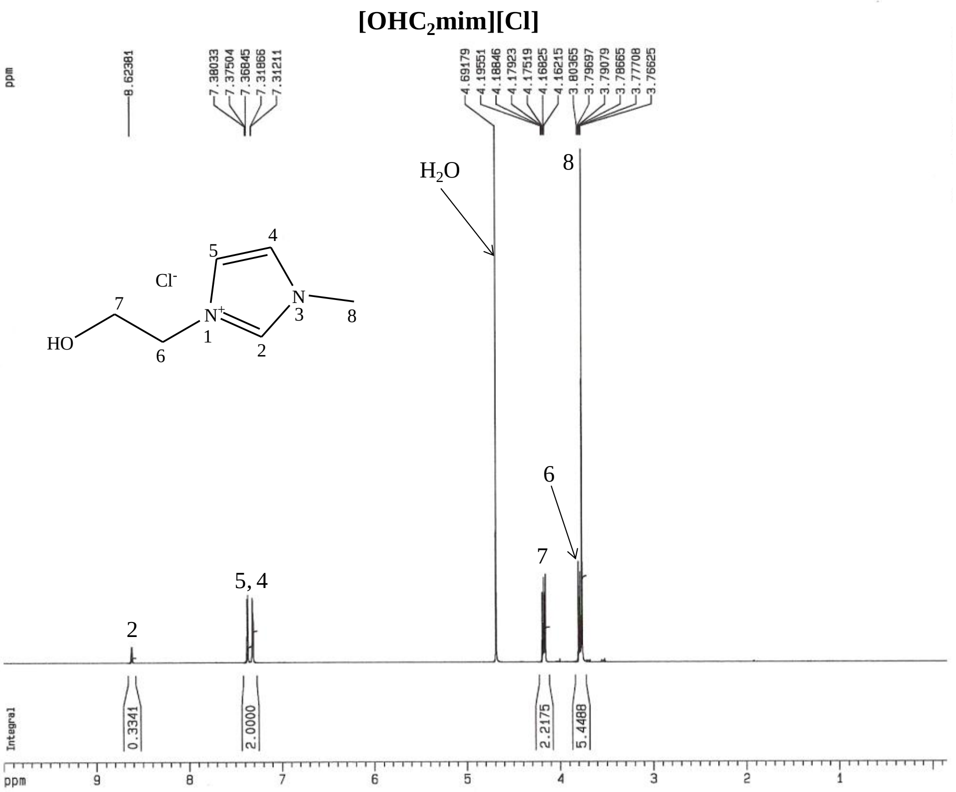

Figure B 9. ^{1}H NMR Spectra of $[OHC_2mim][Cl]$.

$[C_7H_7mim][Cl]$

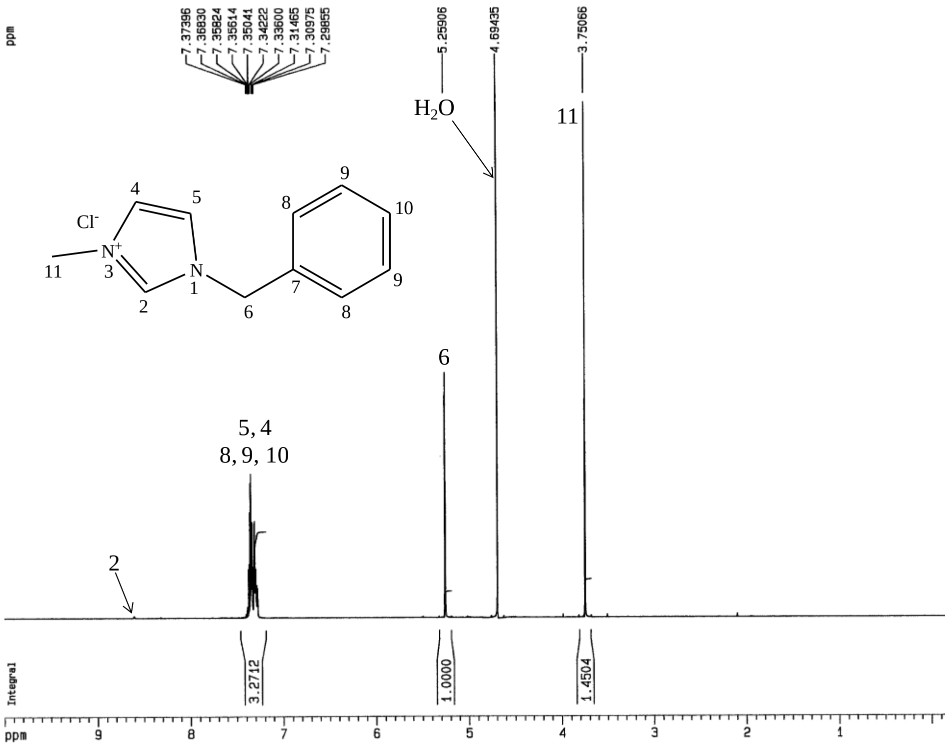

Figure B 10. ^{1}H NMR Spectra of $[C_7H_7mim][Cl]$.

$[C_2mim][Br]$

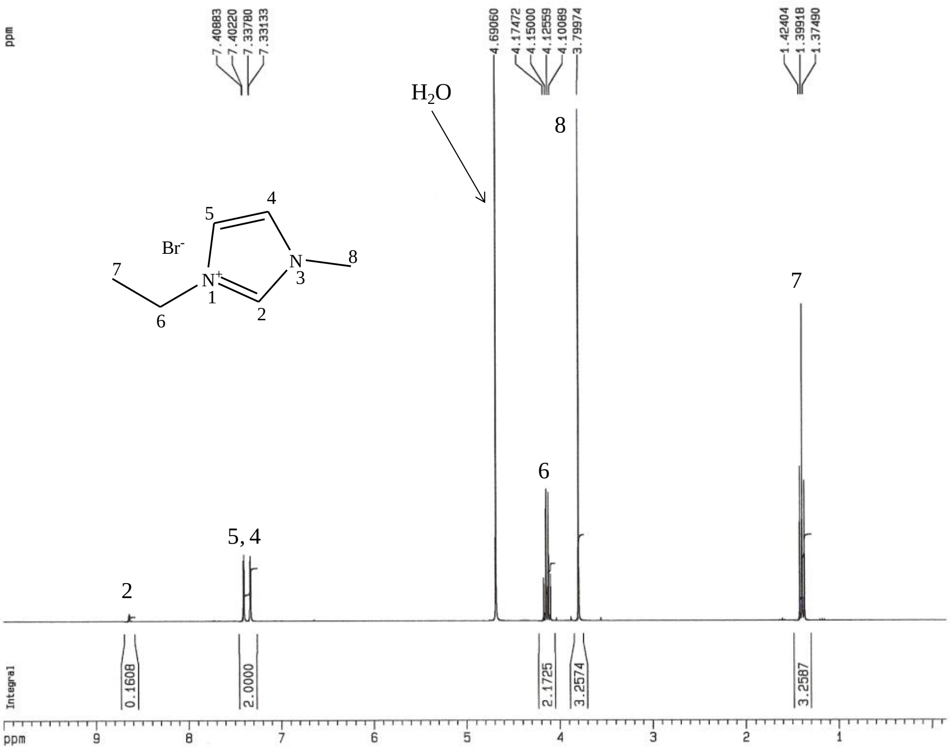

Figure B 11. ^{1}H NMR Spectra of $[C_2mim][Br]$.

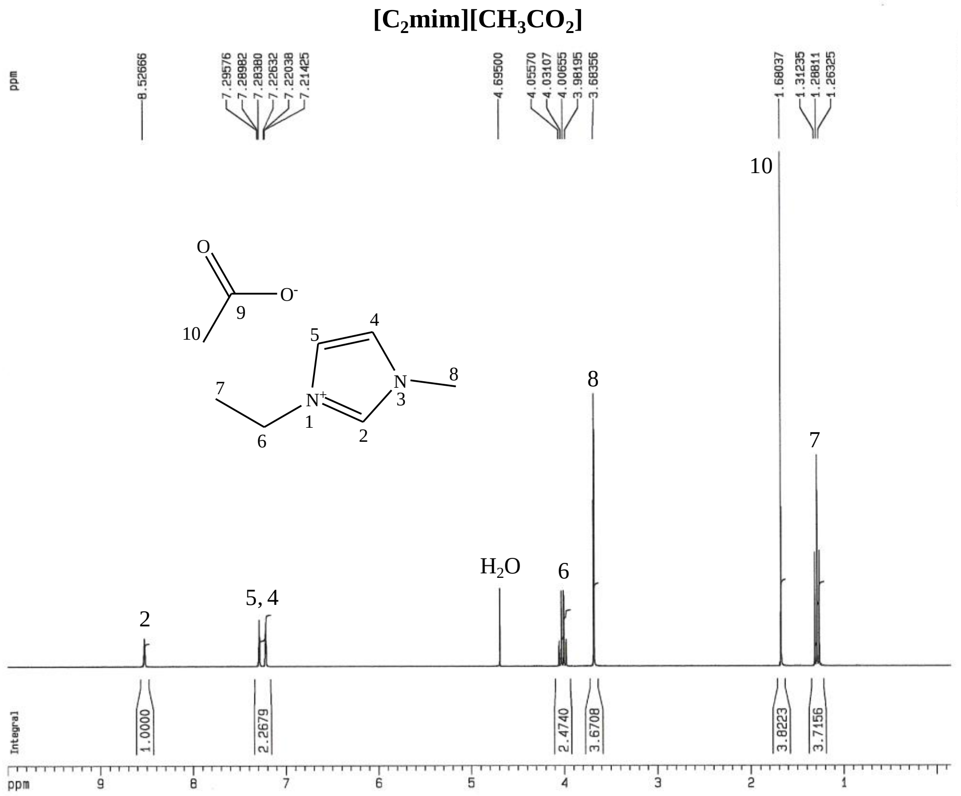

Figure B 12. ^{1}H NMR Spectra of $[C_2mim][CH_3CO_2]$.

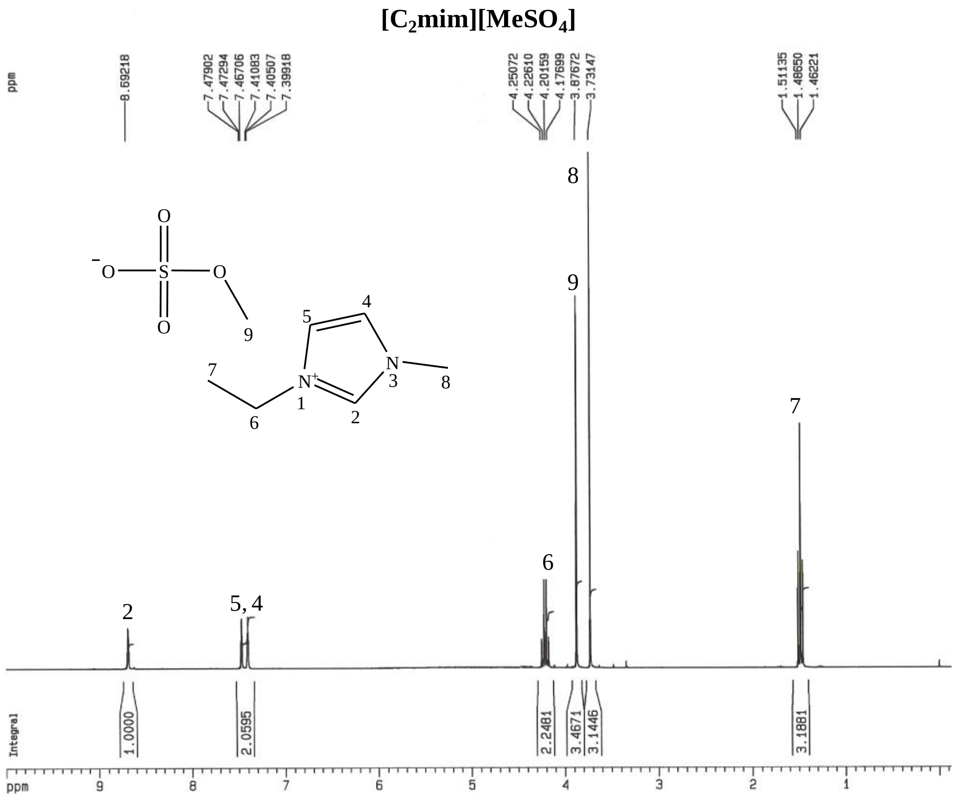

Figure B 13. ^{1}H NMR Spectra of $[C_2mim][MeSO_4]$.

[C_2mim][$EtSO_4$]

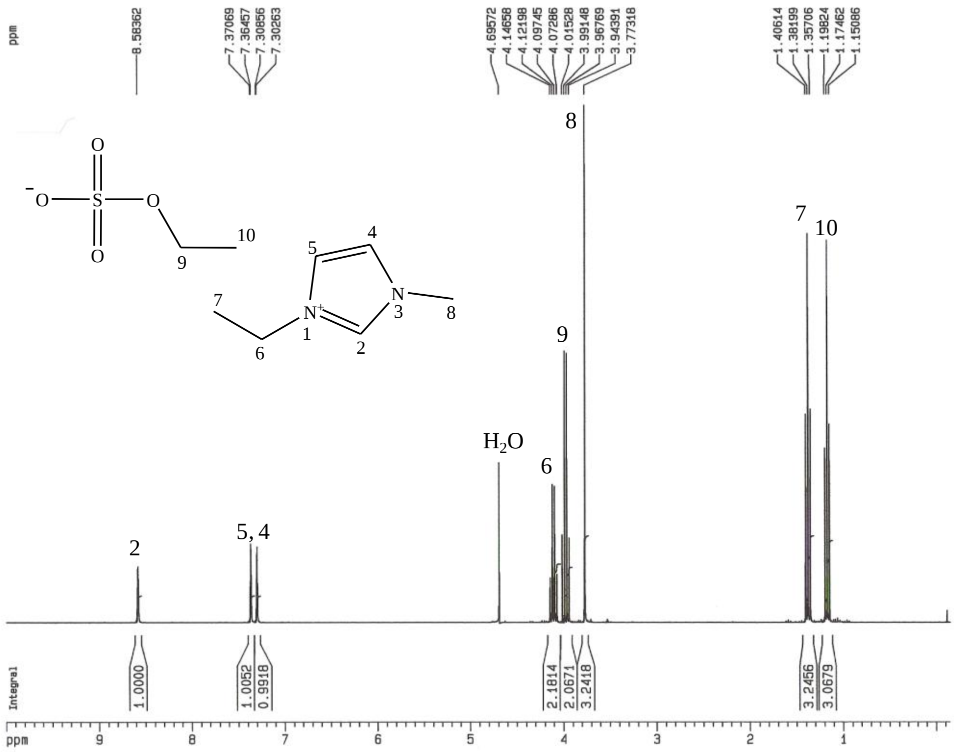

Figure B 14. ^{1}H NMR Spectra of [C_2mim][$EtSO_4$].

[C_2mim][CH_3SO_3]

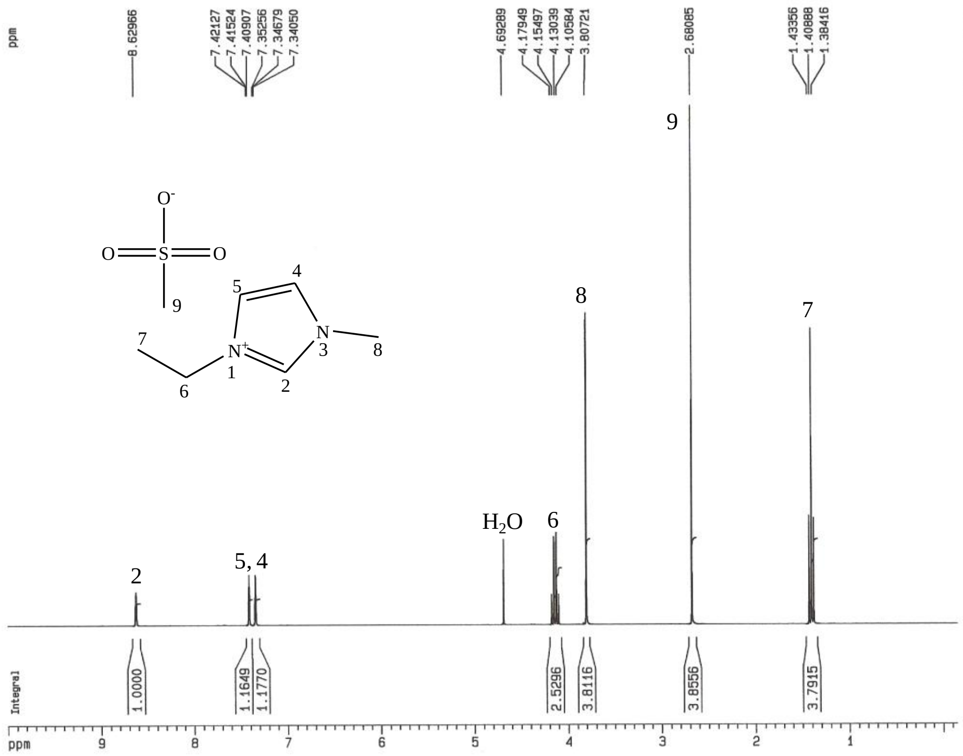

Figure B 15. ^{1}H NMR Spectra of [C_2mim][CH_3SO_3].

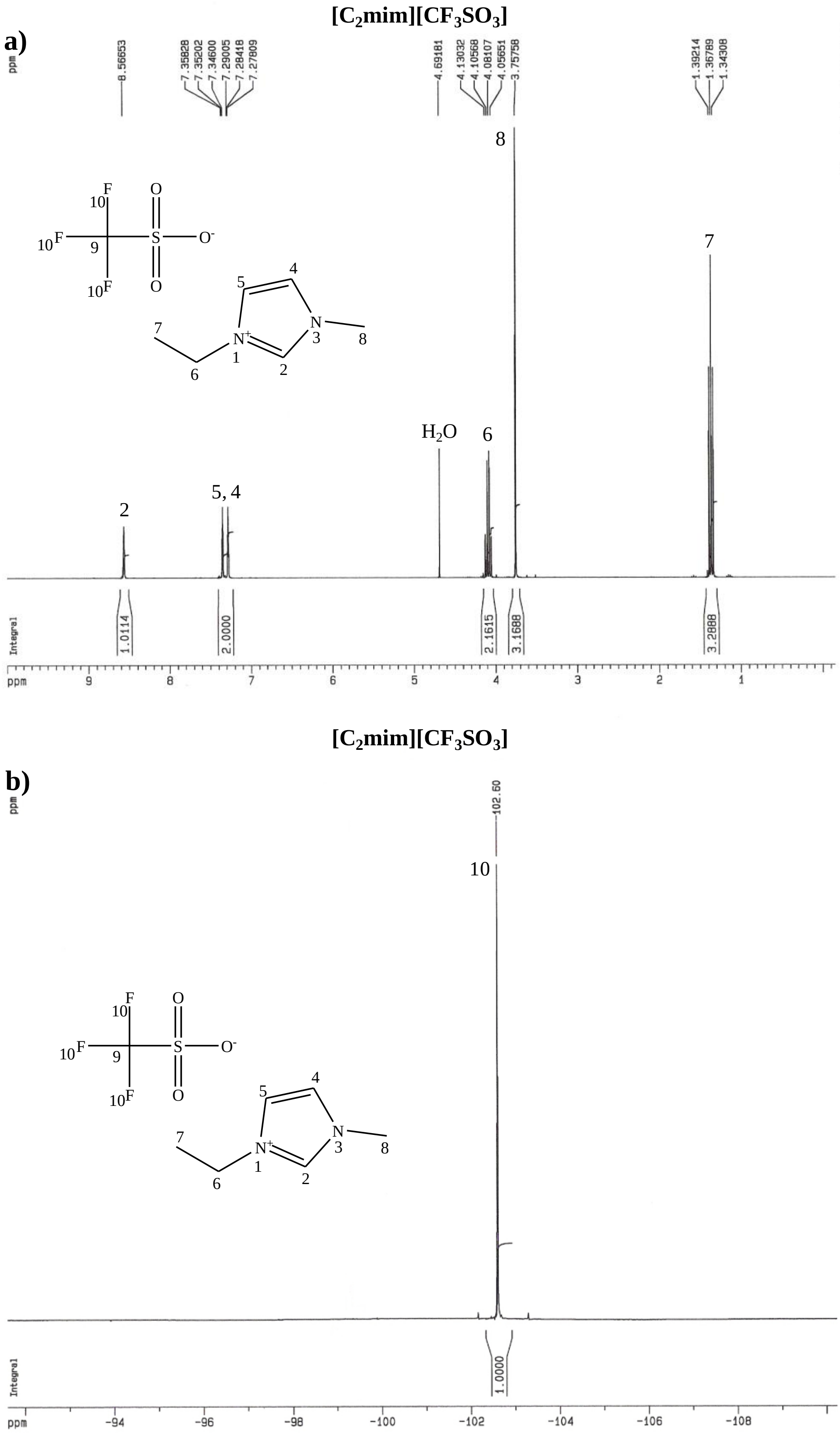

Figure B 16. NMR Spectra of $[C_2mim][CF_3SO_3]$: a) ^1H; b) ^{19}F.

$[C_4mim][Br]$

Figure B 17. ^1H NMR Spectra of $[C_4mim][Br]$.

$[C_4mim][CH_3CO_2]$

Figure B 18. ^1H NMR Spectra of $[C_4mim][CH_3CO_2]$.

[C_4mim][$N(CN)_2$]

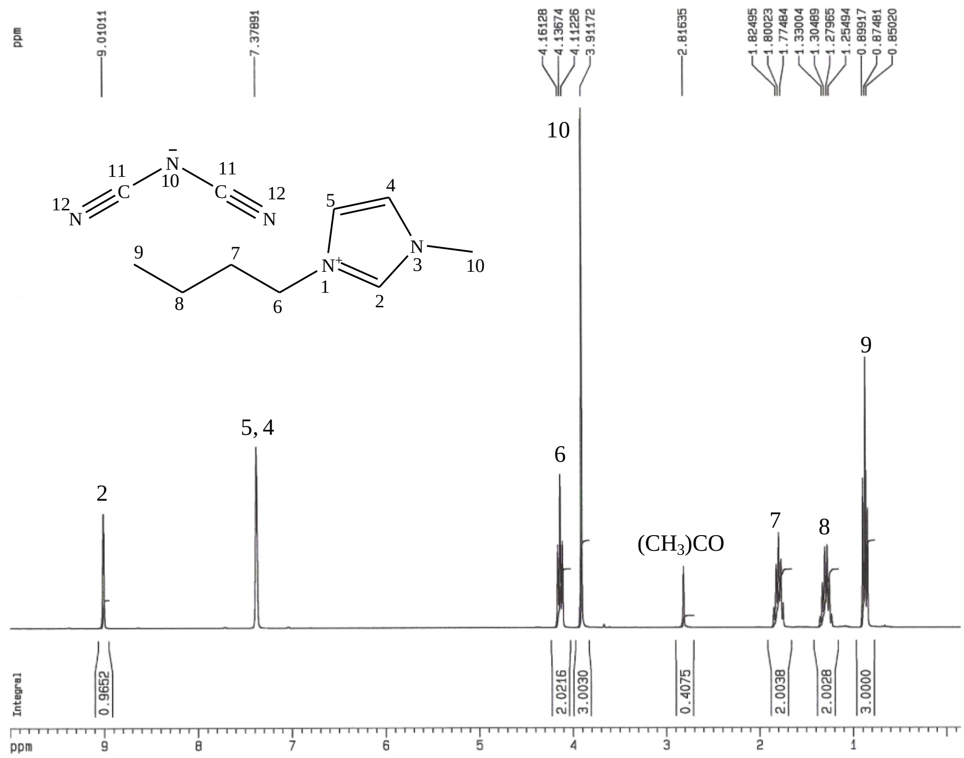

Figure B 19. ^{1}H NMR Spectra of [C_4mim][$N(CN)_2$].

[C_4mim][CH_3SO_3]

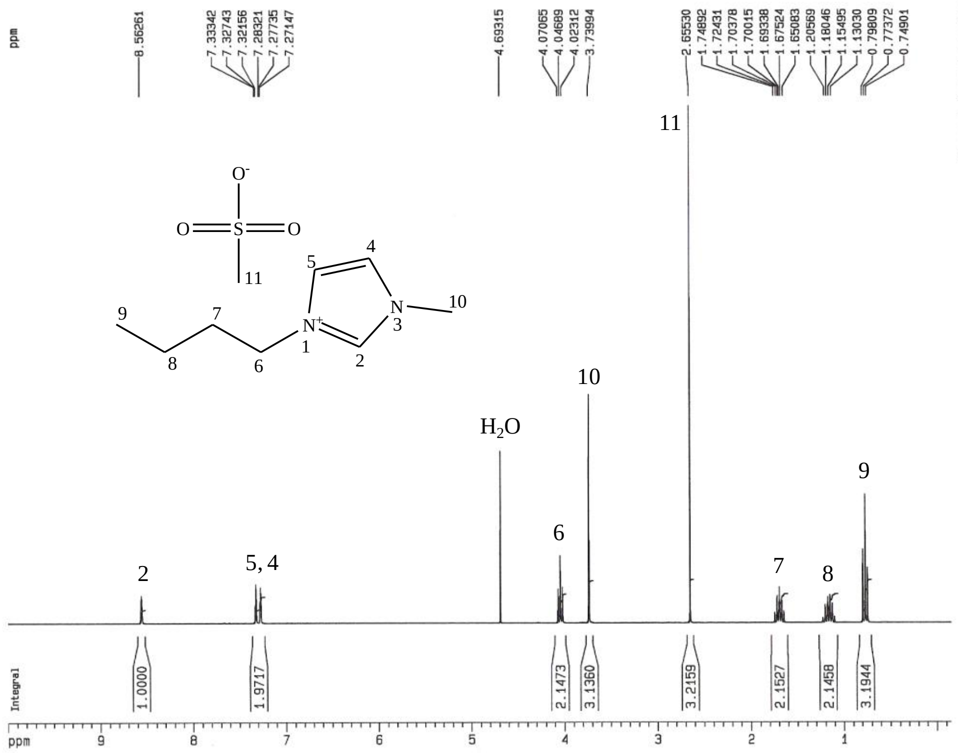

Figure B 20. ^{1}H NMR Spectra of [C_4mim][CH_3SO_3].

[C_4mim][HSO_4]

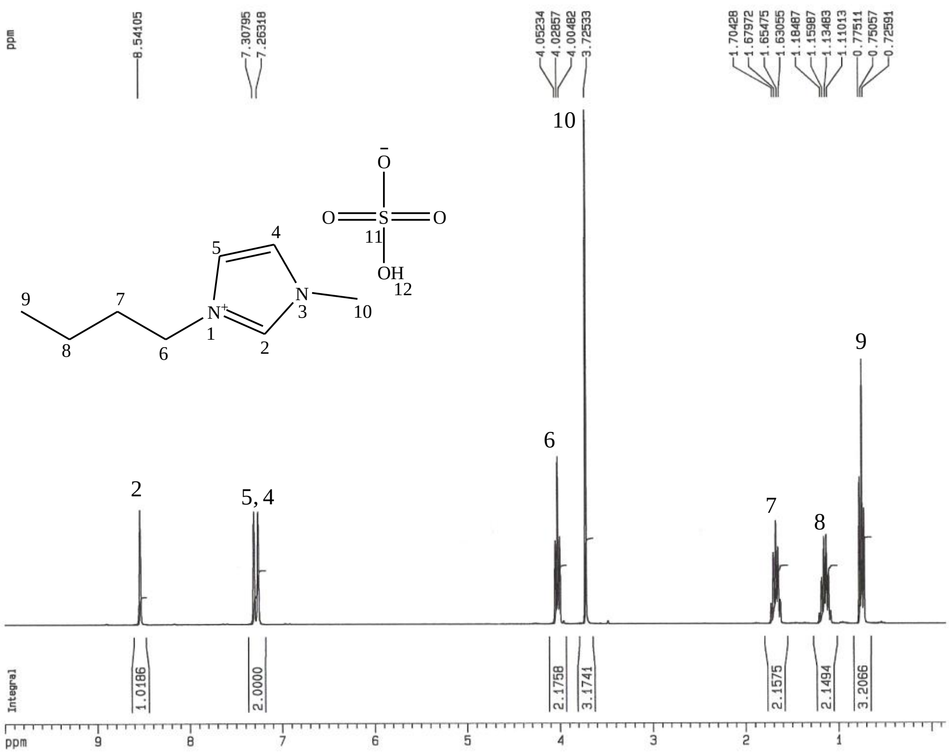

Figure B 21. ^{1}H NMR Spectra of [C_4mim][HSO_4].

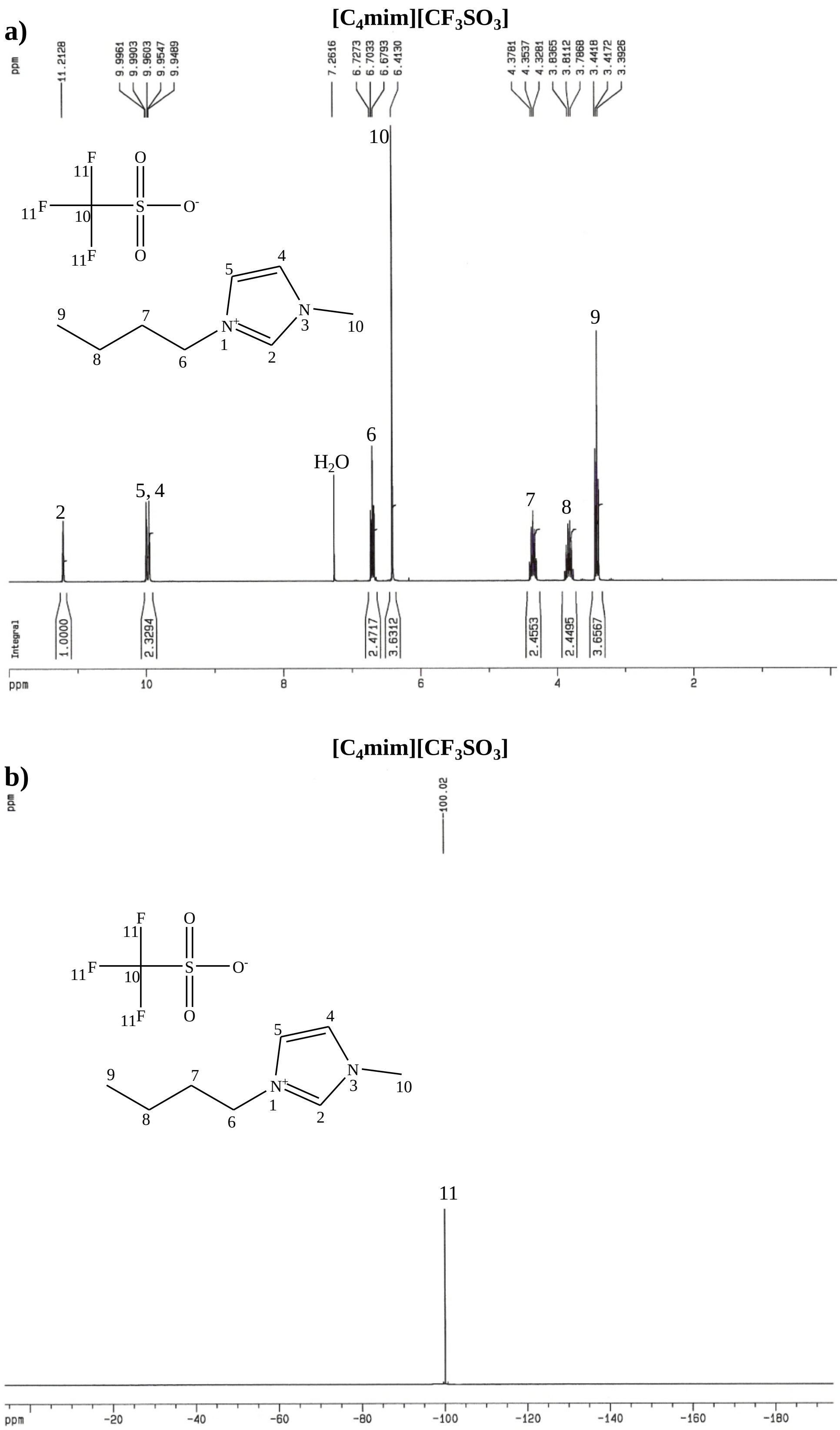

Figure B 22. NMR Spectra of $[C_4mim][CF_3SO_3]$: a) ^1H; b) ^{19}F.

a)

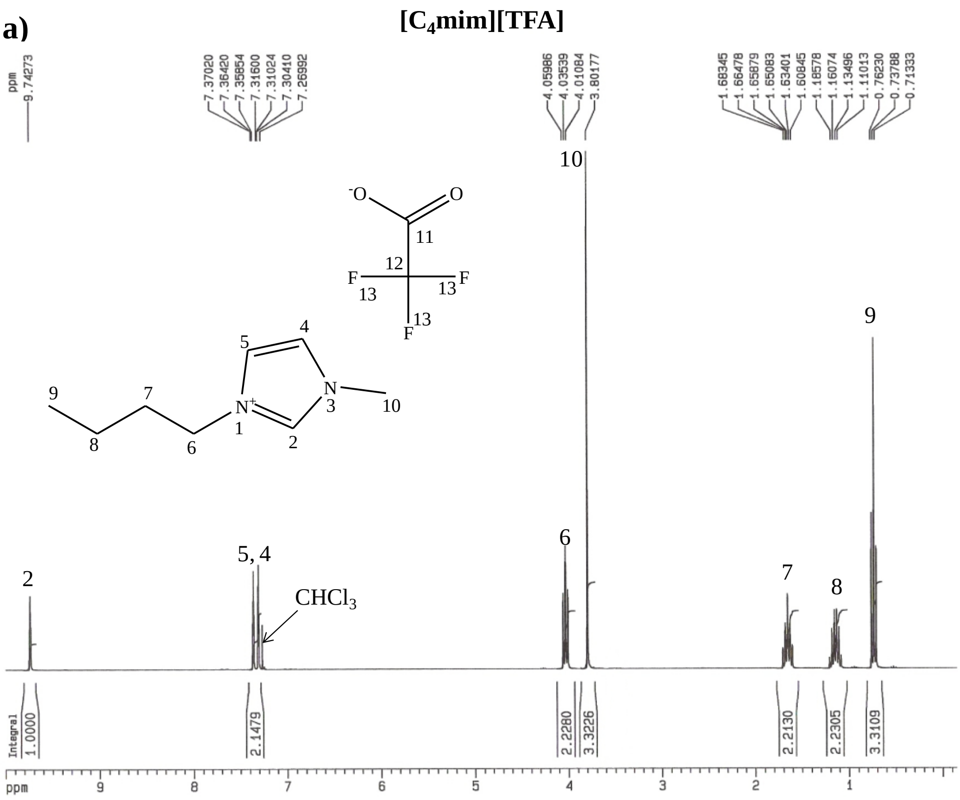

b)

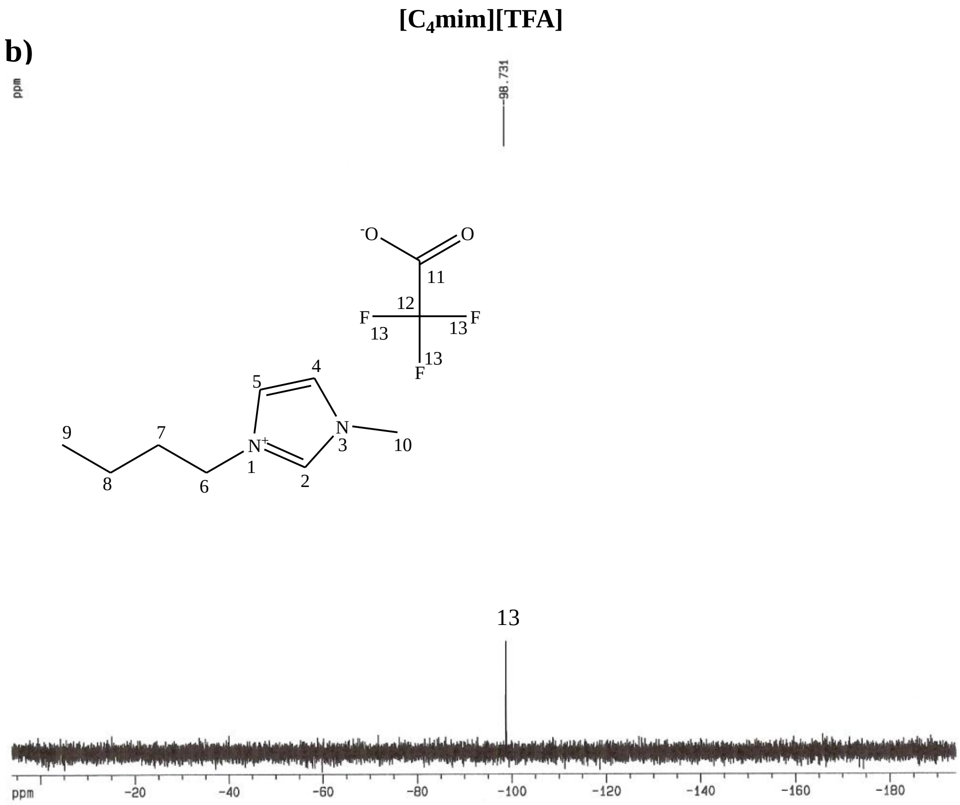

Figure B 23. NMR Spectra of [C_4mim][TFA]: a) ^{1}H; b) ^{19}F.

2. Tables

Table B 1. Experimental binodal curve mass fraction data for the system IL (1) + K_3PO_4 (2) + H_2O (3) at 298 K.

[im]Cl Mr = 104.54		[C_1mim]Cl Mr = 132.59		[C_2mim]Cl Mr = 146.62	
100 w_1	100 w_2	100 w_1	100 w_2	100 w_1	100 w_2
14.071	26.440	40.215	7.716	38.727	4.175
13.364	26.266	36.696	8.386	34.749	6.366
12.892	26.429	33.897	8.938	31.369	7.142
12.333	26.353	30.416	11.312	26.796	8.785
11.909	26.472	27.791	12.334	25.026	10.285
11.469	26.551	25.358	14.071	23.370	11.511
10.953	26.776	22.861	15.973	21.547	13.050
10.496	27.030	21.368	17.092	20.019	14.420
7.475	30.409	19.788	18.484	18.419	15.884
7.009	30.785	18.399	19.692	17.045	17.150
6.296	31.437	16.665	21.215	15.757	18.396
5.581	32.212	15.173	22.492	14.579	19.557
		13.805	23.771	13.550	20.571
		12.578	24.931	12.685	21.426
		11.891	25.617	11.823	22.341
		10.786	26.693	10.781	23.435
		9.207	28.404	10.061	24.238
		7.592	30.292	9.164	25.244
				8.230	26.413
				7.369	27.499
				6.541	28.651
				5.602	30.035

Table B 2. Experimental binodal curve mass fraction data for the system IL (1) + K_3PO_4 (2) + H_2O (3) at 298 K.

[C_4mim]Cl Mr = 174.67				[OHC_2mim]Cl Mr = 162.62	
100 w_1	100 w_2	100 w_1	100 w_2	100 w_1	100 w_2
39.321	3.478	13.932	18.714	67.860	2.316
37.151	4.566	13.531	19.054	64.168	2.772
33.876	5.683	13.021	19.561	54.223	3.718
32.269	6.533	12.675	19.829	49.934	4.554
30.179	7.539	12.304	20.154	45.322	6.918
27.447	8.731	11.083	22.019	38.311	10.589
25.291	10.051	10.426	22.560	34.707	12.735
24.369	10.655	9.792	23.113	30.190	15.750
23.517	11.175	9.113	23.803	28.258	17.120
22.512	11.946	8.530	24.407	21.472	22.289
21.686	12.518	8.024	24.887	67.860	2.316
20.954	13.008	7.648	25.267	64.168	2.772
20.128	13.628	7.152	25.841	54.223	3.718
19.298	14.297	6.735	26.319	49.934	4.554
18.632	14.786	6.329	26.814	45.322	6.918
17.904	15.373	5.986	27.218	38.311	10.589
17.261	15.895	5.635	27.668	34.707	12.735
16.646	16.394	5.313	28.106	30.190	15.750
16.057	16.865	4.977	28.610	28.258	17.120
15.409	17.485	4.507	29.347	21.472	22.289
14.940	17.860	3.804	30.521		
14.343	18.403	2.912	32.157		

Table B 3. Experimental binodal curve mass fraction data for the system IL (1) + K_3PO_4 (2) + H_2O (3) at 298 K.

[amim]Cl Mr = 158.63			
100 w_1	100 w_2	100 w_1	100 w_2
44.178	2.719	14.929	19.269
39.549	4.183	14.461	19.632
37.573	5.123	13.862	20.170
34.552	5.983	13.113	20.911
33.073	6.908	12.533	21.427
31.568	7.611	12.038	21.819
30.238	8.287	11.606	22.222
29.013	9.001	11.107	22.723
27.213	10.187	10.645	23.184
26.089	10.706	10.281	23.525
24.566	11.889	9.964	23.818
23.027	12.958	9.571	24.199
21.720	13.898	9.198	24.594
20.633	14.586	8.864	24.927
19.420	15.559	8.555	25.229
18.306	16.492	8.264	25.519
17.579	16.961	7.804	26.106
16.624	17.803	7.467	26.468
15.716	18.584	6.944	27.055

Table B 4. Experimental binodal curve mass fraction data for the system IL (1) + K_3PO_4 (2) + H_2O (3) at 298 K.

[C_6mim]Cl Mr = 202.73					
100 w_1	100 w_2	100 w_1	100 w_2	100 w_1	100 w_2
42.378	3.902	9.074	21.725	4.247	27.354
35.976	5.403	8.959	21.877	4.192	27.421
33.612	6.214	8.818	21.977	4.121	27.553
31.267	7.301	8.596	22.238	4.050	27.675
29.172	8.245	8.362	22.460	3.955	27.817
27.419	9.054	8.238	22.535	3.908	27.878
25.951	9.812	8.038	22.786	3.859	27.913
24.565	10.488	7.927	22.863	3.796	28.012
23.574	11.200	7.743	23.090	3.734	28.097
22.427	11.794	7.635	23.136	3.674	28.210
21.477	12.342	7.449	23.368	3.575	28.355
20.717	12.886	7.371	23.469	3.504	28.481
20.085	13.472	7.199	23.620	3.390	28.685
19.238	13.869	7.048	23.810	3.341	28.766
18.584	14.336	6.906	24.006	3.199	29.032
17.971	14.732	6.824	24.041	3.112	29.191
17.371	15.141	6.684	24.221	3.033	29.345
16.849	15.528	6.553	24.381	2.948	29.515
16.369	15.888	6.427	24.538	2.852	29.649
15.909	16.229	6.302	24.688	2.798	29.760
15.494	16.575	6.187	24.826	2.746	29.861
14.758	17.246	6.073	24.959	2.685	29.992
14.375	17.489	6.009	24.994	2.626	30.120
14.018	17.743	5.901	25.132	2.542	30.301
13.656	17.960	5.700	25.391	2.482	30.434
13.337	18.195	5.552	25.543	2.406	30.565
12.832	18.758	5.463	25.675	2.359	30.676
12.513	18.911	5.373	25.794	2.316	30.791
12.045	19.408	5.288	25.908	2.237	30.968
11.773	19.573	5.205	26.016	2.174	31.107
11.542	19.758	5.124	26.127	2.105	31.285
11.317	19.938	5.047	26.227	2.047	31.428
11.066	20.011	4.971	26.334	1.959	31.647
10.843	20.136	4.893	26.415	1.907	31.789
10.626	20.273	4.861	26.472	1.800	32.069
10.279	20.651	4.787	26.553	1.713	32.330
10.094	20.781	4.693	26.710	1.606	32.629
9.769	21.111	4.596	26.845	1.489	32.982
9.526	21.284	4.530	26.920	1.385	33.326
9.439	21.405	4.441	27.067		
9.215	21.661	4.327	27.228		

Table B 5. Experimental binodal curve mass fraction data for the system IL (1) + K_3PO_4 (2) + H_2O (3) at 298 K.

[C_1im]Cl Mr = 118.56					
100 w_1	100 w_2	100 w_1	100 w_2	100 w_1	100 w_2
19.992	22.214	8.537	21.342	3.751	24.172
18.153	22.151	8.316	21.507	3.672	24.266
17.569	22.179	7.928	21.785	3.593	24.365
16.842	22.019	7.613	21.839	3.515	24.442
16.310	22.004	7.383	21.842	3.449	24.545
15.702	21.837	7.188	21.898	3.383	24.658
15.232	21.804	7.037	22.060	3.253	24.868
14.665	21.604	6.856	22.103	3.175	24.927
14.250	21.584	6.693	22.173	3.105	25.045
13.788	21.456	6.518	22.169	3.045	25.104
13.421	21.454	6.317	22.300	2.980	25.199
12.974	21.294	6.128	22.401	2.909	25.347
12.578	21.171	5.984	22.391	2.849	25.440
12.244	21.150	5.860	22.431	2.792	25.540
11.886	21.051	5.747	22.520	2.732	25.594
11.618	21.061	5.525	22.622	2.678	25.668
11.303	20.966	5.356	22.867	2.609	25.801
11.049	20.970	5.124	22.812	2.544	25.913
10.773	20.918	4.957	23.181	2.484	26.047
10.536	20.915	4.737	23.174	2.389	26.273
10.312	20.934	4.579	23.412	2.287	26.428
10.089	20.915	4.384	23.396	2.221	26.626
9.925	20.982	4.261	23.702	2.124	26.824
9.694	20.895	4.083	23.733	2.012	27.089
9.483	21.230	3.968	23.894	1.895	27.398
9.108	21.178	3.899	23.966		
8.827	21.297	3.830	24.046		

Table B 6. Experimental binodal curve mass fraction data for the system IL (1) + K_3PO_4 (2) + H_2O (3) at 298 K.

		$[C_2im]Cl$ Mr = 132.59			
100 w_1	100 w_2	100 w_1	100 w_2	100 w_1	100 w_2
25.973	19.523	8.300	16.786	2.758	20.524
24.380	19.553	8.204	16.867	2.674	20.632
23.330	19.258	8.057	16.819	2.599	20.824
22.664	19.286	7.864	16.966	2.521	20.924
22.056	19.190	7.647	17.026	2.456	21.026
21.094	19.015	7.469	17.148	2.392	21.121
20.269	18.773	7.270	17.177	2.338	21.240
19.618	18.871	7.101	17.291	2.278	21.358
18.864	18.744	6.923	17.338	2.232	21.488
18.134	18.613	6.775	17.452	2.140	21.673
17.411	18.495	6.587	17.352	2.024	21.870
16.792	18.363	6.464	17.428	1.943	22.084
16.033	18.079	6.348	17.504	1.814	22.428
15.471	17.954	6.156	17.671	1.733	22.623
14.982	17.887	5.963	17.726	0.847	23.494
14.350	17.597	5.831	17.694	0.829	23.653
13.908	17.513	5.707	17.864	0.813	23.780
13.497	17.446	5.591	17.836	0.795	23.982
13.101	17.390	5.503	17.909	0.782	24.075
12.631	17.208	5.364	17.985	0.766	24.242
12.282	17.117	5.235	18.080	0.754	24.307
11.967	17.059	5.116	18.155	0.731	24.539
11.567	16.884	5.001	18.248	0.706	24.784
11.280	16.829	4.887	18.321	0.688	24.958
11.021	16.804	4.784	18.395	0.670	25.115
10.679	16.623	4.675	18.503	0.657	25.258
10.430	16.620	4.579	18.556	0.642	25.392
10.199	16.593	4.487	18.634	0.626	25.588
9.960	16.545	4.384	18.775	0.605	25.831
9.741	16.505	4.274	18.844	0.586	25.973
9.539	16.458	4.153	18.989	0.564	26.289
9.406	16.544	3.990	19.087	0.550	26.415
9.270	16.627	3.790	19.354	0.530	26.715
9.088	16.605	3.592	19.576	0.510	26.939
8.929	16.600	3.319	20.011	0.494	27.080
8.811	16.672	3.182	19.969	0.478	27.316
8.698	16.748	3.066	20.109	0.459	27.606
8.541	16.733	2.962	20.334	0.432	27.958
8.398	16.722	2.866	20.475		

Table B 7. Experimental binodal curve mass fraction data for the system IL (1) + K_3PO_4 (2) + H_2O (3) at 298 K.

[C_7H_7mim]Cl Mr = 208.69					
100 w_1	100 w_2	100 w_1	100 w_2	100 w_1	100 w_2
43.686	4.760	17.169	16.409	7.802	23.332
40.143	5.651	16.643	16.789	7.490	23.629
37.633	6.455	16.022	17.265	7.220	23.912
35.691	7.147	15.227	17.672	6.960	24.145
33.974	7.876	14.722	18.037	6.707	24.387
32.336	8.534	13.961	18.517	6.475	24.630
30.912	9.219	13.078	19.183	6.259	24.866
29.581	9.839	12.363	19.668	6.027	25.153
28.359	10.342	12.168	19.717	5.699	25.528
27.451	10.810	11.849	20.018	5.409	25.833
26.441	11.153	11.367	20.355	5.043	26.242
25.541	11.535	11.132	20.509	4.775	26.624
24.134	12.436	10.884	20.763	4.385	27.216
23.330	12.786	10.464	21.045	4.044	27.808
22.102	13.576	10.229	21.237	3.784	28.137
21.454	13.796	9.746	21.600	3.639	28.318
20.490	14.425	9.314	21.960	3.416	28.658
19.616	15.008	8.841	22.386	3.178	29.005
18.784	15.550	8.445	22.751	2.744	29.791
17.739	16.069	8.078	23.071	2.217	30.870

Table B 8. Experimental binodal curve mass fraction data for the system IL (1) + K_3PO_4 (2) + H_2O (3) at 298 K.

$[C_2mim][CF_3SO_3]$ Mr = 260.23					
100 w_1	100 w_2	100 w_1	100 w_2	100 w_1	100 w_2
45.772	3.912	12.068	14.488	4.252	21.948
39.539	5.379	11.782	14.696	3.794	22.840
36.122	6.409	11.427	14.807	3.538	23.388
32.628	7.300	11.204	15.051	3.234	24.024
29.869	8.056	10.746	15.217	3.025	24.424
27.650	8.822	10.237	15.531	2.820	24.927
20.642	11.047	9.752	15.767	2.626	25.418
19.564	11.401	9.290	16.356	2.427	25.953
18.556	11.689	8.800	16.756	2.171	26.649
17.732	12.020	8.256	17.280	1.986	27.356
16.958	12.292	7.779	17.753	1.818	27.850
16.338	12.598	7.336	18.157	1.585	28.734
15.680	12.845	6.884	18.346	1.366	29.666
15.069	13.085	6.598	18.855	0.911	30.427
14.509	13.299	6.298	19.209	0.874	30.710
13.982	13.468	6.059	19.653	0.824	31.222
13.599	13.745	5.492	20.198	0.759	31.842
12.842	14.214	5.081	20.898	0.706	32.187
12.429	14.344	4.525	21.349	0.640	32.889

Table B 9. Experimental binodal curve mass fraction data for the system IL (1) + K_3PO_4 (2) + H_2O (3) at 298 K.

$[C_2mim][EtSO_4]$ Mr = 237.29					
100 w_1	100 w_2	100 w_1	100 w_2	100 w_1	100 w_2
28.858	10.669	13.865	19.552	7.916	24.074
27.508	11.463	13.546	19.753	7.731	24.266
26.127	12.058	13.224	19.933	7.466	24.636
24.964	12.692	12.929	20.096	7.207	24.829
23.745	13.264	12.460	20.534	6.937	25.230
22.899	13.830	12.162	20.615	6.649	25.464
22.034	14.321	11.562	21.303	6.321	25.791
21.236	14.792	11.264	21.320	6.020	26.047
20.556	15.238	10.892	21.628	5.793	26.455
19.853	15.674	10.369	22.037	5.413	26.820
19.227	16.021	10.188	22.124	4.982	27.525
19.227	16.021	10.017	22.223	4.573	27.973
18.193	16.865	9.740	22.606	4.162	28.666
18.193	16.865	9.570	22.697	3.584	29.514
17.511	17.059	9.414	22.776	3.276	30.106
17.511	17.059	9.154	23.018	3.046	30.530
16.656	17.830	8.915	23.246	2.768	31.166
16.656	17.830	8.656	23.414	2.520	31.653
15.752	18.367	8.426	23.591	2.174	32.594
14.954	18.857	8.223	23.810		
14.224	19.374	8.110	23.879		

Table B 10. Experimental binodal curve mass fraction data for the system IL (1) + K_3PO_4 (2) + H_2O (3) at 298 K.

$[C_2mim][MeSO_4]$ Mr = 223.27				$[C_2mim][CH_3CO_2]$ Mr = 170.21	
100 w_1	100 w_2	100 w_1	100 w_2	100 w_1	100 w_2
44.344	5.625	13.244	21.370	26.443	9.744
23.640	14.474	12.782	21.748	24.161	11.716
22.835	14.924	12.352	22.105	22.064	13.611
22.076	15.371	11.915	22.346	20.381	15.098
21.454	15.851	11.534	22.648	18.455	16.958
20.748	16.244	11.180	22.975	16.772	18.645
20.123	16.628	10.669	23.358	15.024	20.521
19.604	17.050	10.212	23.741	13.451	22.231
19.064	17.398	9.690	24.326	12.142	23.746
18.603	17.774	9.199	24.723	12.063	23.788
18.081	18.052	8.740	25.047	11.421	24.514
17.555	18.345	8.348	25.423	10.944	24.967
17.137	18.638	8.000	25.824	10.626	25.417
16.324	18.945	7.673	26.150	9.751	26.368
15.984	19.164	7.173	26.708	9.728	26.433
15.301	19.432	6.718	27.145	9.007	27.275
14.954	19.933	6.245	27.772	8.784	27.468
14.751	20.134	5.740	28.389	8.354	28.058
14.630	20.368	5.044	29.296	7.796	28.737
14.055	20.794	4.885	29.302	7.743	28.763
13.760	20.956	3.081	30.379	6.423	30.522

Table B 11. Experimental binodal curve mass fraction data for the system IL (1) + K_3PO_4 (2) + H_2O (3) at 298 K.

$[C_2mim][Br]$ Mr = 191.07					
100 w_1	100 w_2	100 w_1	100 w_2	100 w_1	100 w_2
45.588	3.823	15.817	18.961	9.833	23.771
38.250	7.012	15.490	19.271	9.440	24.132
34.568	7.917	15.137	19.516	9.197	24.349
32.428	8.909	14.832	19.816	9.078	24.445
30.493	9.859	14.519	20.018	8.863	24.687
28.861	10.624	14.162	20.157	8.554	25.005
27.529	11.324	13.897	20.396	8.269	25.350
26.527	12.124	13.600	20.579	7.986	25.605
25.385	12.843	13.335	20.769	7.810	25.801
24.295	13.450	13.100	20.990	7.498	26.179
23.306	13.901	12.661	21.415	7.204	26.481
22.508	14.481	12.384	21.526	6.991	26.712
21.733	14.992	12.170	21.759	6.735	27.008
20.968	15.429	11.958	21.919	6.481	27.226
20.268	15.902	11.743	22.044	6.270	27.539
19.760	16.447	11.539	22.191	6.062	27.775
19.155	16.809	11.197	22.549	5.788	28.181
18.572	17.117	11.011	22.667	5.613	28.446
18.041	17.437	10.865	22.867	5.231	28.987
17.571	17.808	10.685	22.966	4.810	29.628
17.133	18.104	10.545	23.121	4.455	30.218
16.647	18.333	10.252	23.397	3.967	31.092
16.297	18.728	9.951	23.604	3.539	31.888

Table B 12. Experimental binodal curve mass fraction data for the system IL (1) + K_3PO_4 (2) + H_2O (3) at 298 K.

$[C_2mim][CH_3SO_3]$ Mr = 206.26		$[C_4mim][HSO_4]$ Mr = 236.28	
100 w_1	100 w_2	100 w_1	100 w_2
32.063	18.140	59.383	0.551
29.150	18.249	48.248	1.324
18.685	22.738	35.884	2.598
8.377	30.896	25.738	4.786
6.978	33.159	22.740	5.568
6.210	34.120	18.339	6.562
5.699	34.734	16.720	8.001
4.922	36.154	11.279	12.682
4.249	37.579	8.873	15.736
3.856	38.047	4.087	24.013

Table B 13. Experimental binodal curve mass fraction data for the system IL (1) + K_3PO_4 (2) + H_2O (3) at 298 K.

[C$_4$mim][N(CN)$_2$] Mr = 205.26					
100 w_1	100 w_2	100 w_1	100 w_2	100 w_1	100 w_2
47.148	2.129	7.320	14.350	3.326	19.296
42.279	2.846	7.254	14.401	3.288	19.360
38.085	3.443	7.180	14.462	3.248	19.439
35.263	4.361	7.115	14.545	3.210	19.503
32.306	4.814	7.021	14.699	3.173	19.576
30.291	5.498	6.930	14.720	3.135	19.650
28.629	5.987	6.867	14.760	3.098	19.715
27.067	6.330	6.812	14.820	3.063	19.787
25.703	6.749	6.757	14.855	3.030	19.865
24.523	7.058	6.704	14.895	2.999	19.926
23.442	7.359	6.645	14.973	2.963	20.033
22.433	7.608	6.591	15.011	2.921	20.117
21.524	7.896	6.538	15.051	2.872	20.244
20.916	8.206	6.486	15.100	2.822	20.319
20.117	8.436	6.434	15.126	2.779	20.424
19.475	8.564	6.391	15.221	2.739	20.519
18.998	8.834	6.322	15.227	2.700	20.613
18.315	9.032	6.272	15.264	2.662	20.712
17.912	9.234	6.224	15.302	2.618	20.844
17.340	9.361	6.178	15.331	2.576	20.977
16.963	9.609	6.108	15.457	2.536	21.097
16.444	9.743	6.016	15.547	2.496	21.147
15.981	9.880	5.957	15.667	2.458	21.269
15.674	10.068	5.876	15.743	2.414	21.343
15.243	10.163	5.785	15.833	2.373	21.430
14.798	10.282	5.694	15.918	2.313	21.674
14.537	10.459	5.627	16.071	2.256	21.815
14.176	10.542	5.542	16.153	2.203	21.946
13.816	10.636	5.462	16.223	2.159	22.093
13.571	10.814	5.398	16.270	2.117	22.181
13.248	10.918	5.344	16.372	2.072	22.301
13.027	11.076	5.271	16.429	2.032	22.432
12.710	11.136	5.215	16.552	1.992	22.580
12.495	11.300	5.140	16.623	1.955	22.716

12.299	11.457	5.067	16.698	1.912	22.799
12.016	11.533	5.018	16.793	1.876	22.956
11.812	11.708	4.964	16.914	1.839	23.068
11.528	11.750	4.896	16.975	1.804	23.203
11.363	11.853	4.827	17.016	1.758	23.359
11.197	11.992	4.764	17.075	1.722	23.489
10.976	12.048	4.706	17.106	1.658	23.681
10.822	12.184	4.656	17.218	1.582	23.919
10.638	12.184	4.590	17.280	1.067	24.554
10.496	12.312	4.549	17.369	1.041	24.782
10.370	12.404	4.490	17.429	1.023	24.921
10.209	12.415	4.450	17.552	1.004	25.091
10.101	12.502	4.399	17.603	0.989	25.220
9.976	12.612	4.353	17.668	0.968	25.381
9.812	12.615	4.297	17.707	0.946	25.581
9.638	12.849	4.258	17.790	0.925	25.765
9.485	12.920	4.215	17.907	0.907	25.898
9.321	12.948	4.153	17.918	0.882	26.108
9.209	13.044	4.100	17.965	0.861	26.317
9.101	13.119	4.028	18.122	0.845	26.472
8.994	13.230	3.982	18.178	0.828	26.620
8.849	13.240	3.947	18.265	0.806	26.813
8.751	13.324	3.902	18.299	0.789	26.973
8.649	13.422	3.860	18.350	0.755	27.243
8.455	13.610	3.829	18.421	0.731	27.530
8.359	13.698	3.787	18.456	0.706	27.753
8.220	13.714	3.762	18.506	0.688	27.925
8.133	13.797	3.730	18.588	0.656	28.314
8.057	13.863	3.689	18.626	0.519	28.487
7.977	13.940	3.660	18.694	0.510	28.584
7.873	13.962	3.622	18.727	0.500	28.761
7.789	14.020	3.592	18.797	0.488	28.998
7.714	14.089	3.544	18.888	0.466	29.373
7.639	14.155	3.498	18.969	0.443	29.800
7.520	14.155	3.454	19.042	0.420	30.198
7.451	14.223	3.411	19.129		
7.392	14.292	3.368	19.220		

Table B 14. Experimental binodal curve mass fraction data for the system IL (1) + K_3PO_4 (2) + H_2O (3) at 298 K.

$[C_4mim][CF_3SO_3]$ Mr = 288.29					
100 w_1	100 w_2	100 w_1	100 w_2	100 w_1	100 w_2
47.969	1.923	10.935	8.322	7.081	11.433
32.603	4.052	10.554	8.502	6.834	11.698
26.880	4.485	10.215	8.721	6.640	11.983
22.880	4.846	9.919	8.951	6.414	12.200
20.300	5.277	9.614	9.119	6.235	12.448
18.371	5.573	9.392	9.338	6.059	12.683
17.078	5.935	9.215	9.567	5.888	12.897
15.872	6.205	8.938	9.679	5.692	13.027
14.810	6.479	8.743	9.866	5.525	13.391
14.091	6.785	8.516	10.019	5.283	13.890
13.380	7.058	8.333	10.185	5.090	14.096
12.690	7.279	8.164	10.361	4.919	14.300
12.171	7.534	7.949	10.470	4.768	14.548
11.782	7.878	7.707	10.925		
11.304	8.071	7.346	11.158		

Table B 15. Experimental binodal curve mass fraction data for the system IL (1) + K_3PO_4 (2) + H_2O (3) at 298 K.

[C$_4$mim][Br] Mr = 219.12					
100 w_1	100 w_2	100 w_1	100 w_2	100 w_1	100 w_2
53.044	2.210	12.132	18.996	4.795	26.839
41.914	5.021	11.692	19.306	4.621	27.078
35.872	5.766	11.283	19.586	4.401	27.540
33.640	6.686	10.959	19.939	4.304	27.693
31.559	7.575	10.480	20.444	4.232	27.783
30.077	8.456	10.101	20.549	4.085	27.963
28.311	9.123	9.825	20.875	4.026	28.070
27.047	9.841	9.546	21.021	3.949	28.193
26.007	10.340	9.182	21.378	3.858	28.343
24.663	10.781	9.047	21.452	3.771	28.500
23.797	11.331	8.833	21.705	3.689	28.628
23.028	11.867	8.625	21.937	3.584	28.805
21.491	12.856	8.377	22.052	3.484	28.970
21.072	12.900	8.203	22.312	3.392	29.153
20.484	13.307	7.826	22.674	3.305	29.304
19.851	13.708	7.582	22.942	3.242	29.406
19.238	14.049	7.336	23.181	3.160	29.574
18.730	14.435	7.198	23.329	3.050	29.808
18.242	14.802	6.980	23.541	2.943	29.930
17.613	15.002	6.800	23.768	2.765	30.358
17.224	15.396	6.556	24.065	2.575	30.758
16.787	15.694	6.379	24.242	2.457	31.027
15.867	16.433	6.166	24.489	2.369	31.243
15.155	16.850	6.019	24.684	2.277	31.472
14.816	17.088	5.838	24.923	2.196	31.676
14.474	17.296	5.613	25.247	2.069	32.012
14.155	17.513	5.548	25.872	1.881	32.545
13.817	17.633	5.429	26.003	1.715	33.048
13.552	17.794	5.320	26.149	1.540	33.627
13.088	18.289	5.079	26.480		
12.587	18.649	4.916	26.676		

Table B 16. Experimental binodal curve mass fraction data for the system IL (1) + K_3PO_4 (2) + H_2O (3) at 298 K.

[C_4mim][TFA] Mr = 252.24					
100 w_1	100 w_2	100 w_1	100 w_2	100 w_1	100 w_2
44.506	3.982	15.358	14.849	7.138	20.307
40.969	4.631	15.006	15.013	6.936	20.484
35.545	5.421	14.476	15.523	6.748	20.662
33.860	6.280	14.008	15.550	6.484	20.868
32.432	6.935	13.692	15.759	6.227	21.004
30.787	7.579	13.324	16.063	6.040	21.258
29.557	8.122	13.042	16.158	5.860	21.475
28.379	8.596	12.756	16.313	5.691	21.719
27.243	9.120	12.510	16.445	5.515	21.832
26.242	9.566	12.283	16.568	5.248	22.284
25.363	9.928	12.060	16.689	4.884	22.846
24.600	10.317	11.732	16.997	4.637	22.944
23.929	10.828	11.389	17.342	4.409	23.303
23.189	11.235	10.995	17.541	4.122	23.829
22.432	11.565	10.632	17.773	3.838	24.077
21.765	11.824	10.284	17.902	3.623	24.478
21.114	12.194	10.023	18.174	3.412	24.702
20.439	12.526	9.717	18.297	3.230	25.070
19.829	12.829	9.416	18.435	2.999	25.600
19.285	13.079	9.218	18.650	2.603	26.416
18.245	13.542	8.964	18.752	2.297	27.055
17.775	13.755	8.622	19.110	1.925	28.011
17.271	14.028	8.323	19.389	0.806	31.291
16.844	14.191	8.062	19.629	0.634	32.860
16.439	14.351	7.785	19.727	0.473	33.706
16.071	14.517	7.554	19.942	0.403	34.326
15.703	14.682	7.351	20.124		

Table B 17. Experimental binodal curve mass fraction data for the system IL (1) + K_3PO_4 (2) + H_2O (3) at 298 K.

[C_4mim][CH_3CO_2] Mr = 198.26		[C_4mim][CH_3SO_3] Mr = 234.31			
100 w_1	100 w_2	100 w_1	100 w_2	100 w_1	100 w_2
26.443	9.744	46.003	2.594	13.534	21.842
24.161	11.716	40.190	4.949	12.890	22.363
22.064	13.611	37.061	6.348	12.360	22.857
20.381	15.098	34.326	7.760	11.794	23.284
18.455	16.958	31.842	9.092	11.316	23.720
16.772	18.645	29.685	10.314	10.781	24.161
15.024	20.521	27.992	11.255	10.265	24.593
13.452	22.231	27.278	11.755	9.814	24.954
12.142	23.746	25.800	12.670	9.276	25.503
12.064	23.788	24.187	13.785	8.789	25.941
11.421	24.515	23.719	14.090	8.340	26.409
10.944	24.967	22.165	15.097	7.933	26.853
10.626	25.417	21.437	15.702	7.445	27.352
9.751	26.368	20.233	16.498	6.723	28.126
9.728	26.433	19.542	17.082	6.113	28.860
9.007	27.275	18.505	17.779	5.404	29.871
8.784	27.468	17.456	18.658	4.851	30.609
8.354	28.058	16.655	19.356	4.530	30.869
7.797	28.737	15.909	19.886	4.069	31.597
7.743	28.763	14.978	20.554	3.432	32.625
6.423	30.522	14.238	21.258	2.498	34.378

3. Figures

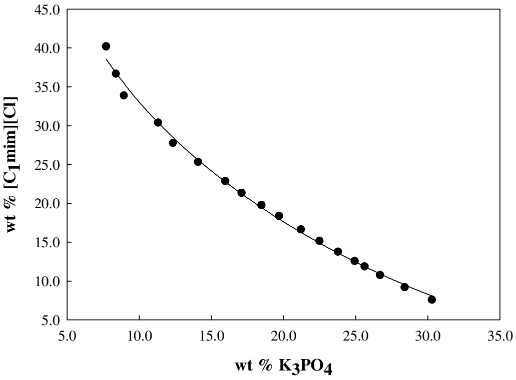
wt % [C_1mim][Cl]
wt % K_3PO_4
45.0
40.0
35.0
30.0
25.0
20.0
15.0
10.0
5.0
5.0
10.0
15.0
20.0
25.0
30.0
35.0

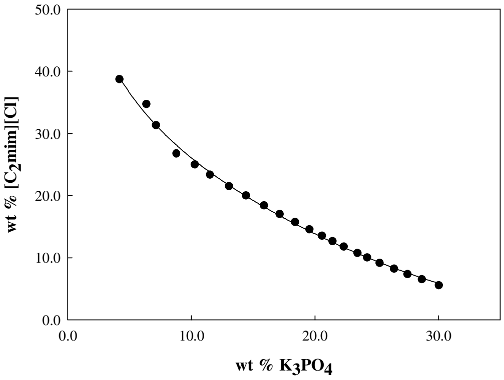
wt % [C_2mim][Cl]
wt % K_3PO_4
50.0
40.0
30.0
20.0
10.0
0.0
0.0
10.0
20.0
30.0

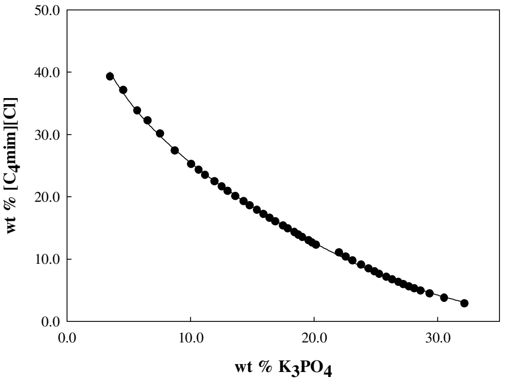
wt % [C_4mim][Cl]
wt % K_3PO_4
50.0
40.0
30.0
20.0
10.0
0.0
0.0
10.0
20.0
30.0

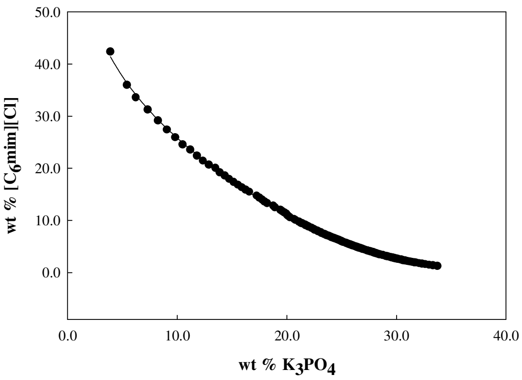
wt % [C_6mim][Cl]
wt % K_3PO_4
50.0
40.0
30.0
20.0
10.0
0.0
0.0
10.0
20.0
30.0
40.0

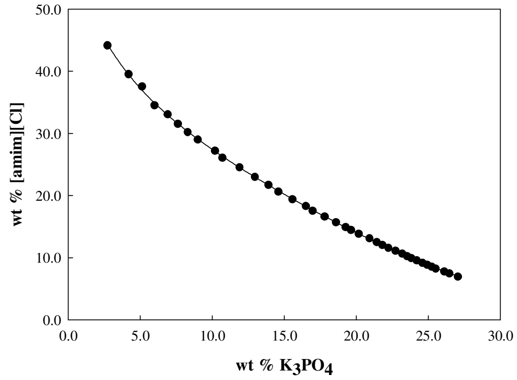
wt % [amim][Cl]
wt % K_3PO_4
50.0
40.0
30.0
20.0
10.0
0.0
0.0
5.0
10.0
15.0
20.0
25.0
30.0

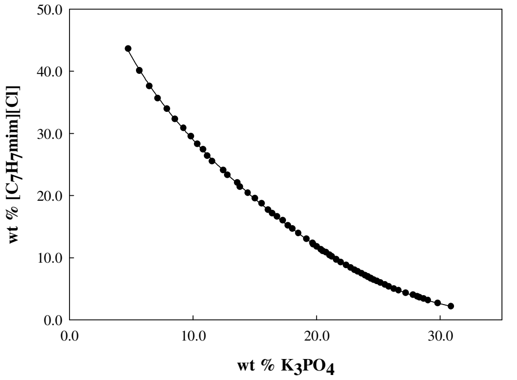
wt % [C_7H_7mim][Cl]
wt % K_3PO_4
50.0
40.0
30.0
20.0
10.0
0.0
0.0
10.0
20.0
30.0

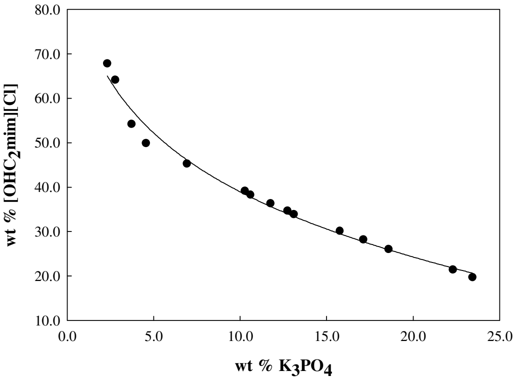
wt % [OHC_2mim][Cl]
wt % K_3PO_4
80.0
70.0
60.0
50.0
40.0
30.0
20.0
10.0
0.0
5.0
10.0
15.0
20.0
25.0

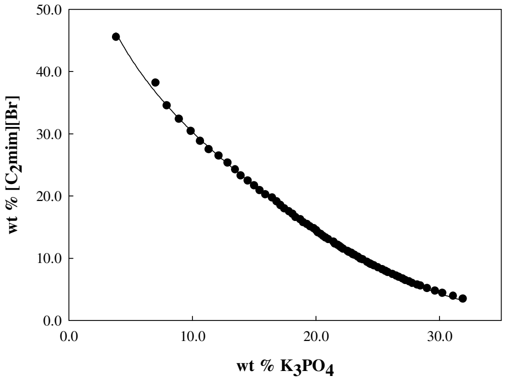
wt % [C_2mim][Br]
wt % K_3PO_4
50.0
40.0
30.0
20.0
10.0
0.0
0.0
10.0
20.0
30.0

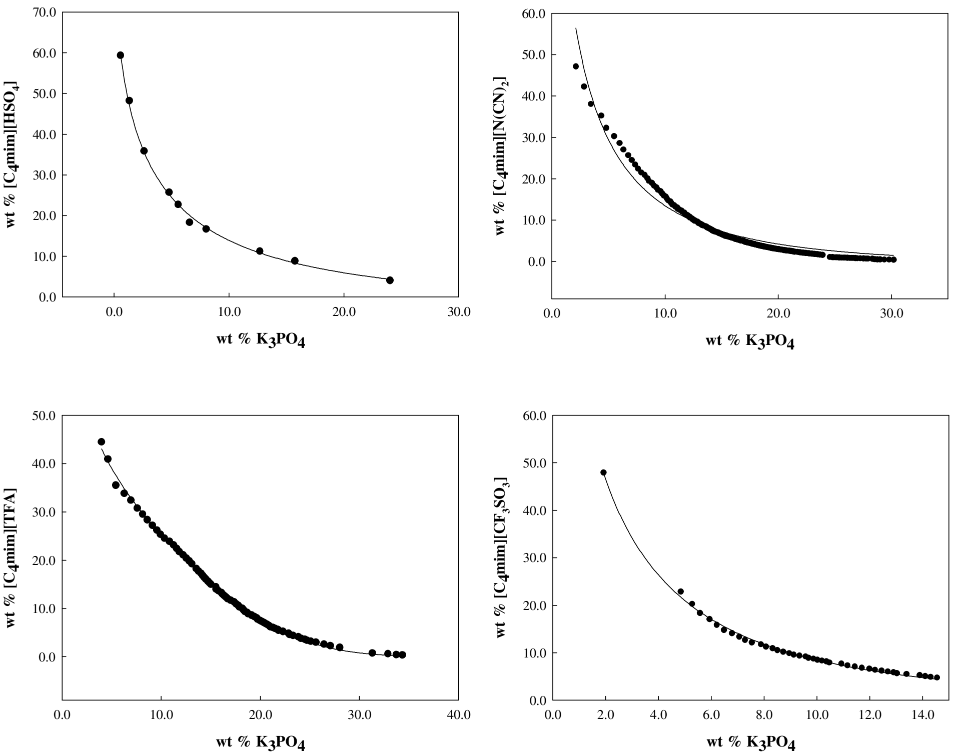

Figure B 24. Experimental values for binodal curve (dots) adjusted with Eq. 5 (dash) for all ILs studied in this work.

3. Calibration Curves

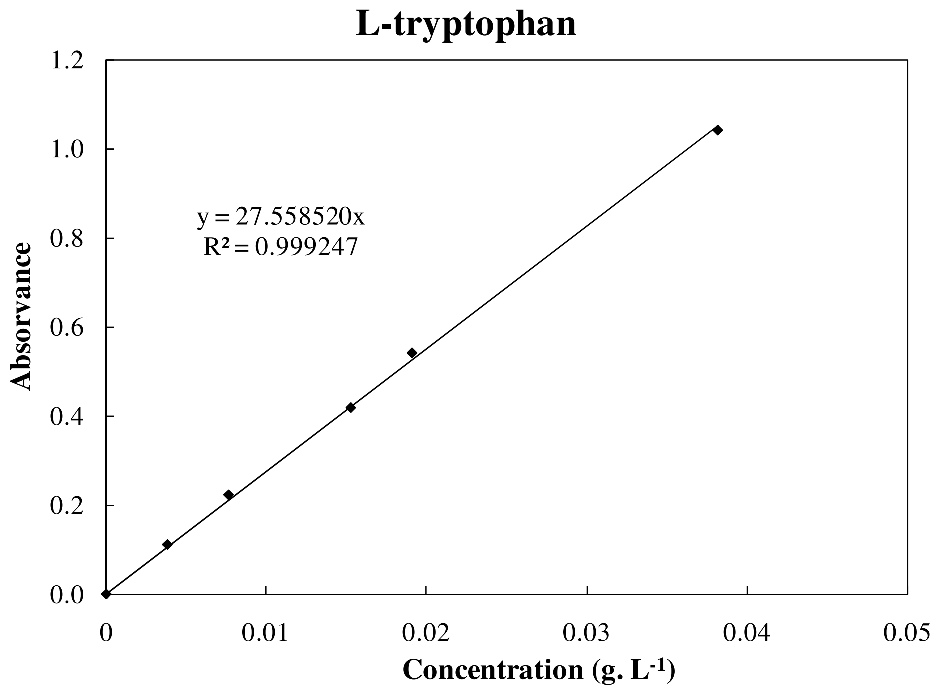

Figure B 15. Calibration curve for L-tryptophan.